PORE NETWORK MODELING OF FISSURED AND VUGGY CARBONATES

A THESIS SUBMITTED TO
THE GRADUATE SCHOOL OF NATURAL AND APPLIED SCIENCES
OF
MIDDLE EAST TECHNICAL UNIVERSITY

BY

SELİN ERZEYBEK

IN PARTIAL FULFILLMENT OF THE REQUIREMENTS
FOR
THE DEGREE OF MASTER OF SCIENCE IN
PETROLEUM AND NATURAL GAS ENGINEERING

JUNE 2008

Approval of the thesis:

PORE NETWORK MODELING OF FISSURED AND VUGGY CARBONATES

submitted by **SELİN ERZEYBEK** in partial fulfillment of the requirements for the degree of **Master of Science in Petroleum and Natural Gas Engineering Department, Middle East Technical University** by,

Prof. Dr. Canan Özgen _____
Director, Graduate School of **Natural and Applied Sciences**

Prof. Dr. Mahmut Parlaktuna _____
Head of Department, **Petroleum and Natural Gas Engineering**

Prof. Dr. Serhat Akın _____
Supervisor, **Petroleum and Natural Gas Engineering Dept.**

Examining Committee Members

Prof. Dr. Ender Okandan _____
Petroleum and Natural Gas Engineering Dept., METU

Prof. Dr. Serhat Akın _____
Petroleum and Natural Gas Engineering Dept., METU

Prof. Dr. Mahmut Parlaktuna _____
Petroleum and Natural Gas Engineering Dept., METU

Assist. Prof. Dr. Evren Özbayoğlu _____
Petroleum and Natural Gas Engineering Dept., METU

Dr. Hüseyin Çalışgan _____
Research Center, TPAO

Date: _____

I hereby declare that all information in this document has been obtained and presented in accordance with academic rules and ethical conduct. I also declare that, as required by these rules and conduct, I have fully cited and referenced all material and results that are not original to this work.

Name, Lastname : SELİN ERZEYBEK

Signature :

ABSTRACT

PORE NETWORK MODELLING OF
FISSURED AND VUGGY CARBONATES

Erzeybek, Selin
M.Sc., Department of Petroleum and Natural Gas Engineering
Supervisor : Prof. Dr. Serhat Akın

June 2008, 104 pages

Carbonate rocks contain most of the world's proven hydrocarbon reserves. It is essential to predict flow properties and understand flow mechanisms in carbonates for estimating hydrocarbon recovery accurately. Pore network modeling is an effective tool in determination of flow properties and investigation of flow mechanisms. Topologically equivalent pore network models yield accurate results for flow properties. Due to their simple pore structure, sandstones are generally considered in pore scale studies and studies involving carbonates are limited. In this study, in order to understand flow mechanisms and wettability effects in heterogeneous carbonate rocks, a novel pore network model was developed for simulating two-phase flow.

The constructed model was composed of matrix, fissure and vug sub domains and the sequence of fluid displacements was simulated typical by primary drainage followed by water flooding. Main mechanisms of imbibition, snap-off, piston like advance and pore body filling, were also considered. All the physically possible fluid configurations in the pores, vugs and fissures for all wettability types were

examined. For configurations with a fluid layer sandwiched between other phases, the range of capillary pressures for the existence of such a layer was also evaluated. Then, results of the proposed model were compared with data available in literature. Finally, effects of wettability and pore structure on flow properties were examined by assigning different wettability conditions and porosity features. It was concluded that the proposed pore network model successfully represented two phase flow in fissured and vuggy carbonate rocks.

Keywords: Pore Network, Two-phase relative permeability, wettability, fissured carbonates

ÖZ

ÇATLAKLI VE KOVUKLU KARBONATLARIN
GÖZENEK AĞ MODELLEMESİ

Erzeybek, Selin
Y. Lisans, Petrol ve Doğal Gaz Mühendisliği Bölümü
Tez Yöneticisi : Prof. Dr. Serhat Akın

Haziran 2008, 104 sayfa

Karbonat kayaçlar, dünya üzerindeki hidrokarbon rezervlerinin büyük bir kısmına sahiptir. Hidrokarbon kurtarımının doğru bir şekilde öngörülmesi için, karbonatların sahip olduğu akış özellikleri doğru tahmin edilmeli ve akış mekanizmaları anlaşılmalıdır. Son yıllarda yaygınlaşan gözenek ağı modellemesi, akış özelliklerinin ve mekanizmalarının belirlenmesinde etkili bir yöntem olarak kullanılmaktadır. Topolojik olarak eşdeğer gözenek ağları, akış özelliklerini doğru olarak belirlenmesini sağlar. Basit gözenek yapıları nedeniyle, gözenek ölçekli çalışmalarda kumtaşları tercih edilmiş olup, karbonat kayaçları için yapılan çalışmalar sınırlıdır. Bu çalışmada, heterojen karbonatlarda iki fazlı akış mekanizmalarının ve ıslanımlık etkilerinin anlaşılması için bir gözenek ağ modeli geliştirilmiştir.

Oluşturulan model matriks, çatlak ve kovuk alt kümelerinden oluşmuş olup, tipik olarak birincil drenaj ve takiben suyla öteleme şeklinde gerçekleşen akışkan ötelemesi serisinin simulasyonu yapılmıştır. Suyla öteleme sırasında gerçekleşen özel mekanizmalar da ayrıca gözönünde bulundurulmuştur. Gözeneklerde,

çatlaklarda ve kovuklarda, fiziksel olarak mümkün olan tüm akışkan konfigürasyonları incelenmiştir. Diğer fazlar arasında araya sıkışmış bir akışkan tabakası şeklindeki konfigürasyonlarda, bu şekilde bulunan bir tabakanın oluşması için gerekli olan kılcal basınç aralıkları belirlenmiştir. Bir sonraki aşamada, oluşturulan modelin sonuçları literatürde bulunan verilerle karşılaştırılmıştır. Son olarak ıslanımlık özelliklerinin ve gözenek yapılarının akış özelliklerine olan etkileri farklı ıslanımlık ve gözenek koşullarında incelenmiştir. Bu çalışmanın sonucunda, oluşturulan modelin, çatlaklı ve kovuklu karbonat kayaçlarında iki fazlı akışı başarıyla temsil ettiğine karar verilmiştir.

Anahtar Kelimeler: Gözenek ağları, iki faz göreli geçirgenlik, ıslanımlık, çatlaklı karbonatlar

To My Parents and My Brother

ACKNOWLEDGEMENTS

I would like to thank my supervisor Prof. Dr. Serhat Akın for his courage, guidance and support throughout my education at METU. His great contributions were extremely beneficial for me during my undergraduate and graduate studies. I also would like to appreciate my thesis committee members, Prof Dr. Ender Okandan, Prof. Dr. Mahmut Parlaktuna, Assist. Prof. Dr. Evren Özbayoğlu and Dr. Hüseyin Çalışgan, for their contributions.

I would like to express my deepest gratitude to my parents, Nimet – Selim Erzeybek and my brother Yunus Serhat Erzeybek, for their continuous love, support and confidence in me. They are always beside me and will be with me despite the distances between us. I greatly acknowledge the supports of Nurcan Tür for her valuable friendship and encouragement throughout this study. She has been more than a home mate for me.

I would like to express my special thanks to Hüseyin Onur Balan for his continuous patience, support and trust. Without his love and his contributions to my life, this study cannot be accomplished.

I wish to thank to my instructors at my department for their valuable contributions to my academic life. Also, I owe special thanks to The Scientific and Technological Research Council of Turkey (TUBITAK) for the financial support throughout my M.Sc. education.

TABLE OF CONTENTS

ABSTRACT iv
ÖZ vi
ACKNOWLEDGEMENTS ix
TABLE OF CONTENTS x
LIST OF TABLES xiii
LIST OF FIGURES xiv
NOMENCLATURE xvi
CHAPTER
1. INTRODUCTION 1
2. LITERATURE REVIEW 4
2.1. Carbonate Reservoirs 5
2.2. Pore Structure of Carbonates 6
2.2.1. Porosity Types in Carbonates 6
2.2.1.1. Primary Porosity 7
2.2.1.2. Secondary Porosity 7
2.2.2. Porosity Classification of Carbonate Rocks 8
2.2.3. Pore Network Modeling Studies for Carbonates 11
2.3. Advanced Studies in Pore Network Modeling 12
3. PORE NETWORK MODELING 15
3.1. Pore Morphology 15
3.2. Network Type 16
3.2.1. Network Dimension 16
3.2.2. Flow Behavior 17
3.2.2.1. Quasi-Static Network Models 17
3.2.2.2. Dynamic Network Models 17
3.2.3. Spatially Correlated and Uncorrelated Networks 19
3.3. Flow Mechanisms 20
3.3.1. Snap – Off 20

3.3.2. Piston – Like Advance 22
3.3.3. Pore – Body Filling 25
4. STATEMENT OF THE PROBLEM 27
5. METHODOLOGY 28
5.1. Construction of Pore Network Model 28
5.1.1. Assigning Matrix Properties 28
5.1.2. Assigning Secondary Porosity Features 30
5.1.3. Constructed Pore Network Model 30
5.2. Simulation of Flow Mechanisms 32
5.2.1. Primary Drainage 32
5.2.1.1. Threshold Pressure Calculation 32
5.2.1.2. Primary Drainage Algorithm 33
5.2.2. Waterflooding (Imbibition) 34
5.2.2.1. Snap – Off 34
5.2.2.2. Piston – Like Advance 34
5.2.2.3. Pore Body Filling 35
5.2.2.4. Waterflooding Algorithm 36
5.2.3. Calculation of Flow Properties 36
5.2.3.1. Phase Area Calculation 36
5.2.3.2. Conductance Calculation 38
5.2.3.3. Saturation Calculation 39
5.2.3.4. Relative Permeability Calculation 39
6. RESULTS AND DISCUSSION 41
6.1. Base Model 41
6.1.1. Saturation Distribution 47
6.1.2. Sensitivity Analysis 48
6.1.2.1. Wettability Analysis 48
6.1.2.2. Effects of Wettability on Imbibition Mechanisms 51
6.1.2.3. Pore Morphology Analysis 52
6.2. Pore Network Model for Vuggy Carbonates 57
7. CONCLUSIONS 62
8. RECOMMENDATIONS 64

REFERENCES 65
APPENDICES
A. Matlab Code for Pore Network Construction 74
B. Code For Primary Drainage 84
B.1. Flow in Primary Drainage 84
B.2. Threshold Pressure Calculation 88
B.3. Conductance Calculation 88
C. Code For Imbibition 90
C.1. Flow in Imbibition 90
C.2. Threshold Pressure Calculation 94
C.3. Threshold Pressure Calculation for Mechanism Type 96
C.3.1. Snap – Off 96
C.3.2. Piston Like Advance 97
C.3.3. Pore Body Filling 99
C.4. Conductance Calculation for Imbibition 100

LIST OF TABLES

TABLES

Table 1 Lucia Classification 10
Table 2 Parameters in Weibull Distribution and Contact Angle Ranges 29
Table 3 Radius Ranges for Elements 31
Table 4 Model Properties for Valvatne (2004) and This Study 44
Table 5 Model Properties for Base Model and Bekri et al. (2004) 45
Table 6 Advancing Angle Ranges for Sensitivity Analysis 49
Table 7 Residual Phase Saturations for Wettability Cases 50
Table 8 Radius Ranges for Sensitivity Analysis 53
Table 9 Vug Size Ranges 57
Table 10 Advancing Angle Ranges for Vuggy Base Model 60

LIST OF FIGURES

FIGURES

Figure 1 World Distribution of Carbonate Reservoirs (SLB, 2008) 6
Figure 2 Choquette and Pray Classification Porosity Types (Moore, 2001).... .9
Figure 3 Choquette and Pray Classification Modifying Terms (Moore, 2001) .9
Figure 4 Revised Lucia Classification Interparticle Pore Space
(Moore, 2001)..... 11
Figure 5 Revised Lucia Classification Vuggy Pore Space (Moore, 2001) 11
Figure 6 Pore Shapes used in Pore Network Models 16
Figure 7 Snap – Off Mechanism (Arc menisci moves into the center)..... 21
Figure 8 Snap – Off Mechanisms (Valvatne, 2004)..... 22
Figure 9 Piston – Like Advance 23
Figure 10 Piston – Like Advance (Modified from Valvatne, 2004) 23
Figure 11 Pore – Body Filling Mechanism 25
Figure 12 Pores and Throats..... 29
Figure 13 Fissure with Variable Size 30
Figure 14 Distribution of Sub Domains 31
Figure 15 Pore Size Distribution..... 31
Figure 16 Phase Area Distribution within Elements..... 37
Figure 17 Phase Area Distribution with Non – Wetting Phase Layer..... 37
Figure 18 Capillary Pressure Curves for Drainage and Imbibition..... 41
Figure 19 Relative Permeability Curves (Drainage) 42
Figure 20 Relative Permeability Curves (Imbibition)..... 42
Figure 21 Comparison of Capillary Pressure Curves with Valvatne (2004) A
(Primary Drainage)..... 44
Figure 22 Comparison of Relative Permeability Curves with
Valvatne (2004) B (Primary Drainage)..... 44
Figure 23 Comparison of Capillary Pressure Curves with
Bekri et al. (2004) (Imbibition)..... 45

Figure 24 Comparison of Relative Permeability Curves with Bekri et al. (2004) (Imbibition) 46
Figure 25 Oil Saturation Distribution (At the end of drainage) 47
Figure 26 Water Saturation Distribution (At the end of imbibition)..... 48
Figure 27 Relative Permeability Curves for Wettability Analysis (Primary Drainage)..... 50
Figure 28 Relative Permeability Curves for Wettability Analysis (Waterflooding) 50
Figure 29 Preference of Imbibition Mechanisms for Different Wettability Conditions 51
Figure 30 Preference of I_n Mechanisms 52
Figure 31 Relative Permeability Curves for Large Sized Element (Primary Drainage)..... 54
Figure 32 Relative Permeability Curves for Large Sized Elements (Waterflooding) 54
Figure 33 Relative Permeability Curves for Small Sized Elements (Primary Drainage)..... 56
Figure 34 Relative Permeability Curves for Small Sized Elements (Waterflooding) 56
Figure 35 Capillary Pressure Curves for Base Model and Matrix (Drainage) . 58
Figure 36 Relative Permeability Curves for Vuggy Base Model (Drainage) .. 58
Figure 37 Relative Permeability Curves for Vuggy Base Model (Waterflooding) 59
Figure 38 Relative Permeability Curves for Vuggy Base Model (Wettability Analysis for Drainage) 60
Figure 39 Relative Permeability Curves for Vuggy Base Model (Wettability Analysis for Waterflooding) 61

NOMENCLATURE

A	Area, L^2
a	Random number
b_{pin}	Length of water-wet corner, L
D	Threshold pressure function
f	Boundary condition parameter
F	Threshold pressure function
g	Conductance, L^4
G	Dimensionless shape factor
k_r	Relative permeability
n	Number of invaded neighbor elements
n_c	Number of corners
Num	Total number of elements
P_c	Capillary pressure, m/Lt^2
P_{c_max}	Maximum capillary pressure during primary drainage, m/Lt^2
r	Radius of curvature, L
R	Radius, L
R_n	Mean radius of curvature, L
S_w	Water saturation, fraction
S_o	Oil saturation, fraction
x	Random number

Greek Letters

α	Corner half angle, radians
β	Angle, radians
γ	Weibull distribution function parameter
δ	Weibull distribution function parameter
θ	Contact angle, radians

θ_{max}	Maximum contact angle for spontaneous imbibition, radians
μ	Viscosity, m/Lt
σ	Interfacial tension, m/t^2
φ_1	Conductance function parameter
φ_2	Conductance function parameter
φ_3	Conductance function parameter
Ω	Effective perimeter, L

Subscripts

a	Advancing
advancing	Advancing
c	Corner
center	Center
corner	Corner
eff	Effective
ins	Inscribed
Max	Maximum
Min	Minimum
nw	Non-wetting phase
o	Oil
p	Phase Type (nw or w)
r	Receeding
receeding	Receeding
t	Total (for element)
T	Total (for model)
w	Wetting phase

CHAPTER 1

INTRODUCTION

Studies in reservoir modeling and oil recovery estimation require accurate prediction of rock and fluid properties, and a good understanding of flow mechanisms. Properties like relative permeability and wettability have significant influence on oil recovery and they should be predicted as close to reality as possible (Honarpour and Mahmood, 1986). Moreover, identification of flow mechanisms is essential since probable phase entrapments can be determined by understanding flow in porous media.

Relative permeability curves are generally obtained by steady or unsteady state experimental methods. Although steady state methods yield accurate and reliable results, they are time consuming. On the other hand, unsteady state methods are less time consuming but resulting uncertainties and have operational constraints like capillary end effects or viscous fingering (Honarpour and Mahmood, 1986). Moreover, effects of wettability cannot be clearly identified by using experimental techniques. Thus, in order to obtain relative permeability curves and investigate effects of wettability, pore network models and pore scale modeling studies are conducted. Pore network modeling is an effective tool in determination of relative permeabilities in cases where experimental methods are not sufficient and successful or heterogeneity in porous media is high.

In early pore scale studies, porous media was represented by sphere packs or bundle of tubes. Fatt (1956) initiated use of pore network models by proposing a new model for porous media by combining sphere pack and bundle of tubes approaches. Later on, studies for homogeneous and isotropic porous media were

conducted by using pore networks and flow mechanisms were simulated (Dullien et al., 1976). After implementation of invasion-percolation theory into pore scale modeling (Larson et al., 1981; Wilkinson and Willemsen, 1983) and enhances in pore space extraction methods, it became possible to obtain relative permeability and capillary pressure curves similar to the experimental results (Heiba et al., 1983; Oren et al, 1997; Blunt, 1997).

In pore scale studies, it is essential to represent porous media accurately. By using topologically equivalent pore network models, it is possible to obtain good matches with simulation and experimental results (Oren et al, 1997). During the last decade, studies in pore network modeling of sandstones increased. By using different pore size determination methods, like NMR (Kamath et al., 1998; Ioannidis and Chatzis, 2000; Moctezuma et al., 2003; Bekri et al., 2004), CT imaging (Piri, 2003), X-ray tomography, topologically equivalent pore space for sandstones can be constructed, since porous media is relatively homogeneous and simple. On the contrary, carbonates have complex and heterogeneous pore space due to secondary porosity features like vugs, fissures and fractures. Representation of the complicated flow behavior and determination of wettability effects within the complex porous media of carbonate rocks, are relatively hard and require additional techniques (Blunt, 2001). Conventional experimental methods are inadequate to determine flow properties and to yield precise pore size distribution of heterogeneous carbonates. Thus, studies in pore network modeling of carbonates are conducted for granular type carbonates (Valvatne, 2004; Nguyen et al., 2005). As for heterogeneous vuggy carbonates, pore network modeling is recently initiated (Kamath et al., 1998; Ioannidis and Chatzis, 2000; Moctezuma et al., 2003; Bekri et al., 2004; Bekri et al., 2005) and for fractures and fissured carbonates, studies are limited (Hughes and Blunt, 2001; Wilson-Lopez and Rodriguez, 2004).

In this study, a pore network model is constructed for simulating two-phase flow in fissured and vuggy carbonates. In Chapter 2, a literature review on pore structure of carbonate rocks is provided. In Chapter 3, pore network modeling and

flow mechanisms are introduced. The statement of the problem will be presented and methodology part will follow in Chapter 4 and 5 respectively. Results and discussion are presented in Chapter 6 and conclusion will be given in Chapter 7.

CHAPTER 2

LITERATURE REVIEW

Pore scale modeling is an effective method in determination of wettability effects on relative permeability and capillary pressure curves. By using topologically equivalent representation of porous media, flow properties can be predicted accurately.

Representing porous media and simulating single and multiphase flow at pore scale are technologically enhancing study areas. During the early stages of network modeling, sphere of packs and bundle of tubes approaches were used to represent porous media. Initially, sphere packs were implemented in flow modeling studies and it was concluded that complex pore geometry in sphere packs prevented the derivation of flow properties (Fatt, 1956). In bundle of tubes approach, flow in porous media could be successfully described by relatively simple mathematical expressions whereas representation of real porous media might not be accurate. Moreover, bundle of tubes approach was not capable for elucidating capillary hysteresis and existence of residual saturation wetting or non-wetting phase saturation (Fatt, 1956; Dullien, 1992). Thus, in order to determine flow properties and understand flow mechanisms and wettability effects, Fatt (1956) demonstrated a pioneering approach where use of tube networks combined with pre-used methods, successfully represented flow properties.

In this study, a pore network model for fissured and vuggy carbonates is developed. Since carbonate reservoirs contain more than 60% of world remaining

oil in place and 40% of the world gas reserves (SLB, 2008), it is essential to understand flow mechanisms and wettability effects in carbonate rocks.

2.1 Carbonate Reservoirs

Carbonates are sedimentary rocks deposited in marine environments. Biological in origin, carbonates are composed of fragments of marine organisms, skeletons, coral, algae and precipitated mostly calcium carbonate. They are chemically active and easily altered. The deposition area directly affects the heterogeneity of carbonate grains. Once carbonate rock is formed, a range of chemical and physical processes begins to alter the rock structure changing fundamental characteristics such as porosity and permeability.

At deposition, carbonate sediments often have very high porosities (35%–75%) but this decreases sharply as the sediment is altered and buried to reservoir depths. As a result, carbonate reservoirs exhibit abrupt variations in rock type distribution (SLB, 2008). Thus, a complex porous media and heterogeneous pore network are present within carbonate rocks and carbonate reservoirs are generally characterized by extreme heterogeneity of porosity and permeability. They can be massive, vuggy and fractured in the organic reef facies or highly stratified, often vertically discontinuous in the back reef and shoal facies (Jardine et al., 1977). Contrary to sandstones, carbonate reservoirs are generally mixed – wet or oil – wet (SLB, 2008).

As mentioned before, most of the hydrocarbon reserves are in carbonate reservoirs. For example, Middle East has 62% of the world proved oil reserves and 70% of these reserves are in carbonate reservoirs. Also, 40% of world's proven gas reserves are in Middle East and 90% of them are again in carbonate reservoirs (SLB, 2008) and world distribution of carbonate reservoirs is illustrated (Figure 1).

Despite the difficulties in characterizing and identifying, it is essential to understand flow behavior in carbonate reservoir in order to forecasting production accurately.

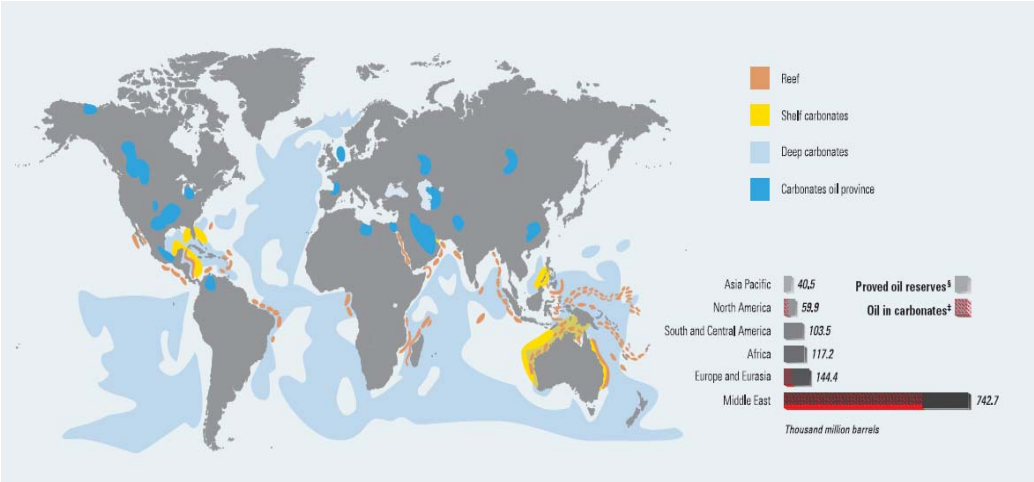

Figure 1- World Distribution of Carbonate Reservoirs (SLB, 2008)

2.2 Pore Structure of Carbonates

2.2.1. Porosity Types in Carbonates

Several mechanisms influence porosity evolution and pore-size distribution in carbonate rocks. Mainly, there are two types of porosity; primary interparticle and secondary. Primary interparticle porosity is formed by deposition of calcareous sand or gravel under the influence of strong currents or waves or by local production of calcareous sand-size particles with sufficient rapidity to deposit particle on particle with little or no interstitial mud. Secondary porosity is formed by dissolution of interstitial mud in calcareous sand and the result is microvuggy porosity resembling inter particle pore space.

2.2.1.1. Primary Porosity

Primary porosity includes pore types which result from depositional processes and which have been modified slightly by compaction, pressure solution, and simple pore filling cement, or dissolution alteration.

According to Murray (1960), primary porosity is originated from framework, mud and sands. Framework material could be organic or inorganic and commonly composed of tightly interlocking crystals of calcite or aragonite. Mud consists of particles that are chemically or biochemically precipitated fine crystals or finely comminuted debris of larger particles. In addition, carbonates can be deposited as sands, which are generally deposited under conditions of sufficiently rapid water movement either to remove the finer particles or to transport and selectively deposit larger particles.

Primary pore types can be destroyed; porosity and pore size may be reduced either by cementation or by cementation in conjunction with replacement. Commonly observed cementing materials are calcite, anhydrite, and quartz. Calcite cement appears to be especially common where the particles are monocrystalline (Moore, 2001).

2.2.1.2. Secondary Porosity

Secondary porosity in carbonates is composed of different features like vugs, fractures and fissures. As mentioned before, in early stages of diagenesis, carbonates are composed of framework material and during diagenesis vugs are formed generally within the framework. Fracture and fissures may be formed by post depositional processes. Their geometry and intensity are dependent on several factors like geomechanical and lithological properties (Peacock and Mann, 2005).

Secondary vugs are void spaces formed by post-depositional processes. Vugs are larger than the simple fitting together of associated mutually interfering crystals or deposited particles. Several mechanisms involve in formation of vugs; replacement of anhydrite, carbonate dissolution, replacement of dolomite and fracturing (Mazullo, 2004).

Fractures have an important role in porosity of carbonate rocks. The style, geometry and distribution of fractures can be controlled by various factors; such as, rock characteristics and diagenesis (lithology, sedimentary structures, bed thickness, mechanical stratigraphy, the mechanics of bedding planes); structural geology (tectonic setting, paleostresses, subsidence and uplift history, proximity to faults, position in a fold, timing of structural events, mineralization, the angle between bedding and fractures); and present-day factors; such as, orientations of in situ stresses, fluid pressure, perturbation of in situ stresses and depth (Peacock and Mann, 2005). Furthermore, lithological competence can control the geometry and distribution of fractures, with more fractures tending to occur in more brittle beds. Sedimentary structure can be considered as weakness points and fractures can initiate at such anisotropies as bedding plane irregularities and fossils. Moreover, bed thickness affects spacing of joint sets within a bed. It is commonly approximately proportional to bed thickness, with joint frequencies tending to be higher in thinner beds than in thicker beds. Also, mechanical behavior of the bedding planes can control fracture propagation and mechanical stratigraphy (Peacock and Mann, 2005).

2.2.2. Porosity Classification of Carbonate Rocks

Porosity classification of carbonate rocks is different and more difficult than the classification in siliciclastic rocks. Since carbonates are composed of fragmental or non-fragmental particles, micrite or sparry calcite cements and may involve fractures, vugs or fissures; their porosity classification requires additional care. Thus, many carbonate sedimentologists propose different porosity classification

methods, generally based on rock fabric, petrophysical properties, modifying terms and timing.

The pore types can be generally classified as intergrain/intercrystal, moldic/intrafossil/shelter and cavernous/fracture/solution enlarged fracture. This general classification was further divided according to visibility and rock fabric related to petrophysical properties by Archie (1952), rock fabric and petrophysical properties by Lucia (1983) (further improvements in 1995 and 1999) and fabric selectivity by Choquette and Pray (1970).

Choquette and Pray (1970) classified basic porosity types according to fabric selectivity and modifying terms (genetic, size and abundance) (Figures 2 and 3). It can be implied that the porosity is mainly based on fabric selectivity and modifying terms. Solid and diagenetic components are defined as fabric. In case of a relationship between fabric components and porosity, the pore type would be fabric selective; otherwise, it would be considered as not fabric selective type. Fabric selectivity mainly depends on the configuration of pore boundary and the position of the pore relative to fabric (Choquette and Pray, 1970).

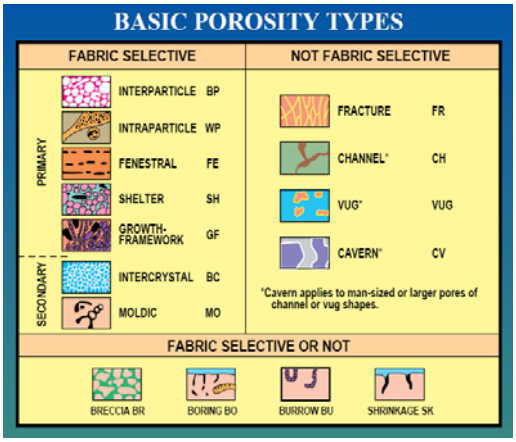

Figure 2- Choquette and Pray Classification Porosity Types (Moore, 2001)

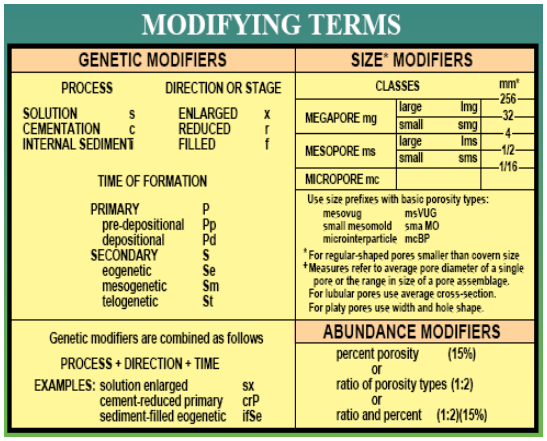

Figure 3- Choquette and Pray Classification Modifying Terms (Moore, 2001)

For primary porosity (syndepositional porosity), fabric selectivity is totally determined by fabric components; where as in secondary porosity, which is formed after final deposition, fabric selectivity depends on the diagenetic history. Moreover, Choquette and Pray generated their classification also on genetic and size modifiers. Genetic modifiers are used for giving more detailed information about the evolution of porosity and size modifiers are used for expressing the size of the pores.

Another commonly used porosity classification is proposed by Lucia (1983), which is based on petrophysical properties. According to Lucia, the pore space in carbonate rocks is divided into two major parts; (1) interparticle pore space and (2) vuggy pore space. Interparticle porosity is subdivided according to particle size and vuggy porosity according to connectivity of the vuggy space (Table 1).

Table 1- Lucia Classification (Lucia, 1983)

Interparticle			Vuggy	
Particle Size			Connection	
Fine	Medium	Large	Through Interparticle Pores	Through Other
< 20 µ	20 - 100 µ	> 100 µ	Separate	Vugs Touching

It can be stated that Lucia's classification mainly depends on fabric and petrophysical properties of the rock. Lucia (1995) proposed a revised form of his classification, where interparticle porosity is classified according to dominant fabric type and vuggy porosity according to again connectivity of the pores and dominant fabric type (Figures 4 and 5). In this revised classification, Lucia mainly followed Dunham's (1962) carbonate rock classification for interparticle pore space; but he further divided the classification according to dominant matrix type and based on size, sorting of grains and crystals. Vuggy pore space was divided into two; separate vug pores and touching vug pores. Separate vug pores are interconnected only through interparticle porosity and either within particles or

significantly larger than particle size (Lucia, 1999). They are typically fabric selective in origin and presence of separate vug porosity increases total porosity but not significantly permeability (Moore, 2001). Touching vug pores, which are non-fabric selective in origin, are significantly larger than particle size and form an interconnected pore system (Lucia, 1999). According to Lucia, fracture porosity should be considered as touching vug pore since fracture porosity affects permeability in carbonate reservoirs.

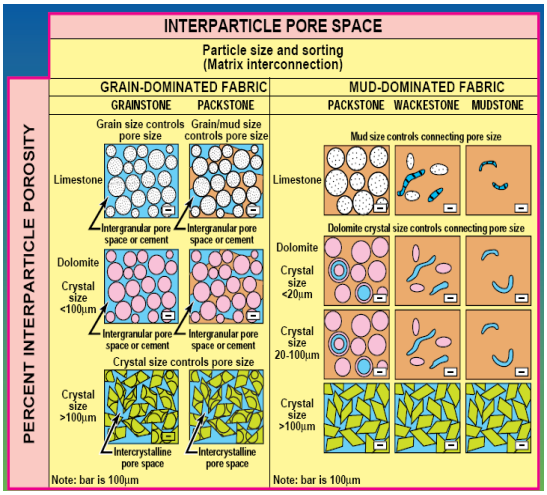

Figure 4- Revised Lucia Classification Interparticle Pore Space (Moore, 2001)

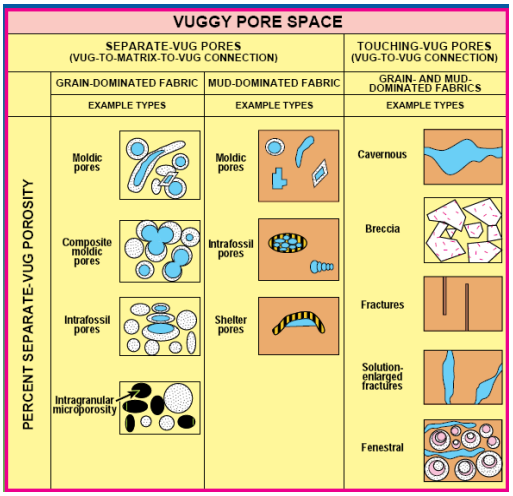

Figure 5- Revised Lucia Classification Vuggy Pore Space (Moore, 2001)

2.2.3. Pore Network Modeling Studies for Carbonates

Pore scale studies for carbonates are more complex because of secondary porosity features like fractures, fissures and vugs, and initiated recently compared to advanced network studies conducted for sandstones. For relatively homogeneous intergranular carbonates, Valvatne (2004) obtained fairly good results for primary drainage capillary pressure curves. In his study, experimental capillary pressure curves of two peloidal grainstone samples were compared to pore network derived capillary pressures. Kamath et al. (1998) developed an uncorrelated pore network model for vugular rocks and obtained poor results for relative permeability curves.

Ioannidis and Chatzis (2000) proposed a dual network model for representation of pore structure for vuggy carbonates. They constructed a dual porosity network model by combining X-ray and CT analysis results. Vugs were superimposed on matrix blocks in an agreement with porosity distribution of the sample.

Moctezuma et al. (2003) constructed a dual network model, composed of matrix, vugs and fractures combining vugs, for a vuggy carbonate. The equivalent pore network model was developed by combining mercury invasion data and NMR measurements. Bekri and Laroche (2004) extended Moctezuma's study to investigate wettability effects on vuggy carbonates and, calculate transport and electrical properties (2005). By constructing a 3-D pore network model, capillary pressure and relative permeability curves were determined which were in agreement with the experimental data. Okabe (2004) and Al-Kharusi (2007) extracted pore space from CT images for carbonates and developed a pore scale simulator for determining flow properties.

As for fractures, microfractures and fissures, Hughes and Blunt (2001) simulated multiphase flow in a single fracture represented by square lattices connected by throats and extended this study to investigate matrix/fracture transfer (2001). For modeling two-phase flow in microfractured porous media, a network model composed of pores, without throats, with variable cross sections was used by Wilson-Lopez and Rodriguez (2004). A recent study is conducted by Erzeybek and Akın (2008) for modeling two – phase flow in fissured and vuggy carbonates. Both fissures and vugs are implemented into pore network and various properties like wettability and pore morphology are examined.

2.3 Advanced Studies in Pore Network Modeling

Technological improvements in computer science and advanced imaging tools like CT and SEM yield enhancements in pore scale modeling. Pore scale studies can be coupled with neural networks to simulate flow in porous media (Karaman, 2002). In addition, use of pore network models is extended to other research areas

such as modeling miscible CO_2 flooding (Uzun, 2005) and flow of Non-Newtonian fluids or NAPLs. In hydrology, pore scale modeling can be used for identification of NAPL behavior within the porous media. Non-Newtonian fluids used in petroleum industry are polymeric solutions with shear-thinning behavior, unlike Newtonian fluids which are conventionally found in reservoirs. Since it is hard to determine relative permeability and capillary pressure curves of NAPLs and Non-Newtonian fluids by experiments, pore network modeling studies can be used for obtaining flow properties for those kinds of fluids.

Jia et al. (1999) conducted visualization experiments and numerical simulations in pore networks for understanding basic aspects of mass transfer during the solubilization of residual non-aqueous phase liquids NAPL. Moreover, Al-Futaisi and Patzek (2004) studied spontaneous and forced secondary imbibition of NAPL invaded sediment by using a 3-D uncorrelated pore network model of a mixed-wet soil.

For simulating Non-Newtonian flow in porous media, studies are recently conducted (Lopez et al., 2003; Balhoff, 2005; Sochi, 2007). Lopez et al. (2003) studied the flow of power law fluids in porous media at pore scale. By using an accurate representation of pore space and bulk rheology (variation of viscosity with shear rate), a relationship between pressure drop and average flow velocity in each pore was defined. They predicted the experimental results successfully but their study was limited to simple shear-thinning fluids. Balhoff (2005) reported pore scale modeling of Non-Newtonian fluids. He used an unconsolidated porous media to simulate flow of polymers and suspensions. He predicted flow properties for steady state flows. Also, viscous fingering patterns of Non-Newtonian fluids were examined during transient displacement.

Sochi (2007) constructed a topologically disordered pore network model and simulated flow of Non-Newtonian fluids. Pressure field was obtained iteratively and volumetric flow rate and apparent viscosity values were determined. Moreover, time-independent category of the non-Newtonian fluids is investigated

using two time-independent fluid models and a comparison between the model and the experimental results was carried out. The yield-stress phenomenon was also investigated and several numerical algorithms were developed and implemented to predict threshold yield pressure of the network.

Apart from the studies conducted for Non-Newtonian fluid and NAPLs, pore scale modeling is used for construction of sedimentary rocks and mechanical properties (Bakke and Oren, 1997; Jin and Patzek, 2003). Bakke and Oren (1997) developed a pore network model by simulating the main sandstone forming geological processes. They successfully modeled sand grain sedimentation, cementation and diagenesis by using the input data gathered from thin section analysis and obtained a topologically equivalent representation of porous media.

Jin and Patzek (2003) developed a depositional model by constructing geometrical structure and mechanical properties of sedimentary rocks. They obtained two and three-dimensional porous media for unconsolidated sand and sandstones. At pore scale, they simulated the dynamic geologic processes of grain sedimentation, compaction and diagenetic rock transformations and obtained mechanical properties. Moreover, the depositional model was used for studying initiation, growth and coalescence of micro-cracks.

Pore network modeling can also be used for modeling advanced processes such as in-situ combustion (Lu and Yortsos, 2001) or coal structure modeling (Tomeczek and Mlonka, 1998). Lu and Yortsos (2001) used a pore network model composed of pores and solid sites, for modeling the effect of the microstructure on combustion processes in porous media. In the model, flow and transport of the gas phase occurred in the pore space with convection, whereas heat transfer occurred in solid phase by conduction. Tomeczek and Mlonka (1998) represented coal with both cylindrical and non-cylindrical pores. By using the experimental porosity, they concluded that not only cylindrical pores but also non-cylindrical, spherical pores contributed. They modified a previously developed random pore model by implementing spherical vesicles.

CHAPTER 3

PORE NETWORK MODELING

3.1. Pore Morphology

In early pore network studies, porous media is described by pores and throats that have circular cross sections or by spheres (Blunt and King, 1992). Applying flow equations and solving mathematical expressions for simple circular cross sections are relatively less time consuming. In circular pores, only one phase can be present and thus, effects of wettability cannot be determined accurately. Moreover, circular cross section does not reflect the real porous space. Therefore, different types of pores are needed in pore networks. That's why pore types with equilateral or irregular triangular, square and star shaped cross sections are generally used for description of porous media (Figure 6) (Oren et al., 1997; Blunt, 1997; Radke et al., 1992; Hui and Blunt, 2000; Valvatne and Blunt, 2003; Patzek, 2000). In recent studies (Patzek and Silin, 2001; Piri and Blunt, 2005), porous media is represented by combination of triangular, circular or square cross-sections.

Blunt and King (1992) simulated two phase flow at pore scale by constructing a pore network consisted of pores and throats with spherical geometry. Oren et al. (1997) described pore space by cylindrical shapes with different dimensionless shape factors. By assigning various shape factors, irregular porous media was represented by topologically equivalent irregular triangles. Thus, irregularity in real porous media was reflected and effects of wettability could be observed.

Radke et al. (1992) investigated wettability effects and oil film formation at pore scale. In their study, they described porous media by star shaped pores for representing the rough surface of real pore space instead of representing it by ideal circular shapes. More recently, Blunt (1997) defined pores and throats by squares, enabling residual wetting phase saturation and oil layering. Fenwick and Blunt (1998) described pores by using equilateral triangles in order to simulate three-phase flow in porous media. By assigning equilateral triangular pores, they observed effects of wettability. Investigation of formation and presence of oil layers yield explanation for oil layer drainage and residual water/oil saturation.

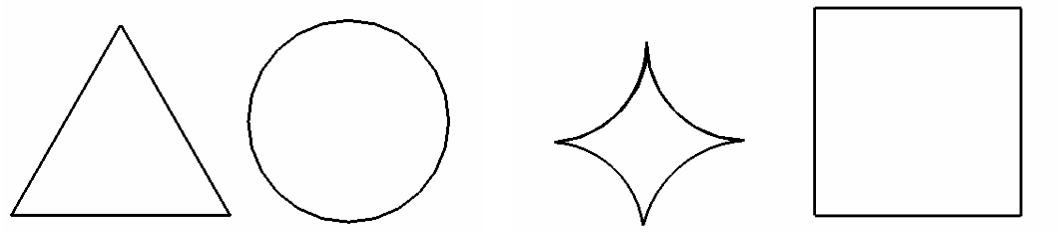

Figure 6- Pore Shapes used in Pore Network Models

3.2 Network Type

3.2.1. Network Dimension

In early pore network studies, 2-D networks were used (Fatt, 1956; Dodds and Lloyd, 1971). Recent advances in computers enabled the use of 3-D networks and pore networks became more popular (Blunt and King, 1992; Nilsen et al., 1996).

Fatt (1956) successfully represented flow properties by using different 2-D tube networks (square, single hexagonal, double hexagonal and triple hexagonal shapes). Dodds and Lloyd (1971) represented porous media by constructing a regular 2-D network of capillary tubes with variable sizes. Blunt and King (1992) simulated two-phase flow in a 3-D pore network model with spherical nodes. Nilsen et al. (1996) successfully reconstructed 3-D porous media of a sandstone

sample reconstructed by using thin section analysis and numerical modeling of main geological processes.

3.2.2. Flow Behavior

In pore scale studies, mainly two types of model are used: quasi-static and dynamic. Quasi-static models involve use of invasion percolation process and capillary forces are dominant. On the other hand, dynamic models require an input flow rate and both capillary and dynamic forces are considered.

3.2.2.1. Quasi-Static Network Models

Fluid flow is dominated either by capillary or viscous forces alone or both. In quasi-static flow, capillary force is the driving force. Thus effects of dynamic aspects are neglected. Final static position of fluid interfaces and configurations are determined in quasi-static networks. Interfacial forces are dominant since capillary number is small (Jia, 2005).

In quasi-static network modeling, invasion-percolation process is implemented for simulating flow in reconstructed porous media. Invasion-percolation process is based on percolation theory (Wilkinson and Willemsen, 1983). Initially, percolation theory is used for describing morphology, conductivity and flow at pore scale (Larson et al., 1981). Percolation process is defined by the fluid flow path determined by the porous media, which is random (Larson et al., 1981). Later on, Wilkinson and Willemsen (1983) defined invasion-percolation describing dynamically flow processes by using constant rate rather than constant applied pressure at pore scale.

3.2.2.2. Dynamic Network Models

Dynamic network models can be used for investigating the effects of both interfacial and viscous forces. In this kind of network model, a certain flow rate is

imposed on network and pressure field is calculated iteratively. Configurations of elements are transiently determined. Since both interfacial and viscous forces are implemented in dynamic network models, the preference between viscous and interfacial forces depends on the capillary number. For low values of capillary number, interfacial forces are dominant whereas for higher values viscous forces are effective. Contrary to quasi-static ones, dynamic networks are not limited to low capillary numbers. Thus, effects of displacement rate on imbibition can be determined easily by using dynamic network models (Jia, 2005).

Dynamic network models are used for investigating flow rate and wettability effects on relative permeability and capillary pressure curves (Koplick and Lasseter, 1985; Dias and Payatakes, 1986a; Lenormand et al., 1988; Mogensen and Stenby, 1998; Hughes and Blunt, 2000; Nguyen et al., 2005). Koplick and Lasseter's (1985) study was the first of its kind where a dynamic model was developed for pore scale modeling. By assuming equal viscosities, 2-phase flow was simulated in porous media which was represented by spherical pores and cylindrical throats. Lenormand et al. (1988) constructed a dynamic model for simulating pore scale immiscible displacement by using a two dimensional porous media constructed by interconnected capillaries. In order to study the effects of viscous and capillary forces on relative permeability, Blunt and King (1992) developed 2-D and 3-D two-phase dynamic models.

Mogensen and Stenby (1998) constructed a 3-D dynamic pore network model for investigating imbibition processes. They observed the effects of contact angle, aspect ratio and capillary number on the competition between piston-like advance and snap-off mechanisms during imbibition. Hughes and Blunt (2000) also constructed a dynamic pore network to study the effects of flow rate and contact angle on relative permeability. They were successful at identifying displacement patterns throughout the imbibition process by varying capillary number, contact angle and initial wetting phase saturation. More recently, Nguyen et al. (2005) developed a dynamic pore network model representing flow in Berea sandstone. They investigated the effects of displacement rate and wettability on imbibition

relative permeability. They recognized the inhibiting effect of displacement rate on snap-off during imbibition.

3.2.3. Spatially Correlated and Uncorrelated Networks

In pore scale studies, there are two main methods used in characterization of porous media: tuning geometric parameters of a regular network model and modeling the random topology of pore space directly. In the first method, a regular network model, which is spatially correlated, is used and corresponding geometric parameters are tuned to match experimental data. Although this method yields more accurate results than simple correlations, predictions are still poor. In the second method, porous media is directly constructed by using only pore size distribution data gathered from thin section analysis. Then, sedimentation and compaction are simulated and a random pore network is obtained. This approach results accurate prediction for sedimentary structures but statistical methods are required for carbonate rocks (Blunt, 2001). In reconstructed pore networks, spatial correlation and connectivity are directly incorporated in the model (Blunt, 2001). Two approaches are mainly used in representing spatial correlation in porous media: short-range correlations like spherical, Gaussian and exponential structures and long-range correlations like fractal concepts (Mani and Mohanty, 1999).

Besides pore size distribution and pore – throat aspect ratio, spatial correlation has also an influence on flow properties. Mani and Mohanty (1999) studied the effects of spatial correlations on multiphase phase flow properties. They observed similar trends in primary drainage and imbibition characteristics for spatially uncorrelated and correlated porous media. Realization independent absolute permeability and capillary pressure curves were obtained. For spatial correlations represented by long-range correlations, realization dependent capillary pressure curves were reported. Also, effects of spatial correlation on primary drainage and imbibition capillary pressure curves were observed. In spatially correlated networks, primary drainage capillary pressure curves were more gradual with respect to the ones in uncorrelated networks. Moreover, higher wetting and non – wetting phase relative

permeability values were obtained during primary drainage as spatial correlation increased. As for imbibition, they reported increase in probability for snap – off and decrease in probability for piston – like advance in spatially correlated systems (detailed information about the processes is presented in Section 3.3).Thus, higher residual non – wetting phase saturation at the end of imbibition were observed as spatial correlation increased. Steeper imbibition capillary pressure curves were obtained for correlated networks with respect to uncorrelated ones (Mani and Mohanty, 1999).

Pore networks are generally assumed to be spatially uncorrelated but it is reported that spatial correlation yields more accurate results with limited predictive capabilities. Thus, Knackstedt et al. (2001) introduced correlated heterogeneity and investigated its effects on two – phase flow properties. They reported significant effect of small-scale correlations on the structure of fluid clusters at breakthrough and at the residual saturation. Also, lower residual phase saturations were observed in correlated heterogeneous pore networks than in the random ones. They concluded that correlated heterogeneity has a strong influence on the final configuration of trapped fluid clusters.

3.3 Flow Mechanisms

In porous media, fluid flow occurs by different mechanisms mainly; snap-off, piston-like advance and pore-body filling. In primary drainage, the elements are assumed to be filled by piston-like advance. On the other hand, during imbibition (for example waterflooding) process, the competition between the flow mechanisms is considered. The detailed descriptions for the mechanisms are provided respectively.

3.3.1. Snap – Off

Snap-off is the invasion by wetting-phase arc menisci present in the corners of an element. The arc menisci displaces the non-wetting phase present in the center

unless piston-like or pore-body filling mechanisms are not favored. Snap–off mechanism is illustrated in Figure 7. During imbibition, initially occurrence of snap-off is controlled. If Roof's criterion is satisfied (Equation 1), the element is assumed to be filled by snap-off (Jia, 2005). Otherwise, the other mechanisms are controlled.

$$\frac{R_{ins}}{R_{throat}} > 3 \qquad (1)$$

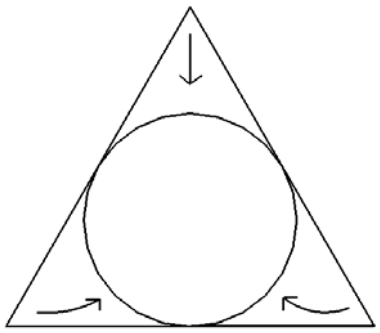

Figure 7 – Snap - Off Mechanism (Arc menisci moves into the center)

Snap-off can occur either spontaneously or in a forced manner (if the oil/ water contact is pinned) (Figure 8). The preference between spontaneous and forced snap-off mechanisms depends on corner half angle and receeding angle values. If the receeding angle value is smaller than the difference between $\pi/2$ and corner half angle, snap-off is spontaneous. Otherwise, snap-off is assumed to be forced with a pinned oil/water contact. The corresponding threshold pressure values are calculated by using the following formulae (Oren et al., 1997).

Spontaneous Snap-Off: $\theta < \frac{\pi}{2} - \alpha$

$$P_c = \frac{\sigma(\cos\theta - 2\sin\theta)}{2R\cot\alpha} \qquad (2)$$

Forced Snap-Off: $\theta > \frac{\pi}{2} - \alpha$

$$P_c = \begin{Bmatrix} \frac{\sigma(\cos\theta - 2\sin\theta)}{2R\cot\alpha}, & \theta \le \pi - \alpha \\ \frac{P_{c\_max}(\cos(\theta_a + \alpha))}{\cos(\theta_r + \alpha)}, & \theta > \pi - \alpha \end{Bmatrix} \quad (3)$$

In case of $\theta = \pi/2 - \alpha$, the element is assumed to be completely filled by wetting phase (Oren and Bakke, 1997).

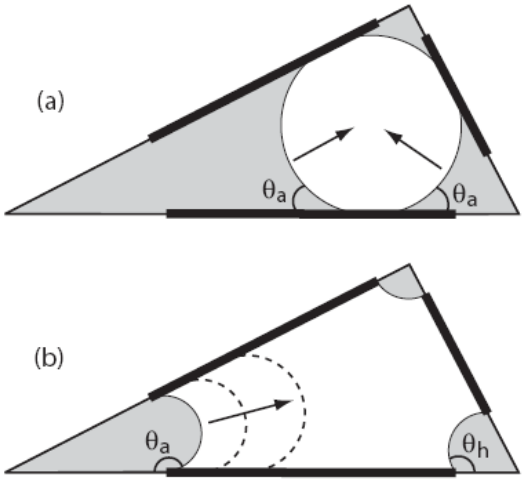

Figure 8 – Snap – Off Mechanisms (θ_a: Advancing Angle, θ_h: Hinging Angle): a) Spontaneous Snap – Off, b) Forced Snap – Off (Valvatne, 2004)

3.3.2. Piston – Like Advance

During piston-like advance filling, non-wetting phase is displaced by an invading interface located in an adjoining invaded element (Oren et al., 1997). An element can be invaded either spontaneously ($\theta \le \pi/2 + \alpha$) or forced ($\theta > \pi/2 + \alpha$) piston like advance mechanism (Figures 9 and 10). Imbibition type and presence of non – wetting phase layers depend on maximum contact angle (θ_{max}) reached (Equation 4) at the end of primary drainage. During imbibition, hinging angle (θ_h) varies

between receeding and advancing angles. As hinging angle reaches advancing angle, the pinned contact will move towards the center.

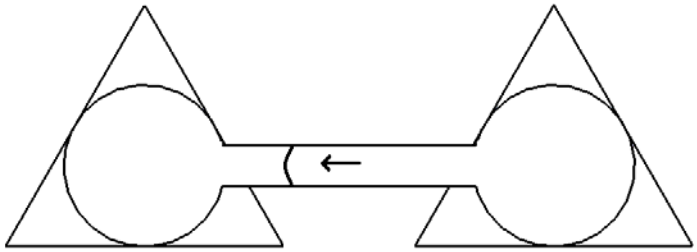

Figure 9 – Piston - Like Advance
(Displacement by an invading interface located in an adjoining invaded element)

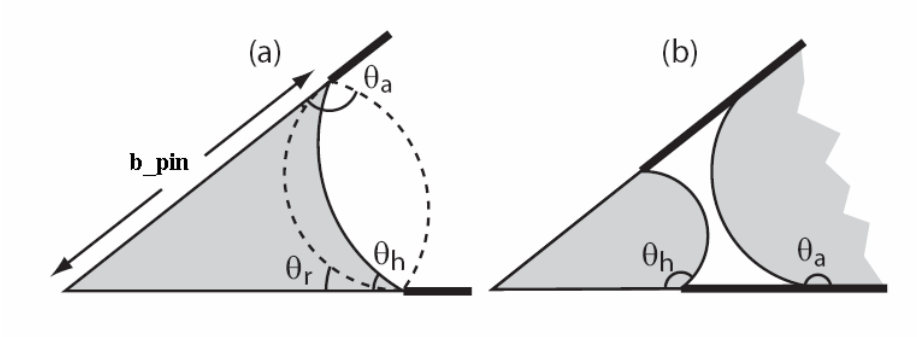

Figure 10 – Piston – Like Advance: a) Hinging Oil/ Water Contact;
b) Sandwiched Oil Layer (Modified from Valvatne, 2004)

In the presence of oil layers, wetting phase saturation and conductance will have two components: triangle corners and center of the element (Hui and Blunt, 2000). Moreover, since non-wetting is squeezed between the wetting phases present in the element, non-wetting phase conductance is calculated by using the thickness of the oil film.

In spontaneous imbibition, capillary pressure will be positive and entrance pressure calculation depends on a maximum advancing angle. On the other hand, negative capillary pressure will be obtained if forced imbibition occurs and oil films may be created.

$$\theta_{max} = \cos^{-1}\left(-\frac{\sin(\alpha+\theta_r)\sin\alpha}{\frac{RP_{c\_max}}{\sigma}\cos\alpha - \cos(\alpha+\theta_r)} \right) \quad (4)$$

During spontaneous imbibition, threshold capillary pressure is calculated by an iterative method by using Equations 5-8 (Hui and Blunt, 2000). Initially, r=R is assumed and β is calculated (Equation 8), then by using Equations 6 and 7, A_{eff} and Ω_{eff} are obtained in order to find P_c from Equation 5. Subsequently, r is evaluated by using Equation 5 and β is re-calculated. The rest of the procedure is straightforward and continues until P_c and r values converge.

$$P_c = \frac{\sigma\Omega_{eff}}{A_{eff}} = \frac{\sigma}{r} \quad (5)$$

$$A_{eff} = \frac{R^2}{2\tan\alpha} - \frac{rb_{pin}\sin(\alpha+\beta)}{2} + \frac{r^2\beta}{2} \quad (6)$$

$$\Omega_{eff} = \left(\frac{R}{\tan\alpha} - b_{pin} \right)\cos\theta + r\beta \quad (7)$$

$$r\sin\beta = b_{pin}\sin\alpha \quad (8)$$

During spontaneous imbibition, if $\theta > \theta_{max}$, negative capillary pressure is obtained (Equation 9) (Patzek, 2000).

$$P_c = \frac{2\sigma\cos\theta}{R} \quad (9)$$

In case of forced imbibition ($\theta > \pi/2 + \alpha$), oil films may be preserved if capillary pressure does not exceed the oil layer stability pressure (Equation 10) (Hui and Blunt, 2000). Threshold pressure is obtained by the same procedure used in primary drainage.

$$P_{stab} = \frac{\sigma\left(\cos\alpha\sin\alpha(2\sin\alpha+\cos\theta)+\sin^2\alpha\cdot\left(\sqrt{4\cos^2\alpha-3\cos^2\theta-4\sin\alpha\cos\theta}\right)\right)}{b_{pin}\left(3\sin^2\alpha+4\sin\alpha\cos\theta+\cos^2\theta\right)} \quad (10)$$

3.3.3. Pore – Body Filling

Pore body filling mechanism is similar to piston-like advance but more than one invaded neighbor elements are effective in filling. Wetting phase invades an element from previously invaded neighbor elements. In Figure 11, pore-body filling mechanism is illustrated. The number of neighbor elements effective during the filling process, n, determines the type of pore-body filling mechanism (I_2, I_3,.., I_n etc.) (Oren et al., 1997).

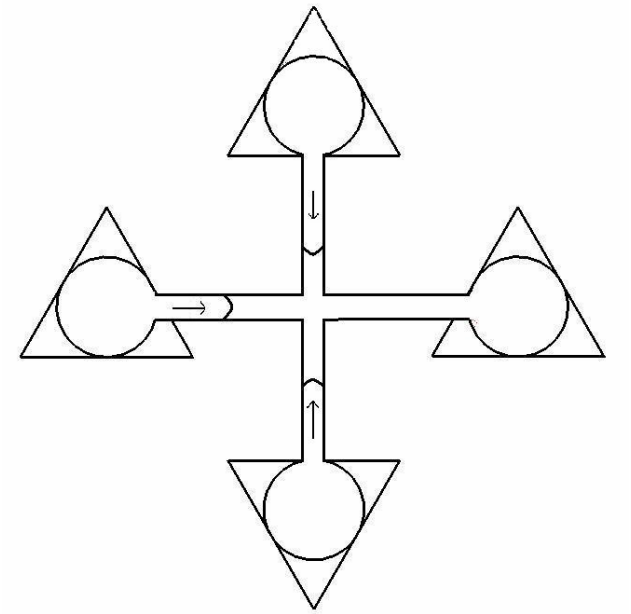

Figure 11 – Pore - Body Filling Mechanism

Like piston-like advance, pore-body filling type imbibition can be either spontaneous or forced. The preference between two mechanisms depends on maximum advancing angle, which is calculated by using Equation 4.

In spontaneous pore-body filling (in other words if $\theta \leq \theta_{max}$) threshold pressure of an element is a function of number of previously invaded neighbor elements and can be calculated by using the following equations (Oren et al., 1997, Patzek, 2000);

$$R_n = \frac{1}{\cos\theta}\left(R_{ins} + \sum_{i=1}^{n} a_i R_{ins\_i} x_i \right) \tag{11}$$

$$P_{c,n} = \frac{2\sigma}{R_n} \tag{12}$$

If only one of the neighbor elements is invaded (n=1), then the mechanism is similar to piston-like advance and threshold pressure is calculated by using the same procedure in piston-like advance. If imbibition is forced, then the threshold pressure is obtained by the same procedure for primary drainage with advancing angle.

CHAPTER 4

STATEMENT OF THE PROBLEM

Carbonates have relatively heterogeneous and complex porous media because of secondary porosity features like fractures, fissures and vugs. The heterogeneous structure of carbonate rocks results difficulties in identification of complex flow mechanisms and determination of flow properties. In pore scale studies topologically equivalent networks yield accurate representation of flow properties. However, it is challenging to represent heterogeneous carbonates accurately and implement a topologically equivalent pore network model for carbonate rocks. Besides its heterogeneous pore structure, carbonate rocks can be mixed wet, resulting heterogeneity also in wettability conditions. Due to their complex pore structure and wettability characteristics, pore scale studies for carbonate rocks are limited.

In this study, a novel pore network model that simulates two-phase flow in fissured and vuggy carbonates is developed. Secondary porosity features are assigned and flow properties within the complex porous media are predicted using this model. Capillary pressure and relative permeability curves for primary drainage and waterflooding mechanisms are obtained. Moreover, by assigning variable contact angle ranges, effects of wettability are observed and mixed wet conditions are simulated straightforwardly.

CHAPTER 5

METHODOLOGY

In this study, a 3-D novel pore network model is developed for simulating two-phase flow in fissured and vuggy carbonate rock. Initially matrix, which is composed of pore and throats, is constructed. The corresponding receeding and advancing angle values are assigned by using normal distribution within a given range for the corresponding wettability conditions. Following that, secondary porosity features (fissures and vugs) are assigned in the model. The elements are constructed for given size ranges, which are obtained from previously conducted thin section analysis and experimental results. Then, capillary pressure and relative permeability curves are obtained for primary drainage and waterflooding mechanisms.

5.1. Construction of Pore Network Model

5.1.1. Assigning Matrix Properties

Matrix is composed of equilateral triangular pores and square throats (Figure 12a-b). First, inscribed radius values are assigned for pores by using Weibull distribution (Equation 13) for given radius ranges (Hui and Blunt, 2000).

$$R_{ins} = \left(R_{Max} - R_{Min}\right)\left(-\delta \ln\left[x\left(1-e^{-1/\delta}\right)+e^{-1/\delta}\right]\right)^{1/\gamma} + R_{Min} \qquad (13)$$

Maximum and minimum radius values are obtained from previously conducted thin section analysis (Hatiboğlu, 2002). Parameters in Weibull distribution function, δ and γ, are chosen (Table 2). Secondly, throat radii are normally distributed by using mode and median of inscribed radius values. Thus, matrix becomes spatially correlated with a maximum coordination number of 6. Also, throat lengths are distributed after obtaining throat radii; by using the statistical properties for radius values, throat lengths are normally distributed.

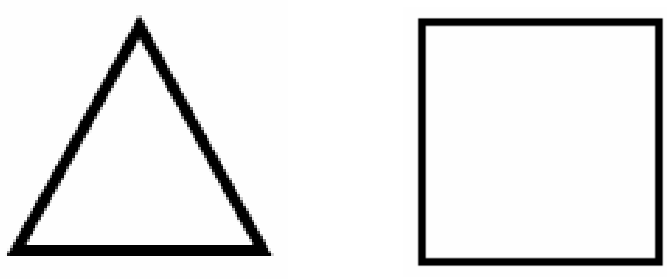

a- Pores **b- Throats**

Figure 12 – Pores and Throats

Table 2 – Parameters in Weibull Distribution and Contact Angle Ranges

γ	1.8
δ	0.1
$\theta_{Receeding}$ (degree)	10 – 25
$\theta_{Advancing}$ (degree)	30 – 160

After constructing matrix which is composed of only pores and throats, receeding and advancing angle values are normally distributed for given angle ranges by satisfying the desired wettability conditions (Table 2). Since carbonate reservoirs are generally oil – wet or mixed – wet, advancing angle range is selected as correspondingly.

5.1.2. Assigning Secondary Porosity Features

The total number of secondary porosity elements is set as 50% of the total number of pores and throats; 30% fissures and 20% vugs. Vugs and fissures are represented by squares with greater inscribed radii which are also obtained using a Weibull distribution for given ranges. Fissures are composed of consecutive elements with variable size (Figure 13) in order to represent the variable aperture within fissures and fractures more realistically. Moreover, consecutive elements of fissures are not connected with throats in order to represent structure of fissures and fractures. Locations of the secondary porosity features and length of fissures are randomly selected. Also, a location which is previously pore or throat or null, may turn out to be a fissure element or vug. Receeding and advancing angle values for fissures and vugs are also normally distributed using the same angle range of matrix. At the end of the model construction process, a spatially semi – correlated pore network model is developed.

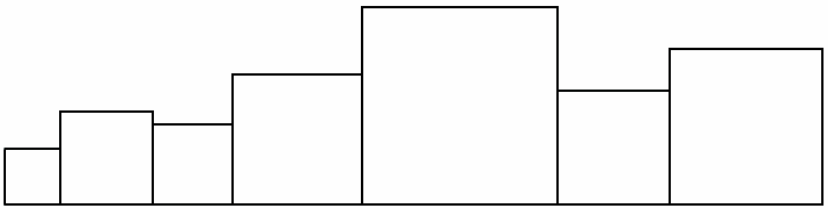

Figure 13 – Fissure with Variable Size

5.1.3. Constructed Pore Network Model

In this study, a 29x29x29 pore network model, composed of matrix, fissure and vug sub domains, is developed (Figure 14). (Null represents non-void element) The constructed pore network model successfully represents a dual pore size distribution (Figure 15). The radius ranges used in Weibull distribution for pores and secondary porosity features are gathered from previously conducted analysis (Table 3) (Hatipoğlu, 2002).

Table 3 – Radius Ranges for Elements

	Pore	Vug	Fissure
R_{max} (μm)	6.5	15	12
R_{min} (μm)	1.2	7	7

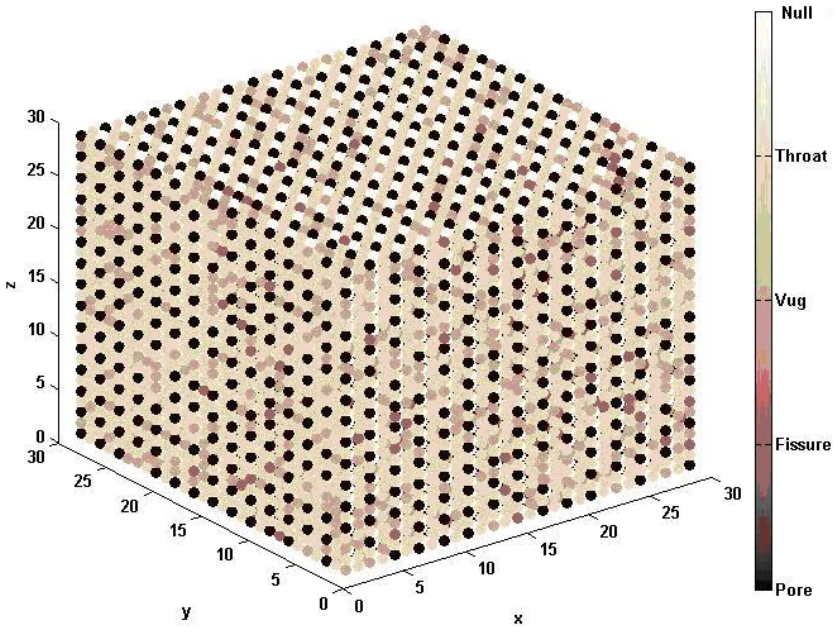

Figure 14 – Distribution of Sub Domains

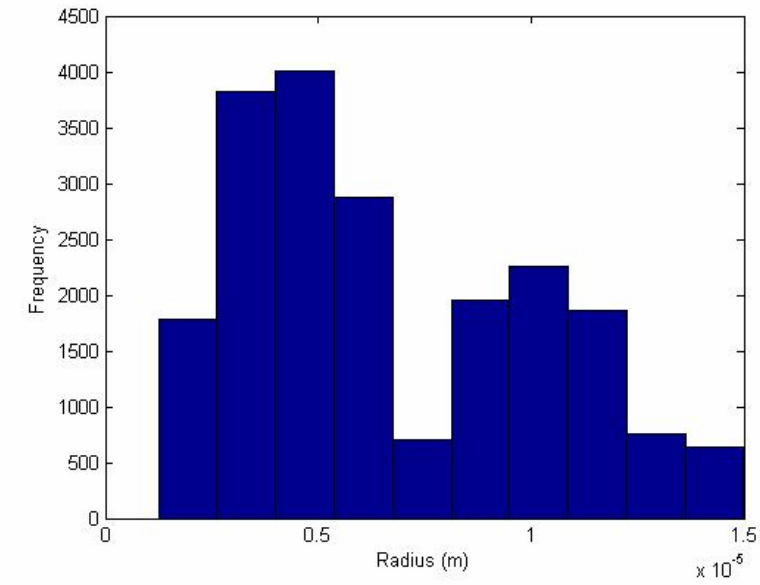

Figure 15 – Pore Size Distribution

The type of cross sections is defined by corner half angle values (α) of elements and area of an element is calculated by considering α (Equation 14), by not directly using geometric equations (Hui and Blunt, 2000).

$$A_t = n_c \cdot R^2 \cdot \cot\alpha \tag{14}$$

Contact angle ranges are selected by bearing in mind that porous media is mixed wet and water is always present in corners. In addition, receeding angle range is assigned such that advancing angle is always greater than receeding angle. Presence of water in corners is guaranteed by the relationship between receeding and corner angles (Equation 15).

$$\theta_{Receeding} + \alpha \leq \pi \tag{15}$$

5.2. Simulation of Flow Mechanisms

5.2.1. Primary Drainage

5.2.1.1. Threshold Pressure Calculation

For simulating two – phase flow in this pore network model, first primary drainage is considered. It is assumed that the system is filled by water prior to oil migration. In primary drainage, receeding angle values are used as contact angle and non-wetting phase enters an element with radius R at threshold pressure of P_c (Oren and et al., 1997);

$$P_c = \frac{\sigma\left(1 + 2\sqrt{\pi G}\right)\cos\theta}{R} F \tag{16}$$

where;

$$F = \frac{1 + \sqrt{1 + 4GD/\cos^2\theta}}{1 + 2\sqrt{\pi G}} \tag{17}$$

$$D = \pi\left(1 - \frac{\theta}{pi/3}\right) + 3\sin\theta\sin\theta - \frac{\cos^2\theta}{4G} \quad (18)$$

$$G = \frac{\sin(2\alpha_1)}{2} \cdot \left(2 + \frac{\sin(2\alpha_1)}{\sin(2\alpha_2)}\right)^{-2} \quad (19)$$

Since the elements are represented by regular geometries, α_i (where i=1, 2,..,n_c) values are equal. During primary drainage, receeding angle is used as contact angle (θ).

5.2.1.2. Primary Drainage Algorithm

Flow of non-wetting phase starts from y=1 to y=29 and all of the elements (pore, throat, fissure or vug) connected to inlet are considered to be prospective elements to be invaded. Initially, threshold pressures of all elements are calculated by using Equation 16 and corresponding pressure values of the inlet elements are listed. An element with minimum threshold pressure is filled by non-wetting phase and current capillary pressure of the system is set to this value. Then, its neighbor elements are controlled to find out whether they can be invaded or not. If a particular capillary pressure exceeds the corresponding threshold pressure of the neighbor element, it is filled and its capillary pressure is set equal to current capillary pressure. If threshold pressure of the neighbor element is greater than the current capillary pressure, the element is added into the pressure list. Subsequently, the minimum pressure in the list is set equal to the capillary pressure of the system and its corresponding element is filled. The same procedure is applied until all possible elements are invaded by non-wetting phase. At each filling step, saturation and conductance of both phases are calculated.

At the end of primary drainage, water is present in corners and oil is in center of the invaded elements. Oil/water contact can be either pinned or not and it is determined by the receeding angle and the corner half angle.

5.2.2. Waterflooding (Imbibition)

Waterflooding starts after primary drainage and two-phase flow properties of the model are obtained for imbibition. All possible flow mechanisms in imbibition, snap-off, piston-like advance and pore body filling, are considered. During imbibition, advancing angle values are used as contact angle. As mentioned before, advancing contact angle values are normally distributed between 30 and 160 degrees range yielding a mixed – wet system. All possible fluid configurations are examined, thus saturation and conductance calculations are conducted by bearing in mind the presence of oil layers, if exists any.

5.2.2.1. Snap – Off

During waterflooding, occurrence of snap – off is controlled first. As mentioned before, if Roof's criterion (Equation 1) is satisfied, the element is assumed to be filled by snap – off process (Jia, 2005). The preference between spontaneous and forced snap – off is determined by relationship between corner half angle and contact angle. Threshold pressure of an element can be obtained for snap – off mechanism by using Equations 2 and 3.

In spontaneous snap – off, if $\theta_h > \theta_a$, the element is assumed to be completely filled by wetting phase present in corners. Otherwise, phase configuration does not change (same as at the end of primary drainage). In forced snap – off, oil / water contact is pinned if $\theta_h < \theta_a$ and A_c is determined by using θ_h otherwise, $\pi - \theta_a$ is used as θ. In case of $\theta = (\pi/2) - \alpha$, the element is completely filled by wetting phase and conductance is calculated accordingly.

5.2.2.2. Piston – Like Advance

In piston – like advance, imbibition can be either spontaneous or forced and the preference depends on $\theta_{Advancing}$ and θ_{Max} (Oren and Bakke, 1997). In spontaneous imbibition, the element is completely filled by the invading wetting phase. As

hinging angle reaches advancing angle, the element will be completely filled by wetting phase. Contrary to spontaneous case, in forced imbibition oil layers can be preserved when suitable conditions exist. In case of forced imbibition, capillary pressure is negative and wetting phase has two components (in corner and in center). Thus, wetting and non – wetting phase areas are calculated by accounting for the presence of oil layers.

Threshold pressure in spontaneous imbibition is calculated by using the aforementioned iterative method (Equations 5-8). During spontaneous imbibition, an element is completely filled by wetting phase and conductance is calculated straightforwardly. In forced imbibition, threshold pressure is obtained by Equation 10 and presence of oil layers is controlled by Equation 9. In case of oil layers, wetting phase has two components; corners and center. Total conductance of wetting phase is obtained by summation of these components. If oil layers are not preserved, the element will be completely filled by wetting – phase and conductance is obtained correspondingly.

5.2.2.3. Pore Body Filling

In pore body filling mechanism, number of previously invaded elements is important. If only one invaded neighbor element (I_1) is present, imbibition will be same as piston – like advance. Threshold pressure and conductance will be calculated by using the same procedure for piston – like advance.

Pore body filling mechanism can occur either spontaneously ($\theta \leq \theta_{max}$) or forced ($\theta \leq \theta_{max}$). In spontaneous imbibition, threshold pressure is calculated by using Equations 11 and 12 and number of terms depends on the number of previously invaded neighbor elements (Oren and Bakke, 1997). As for forced imbibition, threshold pressure is obtained as I_1 mechanism. Phase conductances are determined correspondingly for either spontaneous or forced imbibition.

5.2.2.4. Waterflooding Algorithm

Waterflooding starts after primary drainage and flow occurs from y=1 to y=29. Initially, threshold pressure values, for all waterflooding mechanisms, are calculated for invaded elements in primary drainage. The inlet elements are assumed to be filled by piston-like advance mechanism. For the interior and outlet elements, there is competition between the imbibition mechanisms. First, element is checked for snap-off using Roof's criterion. If snap-off is not favored, threshold pressures for piston like advance and pore body filling mechanisms are compared. Mechanism yielding greater threshold pressure is favored for the corresponding element (Jia, 2005). Then, threshold pressures of inlet elements are listed and element with maximum threshold value is invaded by wetting-phase and its threshold pressure is set equal to current capillary pressure of the system. The neighbors of the invaded element are checked to be filled by wetting phase or not. If it can be invaded, saturation and conductance of the element is calculated. If the neighbor can not be invaded, its threshold pressure is added into the list and procedure continues until the all possible elements are invaded by wetting-phase. Similar to primary drainage, at each filling step, saturation and conductance of both wetting and non-wetting phases are calculated.

5.2.3. Calculation of Flow Properties

5.2.3.1. Phase Area Calculation

For saturation and conductance calculations, wetting and non-wetting phases' areas are determined. Phase areas in the corners and in the center (Figure 16) are calculated by the following formulae (Piri and Blunt, 2005).

$$A_c = \begin{cases} \left(R\frac{\cos(\theta+\alpha)}{\sin\alpha} \right)^2 \sin\alpha\cos\alpha & , \text{if} \quad \alpha+\theta=\frac{\pi}{2} \\ n_c r^2 \left(\cos\theta\left(\cot\alpha\cos\theta-\sin\theta\right)+\theta+\alpha-\frac{\pi}{2} \right) & , \text{if} \quad \alpha+\theta\neq\frac{\pi}{2} \end{cases} \qquad (20)$$

$$A_{center} = A_t - A_c \tag{21}$$

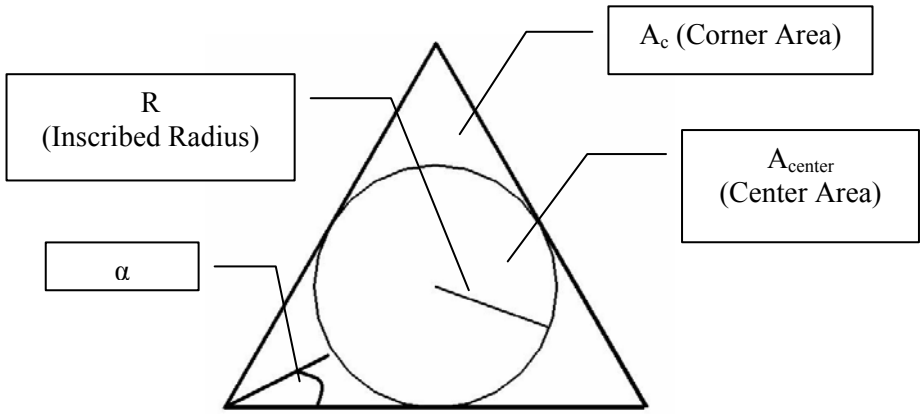

Figure 16 – Phase Area Distribution within Elements

In presence of non-wetting phase layers (Figure 17) preserved during imbibition, area of layer is obtained by the following relations;

$$A_{w\_corner} = n_c r^2 \left(\cos\theta_h \left(\cot\alpha \cos\theta_h - \sin\theta_h \right) + \theta_h + \alpha - \frac{\pi}{2} \right) \tag{22}$$

$$A_{Layer} = A_c - A_{w\_corner} \qquad (A_c \text{ with } \theta = \mu - \theta_{Advancing}) \tag{23}$$

$$A_{Wetting} = A_{w\_corner} + A_{center} \tag{24}$$

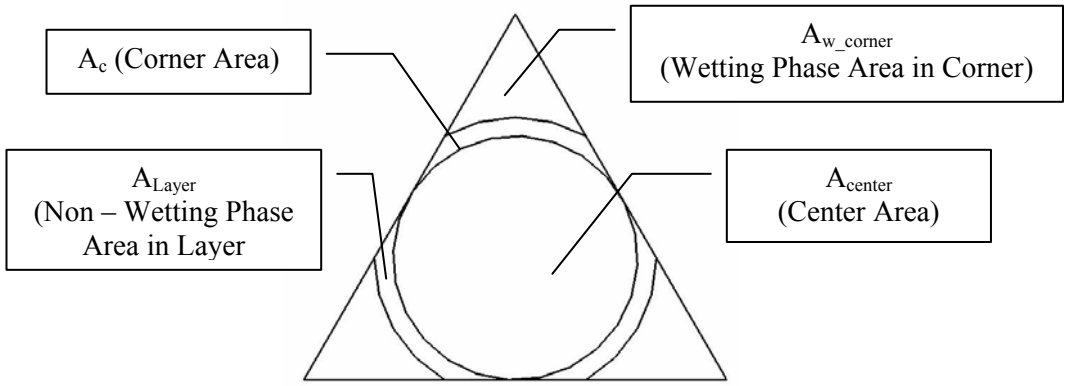

Figure 17 – Phase Area Distribution with Non – Wetting Phase Layer

5.2.3.2. Conductance Calculation

Conductance of an element completely occupied by single fluid is given as (Hui and Blunt, 2000);

$$g_t = \frac{\pi\left(\sqrt{A_t/\pi} + R\right)^4}{128} \tag{25}$$

If two phases are present within the element, one residing in center and the other in corner, conductances of both phases are given by the following equations (Hui and Blunt, 2000);

$$g_{center} = \frac{\pi\left(\sqrt{A_{center}/\pi} + R\right)^4}{128} \tag{26}$$

$$g_c = \begin{cases} \dfrac{A_c^2(1-\sin\alpha)^2 \cdot (\varphi_2\cos\theta - \varphi_1)\varphi_3^{\,2}}{12 n_c \sin^2\alpha (1-\varphi_3)^2 \cdot (\varphi_2 + f\varphi_1)^2} & , \text{if} \quad \theta < \dfrac{\pi}{2} - \alpha \\ \dfrac{A_c^2(1-\sin\alpha)^2 \tan\alpha \varphi_3^{\,2}}{12 n_c \sin^2\alpha (1-\varphi_3)(1+f\varphi_3)^2} & , \text{if} \quad \theta > \dfrac{\pi}{2} - \alpha \end{cases} \tag{27}$$

Where;

$$\varphi_1 = \frac{\pi}{2} - \alpha - \theta$$

$$\varphi_2 = \cot\alpha \cdot \cos\theta - \sin\theta$$

$$\varphi_3 = \left(\frac{\pi}{2} - \alpha\right)\tan\alpha$$

f= 1 (indicating boundary condition at fluid interface. f= 1 represents no – flow boundary)

At the end of the imbibition process, if non – wetting phase is preserved as layer within elements, corresponding wetting and non – wetting phase conductances are obtained by following equations (Hui and Blunt, 2000);

$$g_{Layer} = \frac{A_{Layer}^3 (1-\sin\alpha)^2 \tan\alpha \varphi_3^{\,2}}{12 n_c A_c \sin^2\alpha (1-\varphi_3) \cdot \left(1 + f_1\varphi_3 - (1-f_2\varphi_3)\sqrt{\frac{A_{w\_corner}}{A_c}}\right)^2} \tag{28}$$

$$g_{wetting} = g_{center} + g_{w\_corner} \tag{29}$$

Where g_{w_corner} is calculated by using A_c=A_{w_corner}.

5.2.3.3. Saturation Calculation

Saturation of each phase within an element is obtained by the ratio of phase area to the total area of the model. At each filling step, phase saturations are obtained by the summation of saturations of corresponding phase at each element.

$$S_p = \frac{A_p}{A_T} \tag{30}$$

$$S_T = \sum_{i=1}^{Num} \frac{A_{p\,i}}{A_T} \tag{31}$$

5.2.3.4. Relative Permeability Calculation

In pore network modeling studies, Poiseuille's law is applied and phase flow rates are obtained. Then, relative permeability is obtained by dividing the phase flow rate to total flow rate of the system.(Oren and Bakke, 1997; Patzek, 2000; Piri and Blunt, 2005). In this study, relative permeability is defined as the ratio of phase conductance to total conductance of the system in order to minimize time consumption. Since the model is initially filled by water, total conductance of the

system is defined with respect to water conductance. Total conductance and relative permeability of a particular element are defined as;

$$g_T = \sum_{i=1}^{Num} \frac{\pi\left(\sqrt{A_{ti}/\pi} + R_i\right)^4}{128} \tag{32}$$

$$k_{rp} = \frac{\sum_{i=1}^{Num} g_{pi}}{g_T} \tag{33}$$

CHAPTER 6

RESULTS AND DISCUSSION

6.1 Base Model

A pore network model with 29x29x29 elements and a maximum coordination number of 6 is used to model two-phase flow in fissured and vuggy carbonates. By using the aforementioned methodology (in Chapter 5) for the constructed pore network model, capillary pressure and relative permeability curves are obtained for drainage and imbibition (Figures 18-20). As it is implied from capillary pressure curves, the constructed pore network model successfully represents two – phase flow in fissured and vuggy carbonates (Figure 18). Because of the filling algorithm, a trend, rather than a smooth line, for capillary pressure is obtained. Capillary pressure curve of primary drainage reflects the dual porosity system present in model by the reflection of the curve at S_w= 0.89.

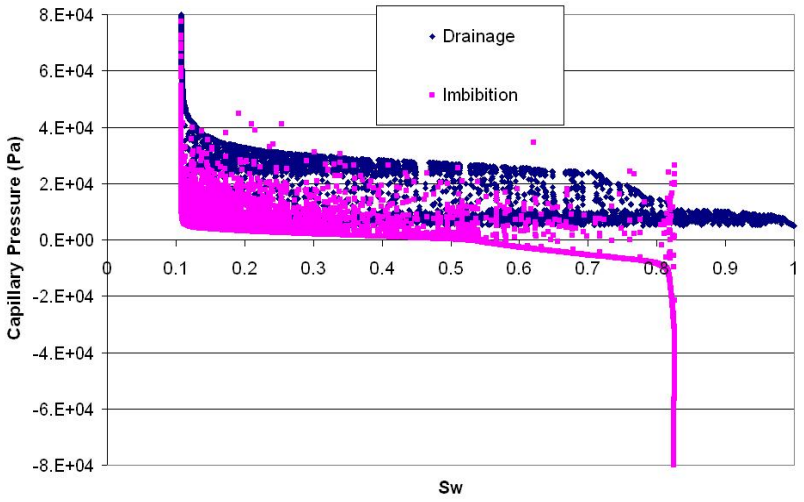

Figure 18 – Capillary Pressure Curves for Primary Drainage and Imbibition

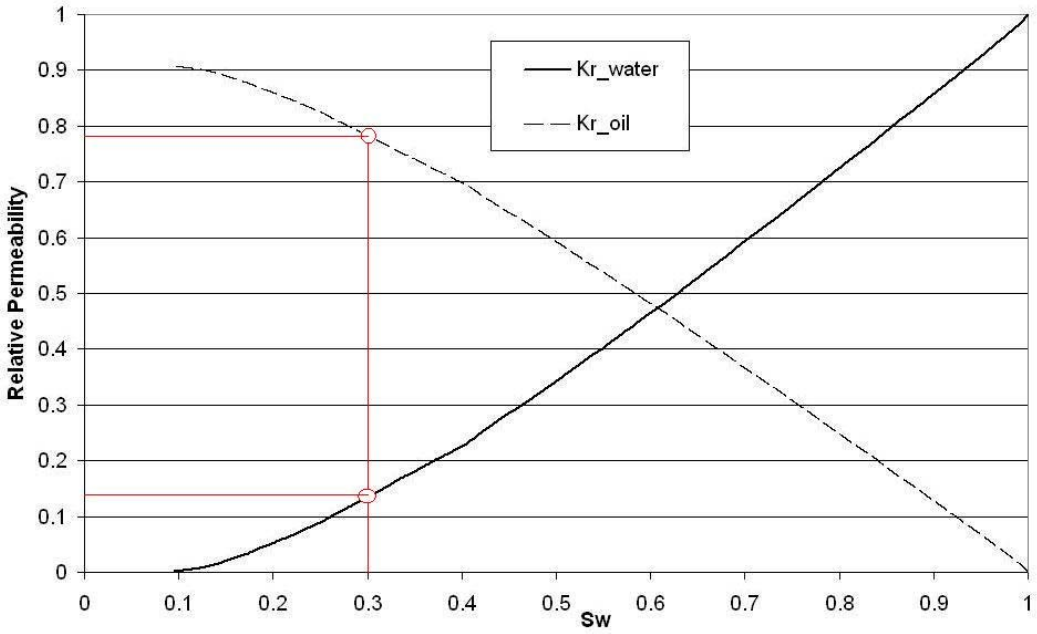

Figure 19 – Relative Permeability Curves (Drainage)

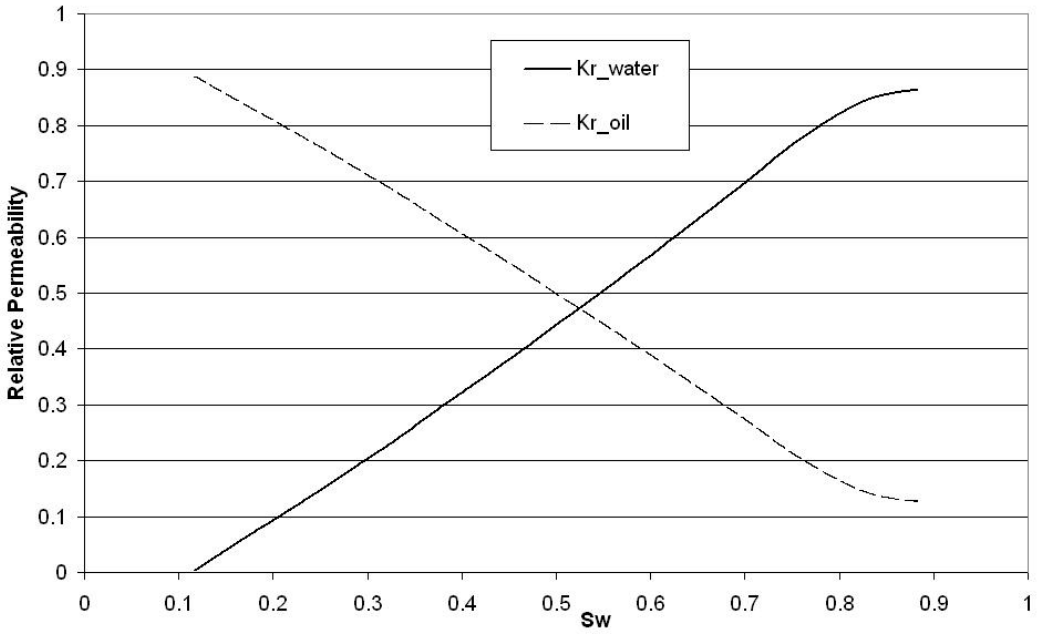

Figure 20 – Relative Permeability Curves (Imbibition)

In typical porous media such as sandstones, relative permeability curves are concave. For such a system at a particular saturation, the summation of relative

permeabilities is less than one, indicating phase interference. On the other than, for fractured media X – type relative permeability curves are reported (Romm, 1966). That is to say, the summation of relative permeability values at a particular saturation is equal to 1 (no phase interference). However, recent studies (Akın, 2001) indicate that concave relative permeability curves are possible for fractured media. In the present study, relative permeability curves are obtained for primary drainage and imbibition (Figures 19 and 20). It is observed that the curves are neither concave nor linear. This is validated by the summation of relative permeability values at a particular saturation. For example, for primary drainage, at S_w= 0.3, water relative permeability is 0.14 where as oil relative permeability is near 0.78 (summation is 0.92), indicating phase interference.Valvatne (2004) reported capillary pressure and relative permeability curves for a mixed – wet intergranular carbonate sample. The sample has pores and throat with 0.1 μm radius mainly. He obtained capillary pressure curve for primary drainage with receeding angles in 25-65 range, fixed advancing angle of 140° and interfacial tension of 0.48 N/m for mercury and air. Capillary pressure curve obtained for the same wettability conditions is compared with the one in Valvatne's study (Figure 21) with adjusted pore base model (Table 4). Also, capillary pressure curve obtained in this study is smoothed as representing the general trend for comparison. Effects of secondary porosity features are not recognizable since smaller radius ranges for the elements are assigned (Table 4) resulting in a relatively homogeneous porous media. On the other hand, in relative permeability curves, secondary porosity effects are amplified (Figure 22). Valvatne used intergranular carbonate sample which was relatively homogeneous and reported concave relative permeability curves. Base model (for fissured and vuggy carbonate rock) is modified for simulating primary drainage with the same wettability conditions (Table 4). It is observed that due to the secondary porosity features the model resulted in linear relative permeability curves (Figure 22). Also, cross over points are at close water saturations with different relative permeabilities. This is due to the flow algorithm used in this study and pore morphology. In other words, greater element sizes resulted higher saturation and conductance.

Table 4 – Model Properties for Valvatne (2004) and This Study

		Base Model (This Study)	Valvatne (2004) A	Valvatne (2004) B	Adjusted Base Model
Pores (µm)	R_{max}	6.5	0.1	0.1	0.65
	R_{min}	1.2	0.1	0.1	0.12
Fissures (µm)	R_{max}	12	-	-	1.2
	R_{min}	7			0.7
Vugs (µm)	R_{max}	15	-	-	1.5
	R_{min}	7			0.7
Receeding Angle (degree)		10- 25	25-65	25-65	25-65
Advancing Angle (degree)		30-160	140	116-120	110-130
Interfacial Tension (N/m)		0.0447	0.48	0.0299	0.48

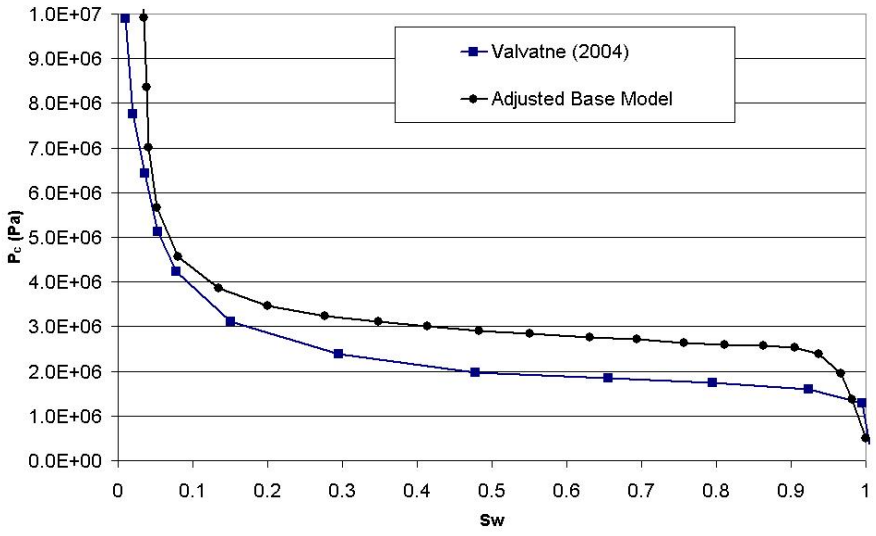

Figure 21 – Comparison of Capillary Pressure Curve with Valvatne (2004) A (Primary Drainage)

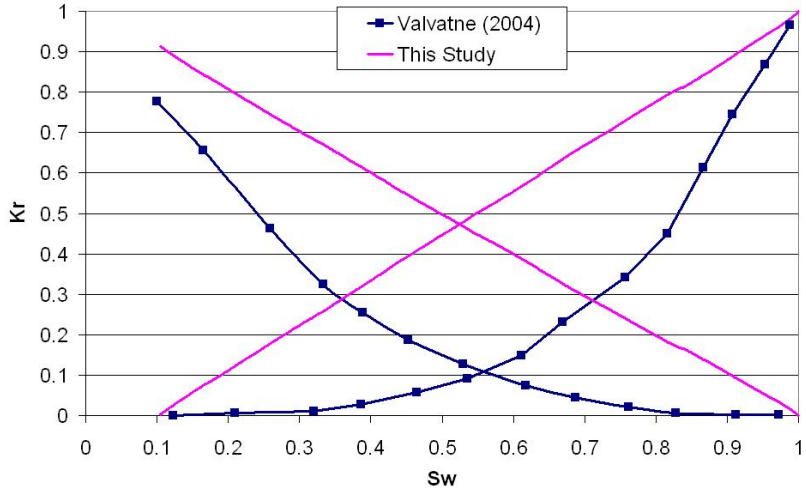

Figure 22 – Comparison of Relative Permeability Curves with Valvatne (2004) B (Primary Drainage)

The results of the pore network model are compared with the ones reported by Bekri et al. (2004) (Figures 23 and 24). They reported capillary pressure and relative permeability curves for a vuggy system with a fixed advancing angle of 180° during imbibition. They used an algorithm in which vugs, with connecting throats, are invaded first. Matrix is assumed to be filled after invasion of vugs at a significant threshold pressure. Results are compared with the ones obtained for the same wettability conditions (Table 5) by using smoothed capillary pressure curve.

Table 5 – Model Properties for Base Model and Bekri et al. (2004)

		Base Model (This Study)	Bekri et al. (2004)
Pores (µm)	R_{max}	6.5	1
	R_{min}	1.2	0.01
Fissures (µm)	R_{max}	12	-
	R_{min}	7	
Vugs (µm)	R_{max}	15	3000
	R_{min}	7	3
Receeding Angle (degree)		10- 25	0
Advancing Angle (degree)		30-160	180
Interfacial Tension (N/m)		0.0447	

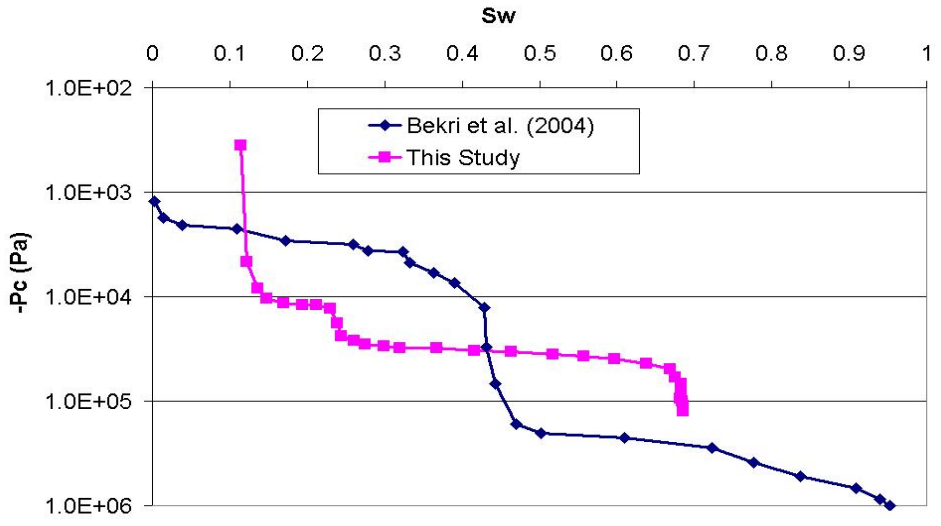

Figure 23 – Comparison of Capillary Pressure Curves with Bekri et al. (2004) (Imbibition)

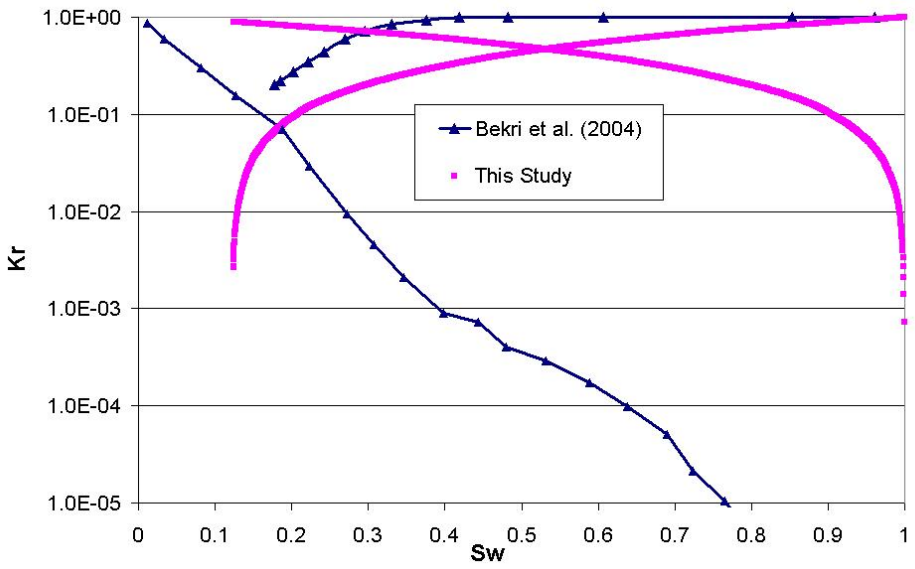

Figure 24 – Comparison of Relative Permeability Curves with Bekri et al. (2004) (Imbibition)

Bekri et al. (2004) reported that the vugs were effective at water saturations below 0.45 and above that value matrix became dominant. Since in their algorithm, filling priority was given to vugs (i.e., vugs were filled first and then matrix was invaded), effect of secondary porosity features on capillary pressure curve was significant. In this study, no priority is given to secondary porosity features thus their effect is not as significant as the one in Bekri's study (Figure 23). A shift in the curve is observed at water saturation of 0.22. Bekri et al. (2004) reported the effects of vug on relative permeability curves for water saturation below 0.45 (Figure 24). End point saturations and corresponding relative permeability values are different mainly because of the difference in pore size distributions and receeding angle ranges (Figure 24). Bekri et al. (2004) used a matrix composed of pores and throats in 0.01-1 μm radius range and vugs with throats in 3-3000 μm size. However, in this study, pore size distribution is different, with larger matrix and smaller vugs. Also, receeding angle was fixed at zero degrees, but in this study receeding angle values are distributed in 10-25° range. Bekri et al. (2004) concluded that wetting phase relative permeability was affected by vugs and matrix, while non – wetting phase was mainly controlled by vugs. They observed small values for oil relative permeability where as higher values for water. Results

obtained for wetting – phase relative permeability values are at the same order of magnitude with Bekri's results. On the other hand, for non – wetting phase relative permeability curves, Difference in several orders of magnitude is observed because of the differences in pore size data and receeding angles. Bekri et al. (2004) used small sizes for matrix and larger sizes for throats and they assumed that vugs were connected by throats. However, in this study, fissures and vugs are directly connected to each other and then to matrix. It is concluded that an agreement in the trends of curves rather than values is obtained for the results and the ones in Bekri et al. (2004).

6.1.1. Saturation Distribution

Oil and water saturation distributions for drainage and imbibition are illustrated (as the color becomes lighter, saturation increases) (Figures 25 and 26). Higher saturations are observed in areas where fissures and vugs are present. This is expected since during imbibition, first larger elements are filled as threshold P_c is small.

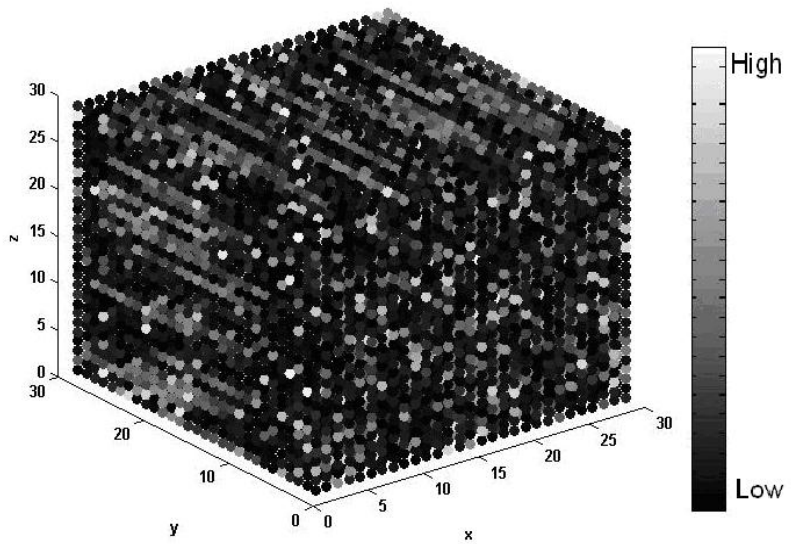

Figure 25 – Oil Saturation Distribution (At the end of drainage)

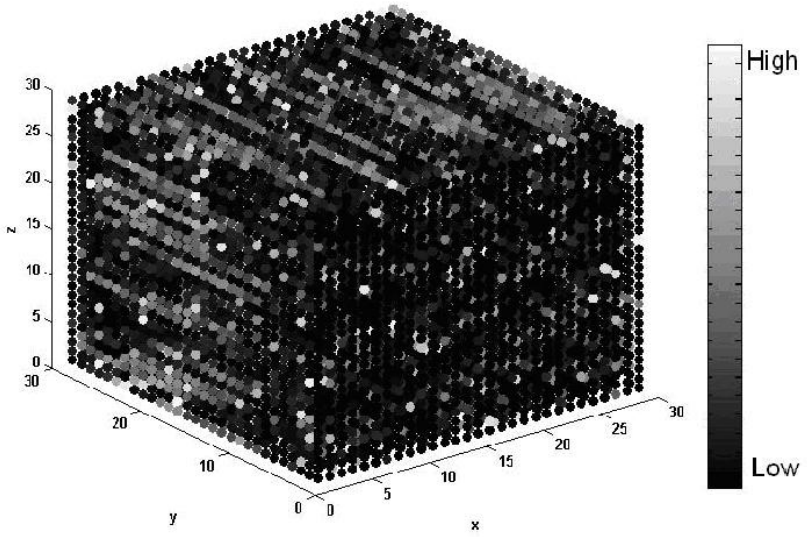

Figure 26 – Water Saturation Distribution (At the end of imbibition)

6.1.2. Sensitivity Analysis

After obtaining two-phase flow properties for primary drainage and waterflooding, sensitivity analyses are conducted in order to analyze the results. For investigating the effects of wettability, different wettabilities are assigned to different sub domains (i.e., matrix, fissures and vugs). Moreover, effects of pore morphology are investigated by changing element sizes on base model. Results are compared with the base model and literature.

6.1.2.1. Wettability Analysis

In the base model, receeding and advancing angle values are normally distributed between 10 to 25 degrees and 30 to 160 degrees ranges respectively, yielding a mixed wet porous media. It is logical to represent porous media for carbonate rocks as mixed wet, since carbonate reservoirs are generally oil – wet or mixed – wet (SLB, 2008). In wettability analysis, advancing angle range is changed and different wettability types are assigned for the elements (Table 6). Initially, the system is considered to be completely water – wet and the corresponding results are obtained. In the second case, wettability is changed to oil – wet and results are

examined. In last case, matrix (pores and throats) is assumed to be water – wet, where as the secondary porosity features (vugs and fissures) are oil – wet.

Table 6 – Advancing Angle Ranges for Sensitivity Analysis (degree)

	Matrix		Vug		Fissure	
Wettability	Max	Min	Max	Min	Max	Min
Base Model	160	30	160	30	160	30
Water-Wet	90	30	90	30	90	30
Oil-Wet	150	90	150	90	150	90

Capillary pressure and relative permeability curves are obtained for all wettability scenarios for primary drainage and waterflooding (Figures 27 and 28). Since only advancing angle ranges are modified, wettability effects are amplified in imbibition relative permeability curves. As the system becomes more water wet, end point relative permeability values are affected and residual oil saturation decreases (for all water – wet case compared to base model) (Table 7). For strongly water – wet systems, end point relative permeability for water is below 0.1 yielding lower residual oil saturation. By comparing results of all water wet and partially water wet (matrix is water wet, vugs and fissures are oil wet) cases, effect of secondary porosity features on non-wetting phase relative permeability can be observed. End point relative permeability values are changed as secondary porosity features become oil wet, This indicates that non-wetting phase relative permeability is mainly controlled by secondary porosity features at small wetting – phase saturation. Similar results were reported obtained by Moctezuma et al. (2003) and Bekri et al. (2004) for carbonate relative permeability curves. In addition, it can be stated that matrix has a significant influence on relative permeability curves. In partially water – wet case, relative permeability curves show a similar trend with all water – wet case but with different end point relative permeability values. As for all oil – wet case, a shift in cross over point (less than 0.5) is observed on the other hand; the remaining curves indicate a water – wet system. This result confirms with the situation commonly observed in oil – wet reservoirs.

Table 7 – Residual Phase Saturations for Wettability Cases

	Residual S_w	Residual S_o
Base Model	0.87	0.13
All Water Wet	0.98	0.02
All Oil Wet	0.76	0.24
Partially Water Wet	0.92	0.08

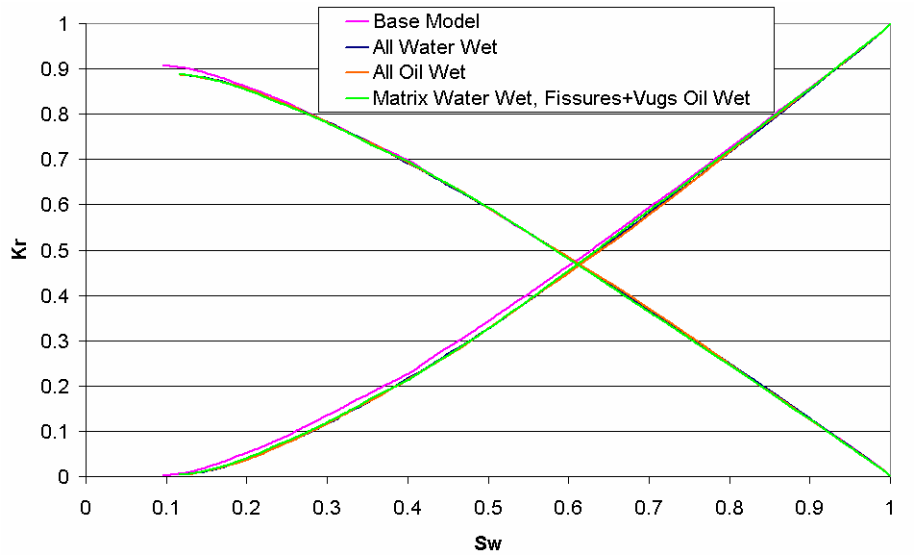

Figure 27 – Relative Permeability Curves for Wettability Analysis (Primary Drainage)

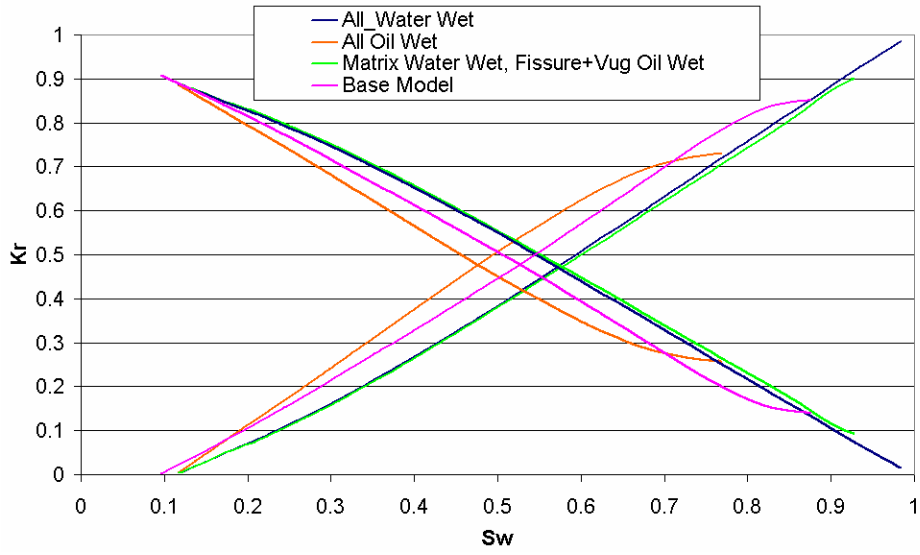

Figure 28 – Relative Permeability Curves for Wettability Analysis (Waterflooding)

Also, end point relative permeability values are changed when a decrease in non – wetting phase and an increase in wetting – phase relative permeability values are

observed. Similar results for recovery and end point relative permeability values were reported by Blunt (1997). Effects of wettability on oil recovery were examined for sandstone reservoirs and it was concluded that residual oil saturation increases, as model becomes more oil wet. Thus, results obtained for all oil – wet case are validated by the results obtained in Blunt's study. It can be concluded that the developed model reflects the wettability effects successfully.

6.1.2.2. Effects of Wettability on Imbibition Mechanisms

During wettability analysis, it is observed that wettability has drastic influence on relative permeability values. Since in imbibition, relative permeability of non-wetting phase is directly related to layer stability and phase entrapments, which mainly depend on contact angle, wettability affects imbibition flow mechanisms as well as other flow properties. In order to illustrate the changes in mechanisms with respect to wettability, sensitivity analyses are conducted by using topologically identical pore network models with different advancing angle values. The model consists of 80% matrix, 10% fissures and 10% vugs. The results are presented for base model (mixed –wet), water – wet and oil – wet cases (Figure 29).

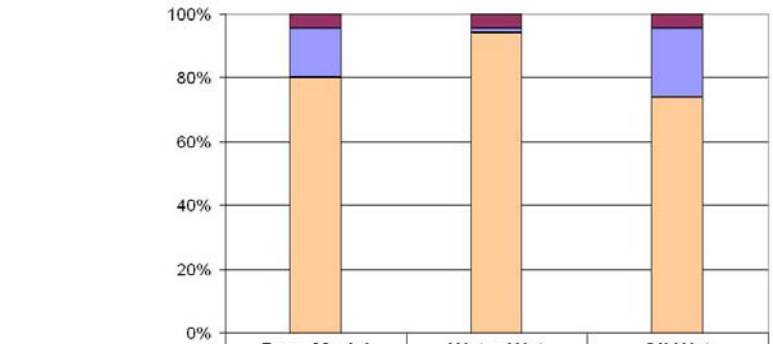

	Base Model	Water Wet	Oil Wet
Piston-Like Advance	841	841	841
Snap-Off	3016	302	4236
Pore Body Filling	15643	18357	14423

Figure 29 – Preference of Imbibition Mechanisms for Different Wettability Conditions

This indicates that in water – wet conditions, wetting phase connectivity is higher yielding suitable conditions for non – wetting phase sweeping. As mentioned before, in water – wet porous media, residual oil saturation is lower and this situation is validated by the higher preference of pore – body filling mechanism, which is successful at oil sweeping. Patzek (2000) reported preference of imbibition mechanism in oil – wet sandstone. It was stated that snap – off is generally preferred in throats while pore – body filling is dominant in pores. In his study, filling mechanisms of throats were examined separately. In this study, it is observed that pore – body filling mechanism is the main mechanism in oil – wet sandstones. Since throats are not examined separately, comparison can not be done. For each cases, I_n mechanism preference during pore – body filling is examined It is concluded that mainly I_4 mechanisms is preferred in most cases (Figure 30). For I_6 mechanisms, higher preference is observed in water – wet case. It is concluded that snap – off is generally preferred in oil – wet porous media where as, pore – body filling mechanism is dominant in water – wet conditions.

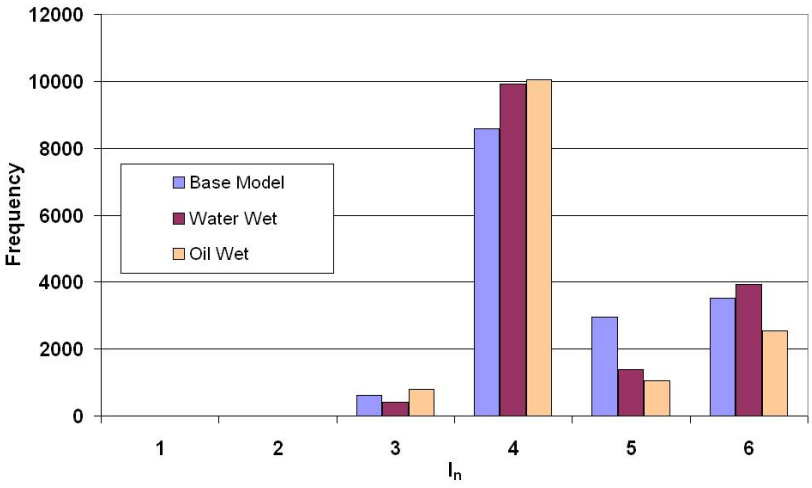

Figure 30 – Preference of I_n Mechanisms

6.1.2.3. Pore Morphology Analysis

By changing inscribed radius ranges for fissures, vugs and matrix sub domains consecutively, effect of element size is investigated. Variation from the base case

is studied by assigning either large or small radius range values for each sub domains respectively. Cases for only large or small fissures, vugs, fissures and vugs, and pores are considered. In Table 8, large and small inscribed radius ranges assigned for sub domains are presented. Base model is simulated by using only large/small fissures, vugs, fissures and vugs, and pores; during each simulation study only one sub domain (except for large/small fissure and vug case) is changed.

Table 8 – Radius Ranges for Sensitivity Analysis (µm)

	Pore Size		Vug Size		Fissure Size	
Size	**R_max**	**R_min**	**R_max**	**R_min**	**R_max**	**R_min**
Base Model	6.5	1.2	15	7	12	7
Large Case	10	5	20	15	25	15
Small Case	3	0.5	8	6	6	3

Large Sized Elements

Relative permeability curves of each case for drainage and imbibition are illustrated (Figures 31 and 32). It can be concluded that large or small element sizes have minor effects on end point relative permeability values as well as on cross over points during primary drainage.

As inscribed radius increases, shifts in cross over points and changes in concavity of drainage relative permeability curves are observed. For large sized vugs and fissures case, drainage relative permeability curve becomes nearly straight. Also, in large sized vugs case, drainage relative permeability curve shows a straight-line trend (i.e. X-type relative permeability curves). As for only large sized fissures or pores cases, the effects are somewhat different; an increase in fissure or pore size yields similar results with base model for both drainage and imbibition. Large sized fissures behave like vugs and do not cause any change indicating abundance of fissures. Large sized pores eliminate the effects of secondary porosity features

and yield more concave relative permeability curves approaching towards to relatively homogeneous porous media.

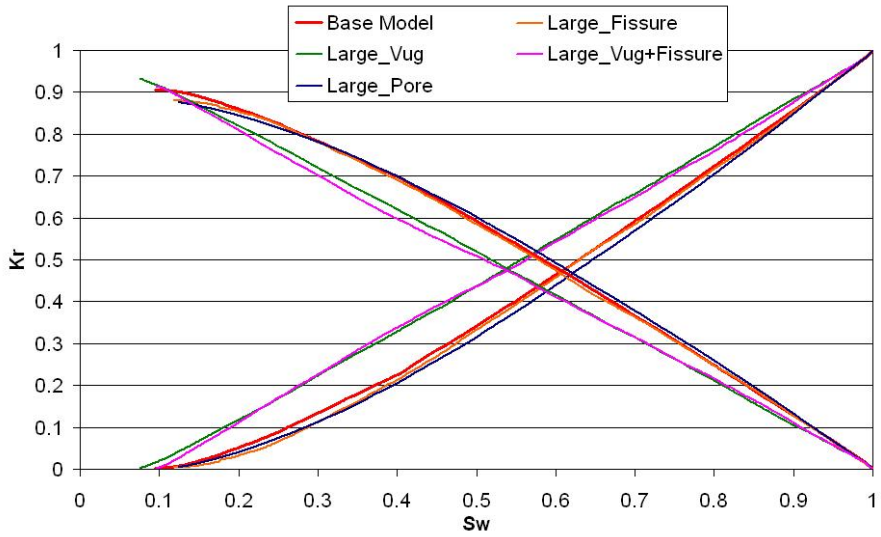

Figure 31 – Relative Permeability Curves for Large Sized Elements (Primary Drainage)

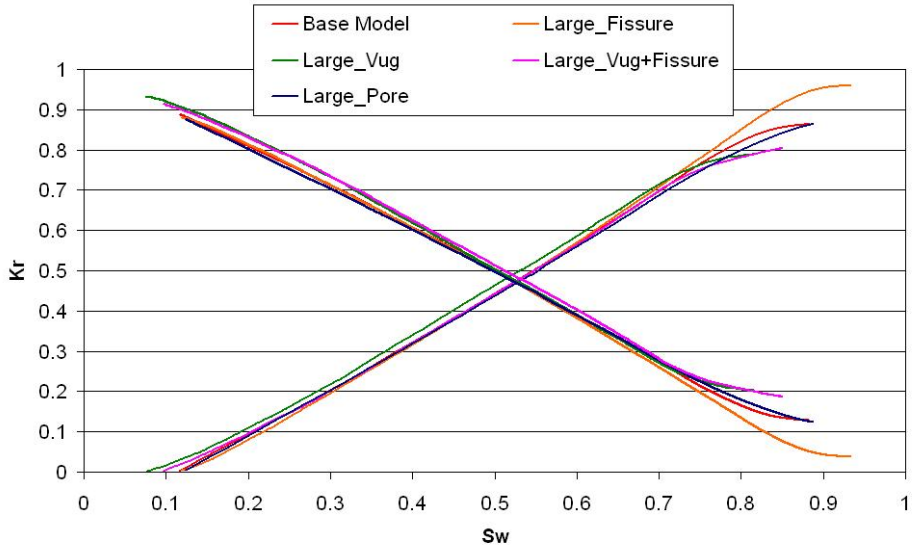

Figure 32 – Relative Permeability Curves for Large Sized Elements (Waterflooding)

It can be concluded that for large sized elements, especially vugs and fissures, porous media behaves like fractured or microfractured porous medium. Similar results were reported previously (Romm, 1966; Babadagli and Ershaghi, 1993; Wilson-Lopez and Rodriguez, 2004). Larger vugs and fissures also effect imbibition by yielding higher end point water relative permeability values; larger vugs and fissures, and vug cases, result a system which has less water – wet behavior than the base model. As mentioned before, as the system becomes more oil – wet (a shift in cross over saturation towards left), residual oil saturation increases and thus end point oil relative permeability decreases significantly. It can be stated that size of secondary porosity features, in other words secondary porosity value, obviously affect non – wetting phase recovery and wettability behavior of a system.

Small Sized Elements

Small values for radius ranges are assigned and pore network model with small sized elements is constructed. Two-phase relative permeability curves for primary drainage and imbibition processes are illustrated (Figure 33 and 34). During primary drainage, effects of small sized vugs and pores are more obvious with respect to small sized fissures or fissures and vugs cases. As vugs get smaller, they act like pores and reduce the effect of secondary porosity features thus, relative permeability curves become more concave with respect to base model curve approaching towards to a single porosity system. Contrary to small sized vugs case, small sized pores significantly increase the effects of secondary porosity features during primary drainage. Thus, curvature of relative permeability curves decreases and they become straighter reflecting a fractured system.

As for small sized fissure and small sized vug and fissure cases, the effects are not obvious in primary drainage and imbibition. Similar results with the base model are obtained but minor increases in end point water relative permeability are observed in primary drainage curves.

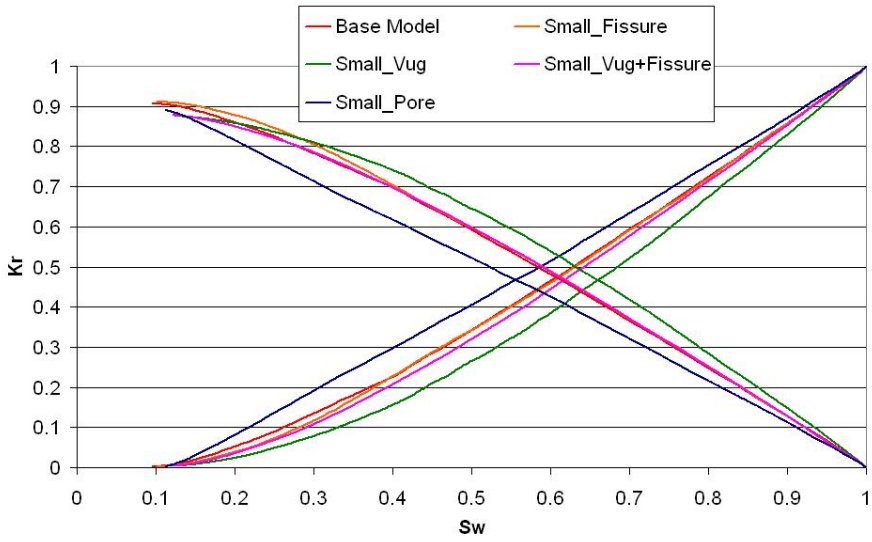

Figure 33 – Relative Permeability Curves for Small Sized Elements (Primary Drainage)

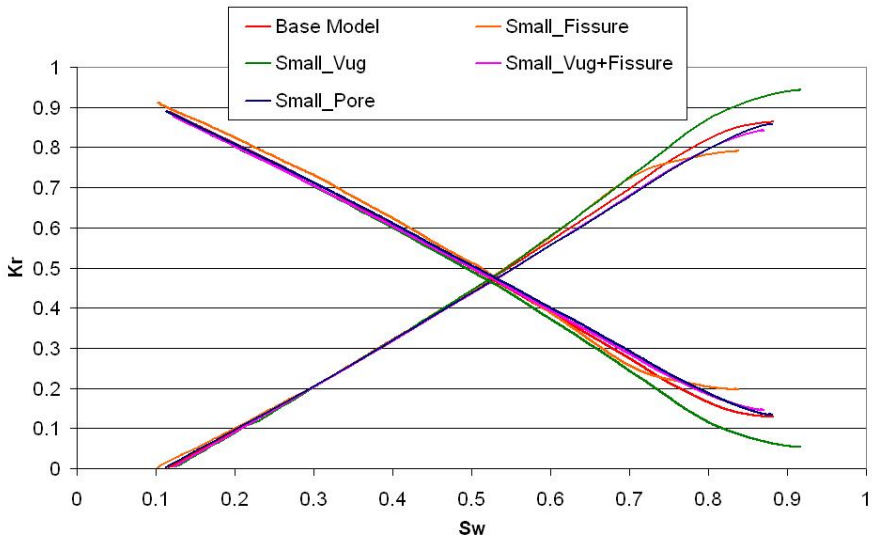

Figure 34 – Relative Permeability Curves for Small Sized Elements (Waterflooding)

During imbibition process, size of the elements affect end point relative permeability values, but cross over points. It can be observed that smaller vug sizes results in end point wetting phase relative permeability values less than 0.1 As fissures get smaller, residual oil saturation increases with relatively higher wetting phase end point relative permeability values. In the other cases, minor

changes are observed in end point relative permeability values. However, in small sized pore case, effect of secondary porosity features is observed by relatively straight curves during imbibition. Also, a shift in cross over saturation point towards higher water saturation direction in drainage relative permeability curve indicates that smaller vug sizes result a more water – wet behavior (i.e., an end point water relative permeability smaller than 0.1 in imbibition.

6.2 Pore Network Model for Vuggy Carbonates

In order to investigate the effects of secondary porosity features, base model is modified for vuggy carbonates. In this case, a pore network model using same element radius and contact angle ranges, is constructed to eliminate fissures from the model. Also, mean and standard deviation values used in throat size distributions are decreased by 50% percent in order to have low porosity in matrix, thus increasing the dominancy of secondary porosity features. Results are compared with the pore network modeling studies conducted for vuggy carbonates (Ioannidis and Chatzis, 2000; Moctezuma et al., 2003; Bekri et al., 2004 and 2005). Smoothed capillary pressure curves for base model and matrix are obtained (Figure 35). Effect of secondary porosity features are amplified in capillary pressure curve for drainage by the shift in the curve at 0.96 water saturation. Similar results are obtained for fissured and vuggy carbonates in this study (Figure 18).

Effects of pore morphology are investigated by assigning smaller values for radius ranges (Table 9) for vug size and vuggy base model is modified correspondingly.

Table 9 – Vug Size Ranges

	Vug Size (μm)	
	R_max	**R_min**
Vuggy Base Model	15	7
Smaller Vug Size	9	4

The results are obtained for matrix (without vugs), vuggy base model and smaller sized vuggy model (Figures 36 and 37).

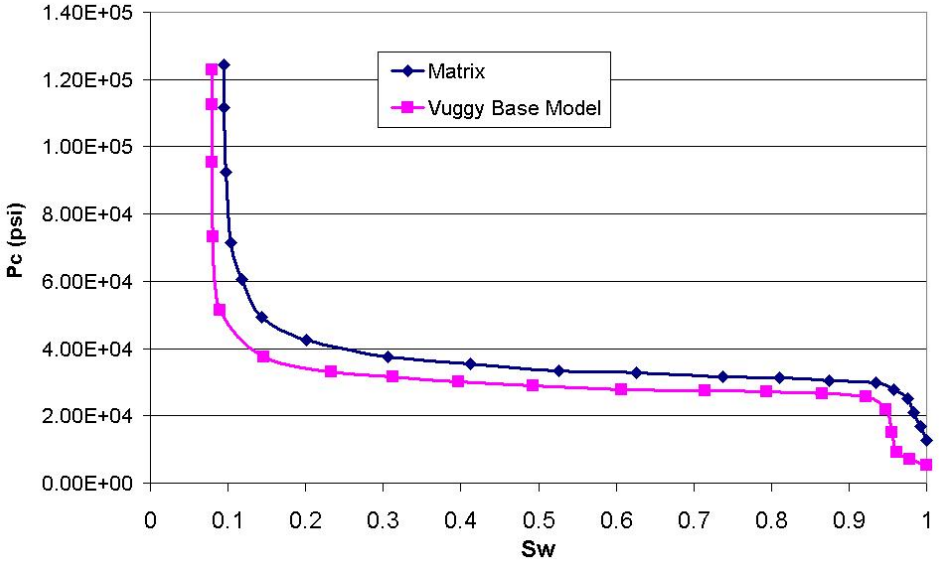

Figure 35 – Capillary Pressure Curves for Base Model and Matrix (Drainage)

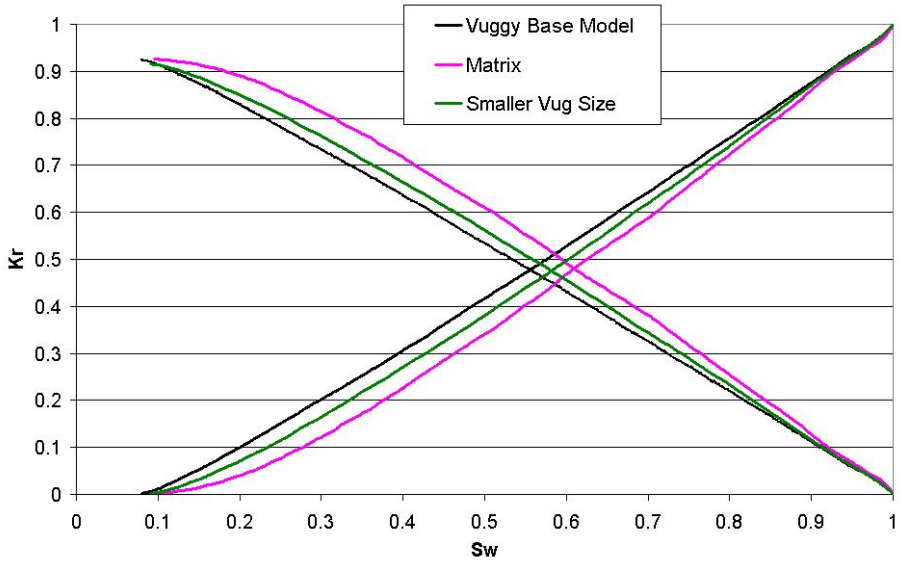

Figure 36 – Relative Permeability Curves for Vuggy Base Model (Drainage)

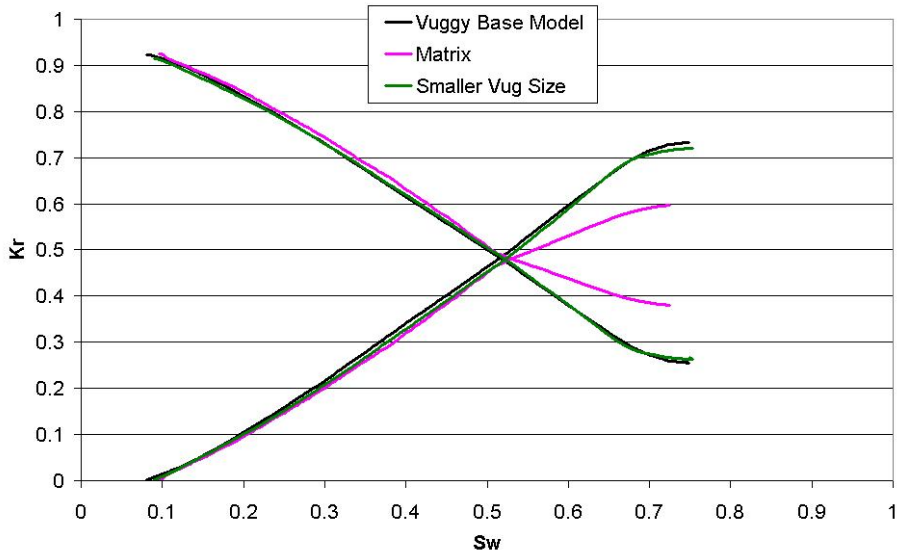

Figure 37 – Relative Permeability Curves for Vuggy Base Model (Waterflooding)

By comparing the results for the aforementioned cases, it can be concluded that primary drainage and waterflooding relative permeability curves successfully represent the effects of secondary porosity features by yielding straight line (i.e. X – type relative permeability curve). This result is reasonable since consecutive vugs act like fractures and similar results were reported previously for fractured porous media (Romm, 1966; Babadagli and Ershaghi, 1993; Wilson-Lopez and Rodriguez, 2004). In only matrix case (without secondary porosity features), concavity of relative permeability curves increases, indicating a relatively homogeneous porous media for primary drainage. Comparison between vuggy base model and matrix curves yields that the pore network model successfully represents a dual porosity system (Figure 35). In addition, as vugs get smaller, they act as pores and yield relatively more concave relative permeability curves for primary drainage. Also, shifts in cross over points are observed. For imbibition process, it is concluded that cross over point does not change as pore morphology changes. End point relative permeability values change however. As the dominancy of vugs decreases, end point relative permeability values for wetting – phase increases. This result is reasonable since the matrix is constructed as a low porosity system and non – wetting phase recovery decreases due to high wetting – phase end point relative permeability. Non – wetting phase breakthrough during

primary drainage in vuggy carbonates can take place at values of capillary pressure much lower than capillary pressure of the matrix at breakthrough. In addition, depending on the degree of interconnectedness of the secondary pore network and the distribution of vuggy porosity, very different values of non – wetting phase saturation can be attained in carbonates characterized by the same value of breakthrough capillary pressure.

Wettability effects on capillary pressure and relative permeability curves are also examined by using different advancing angle ranges (Table 10). The vuggy base model is modified and cases for all water – wet, all oil – wet and partially water – wet (matrix water – wet, vugs oil – wet). The results are compared with vuggy base model and matrix model (Figures 38 and 39).

Table 10 – Advancing Angle Ranges for Vuggy Base Model (in degrees)

	Pore		Vug	
	Max	Min	Max	Min
Vuggy Base Model	160	30	160	30
Water-Wet	75	30	75	30
Oil-Wet	160	105	160	105

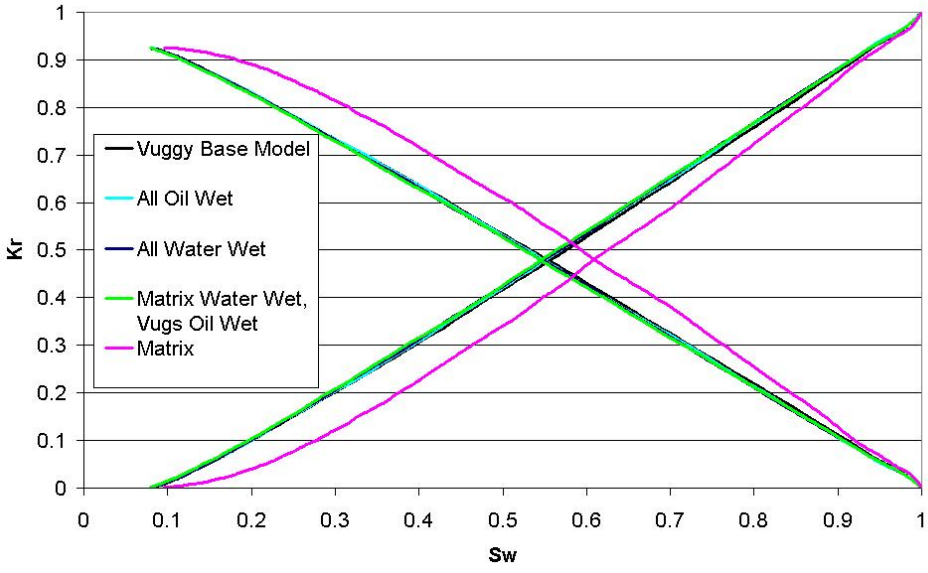

Figure 38 – Relative Permeability Curves for Vuggy Base Model (Wettability Analysis for Drainage)

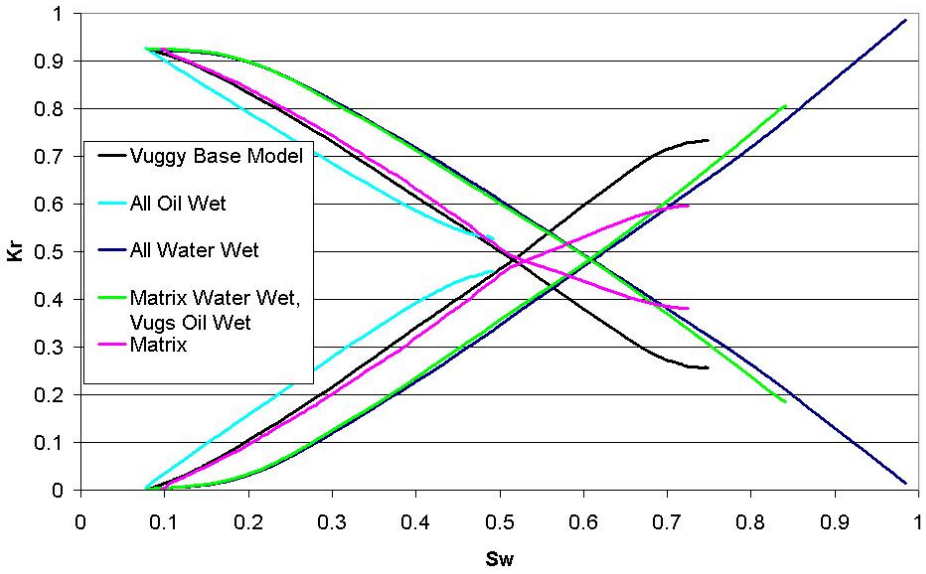

Figure 39 – Relative Permeability Curves for Vuggy Base Model (Wettability Analysis for Waterflooding)

Similar results with the base model are obtained for vuggy pore network model during wettability analysis. It can be observed that as the system becomes more water – wet, the end point relative permeabilities are affected and residual oil saturation decreases, similar to the results obtained by Blunt (1997). In primary drainage, wettability effects cannot be observed significantly since for all cases, receeding angle values are distributed within the same range. Wettability effects are obviously recognized in waterflooding. It is concluded that wettability drastically affect end point relative permeability values and thus residual oil saturation. Non – wetting and wetting – phase relative permeabilities are mostly affected by matrix, since for the cases in which matrix is water – wet, high non – wetting phase recoveries are observed. Bekri et al. (2004) reported similar results wettability contrast between secondary porosity features and matrix. It was stated that non – wetting phase mobility was favored as matrix becomes less oil – wet. Also, Moctezuma et al. (2003) demonstrated that as vugs became more oil – wet, end point relative permeability values were affected obviously and similar results are reported in this study. As a result, it can be concluded that the proposed pore network model successfully represents two – phase flow in vuggy carbonate rocks and, effects of matrix and secondary porosity features are reasonably illustrated.

CHAPTER 7

CONCLUSIONS

Two-phase flow in fissured and vuggy carbonates was studied by developing a new pore network model that consists of several sub-networks including matrix, vug and fissures. The matrix was constructed as spatially correlated since pore and throat radii were statistically related, where as the secondary porosity features were assigned randomly yielding a spatially uncorrelated pore network model. Primary drainage and imbibition processes were simulated and corresponding flow properties were determined. In order to investigate the effects of wettability on flow properties and mechanisms in heterogeneous carbonate rocks, sensitivity analyses were conducted for different wettability types. In addition, effects of pore morphology were examined and results were compared with the base model and literature. The following conclusions are drawn from the results obtained in this study:

- Heterogeneous porous media can be successfully represented by sub networks composed of matrix and secondary porosity features similar to the one constructed in this study,

- Wettability significantly influences on capillary pressure and relative permeability curves and thus residual oil saturation. End point relative permeability values are directly affected by wettability type.

- As the system becomes more water wet, residual oil saturation decreases and end point water relative permeassbility increases. This indicates that, higher recovery is favored for strongly water – wet systems, as it is reported in literature previously.

- In heterogeneous carbonates, matrix wettability directly affects end point relative permeability values. As matrix becomes oil – wet recovery decreases.

- It is observed that wettability type also influences on flow mechanisms, snap – off, piston –like advance and pore body filling, during imbibition. The preference between the mechanisms depends on contact angle and as system becomes water – wet, pore body filling mechanism is favored. In oil – wet systems, snap – off is mainly preferred.

- Pore morphology directly affects flow properties especially during primary drainage. As sizes of secondary porosity features increase, the system behaves like fractured media yielding linear relative permeability curves. As vugs and fissures get smaller, effect of secondary porosity features decreases and concavity of relative permeability curves increases.

- As vugs and fissures get larger, cross over point shifts to lower wetting phase saturation for primary drainage. This indicates that wettability behavior of a system is altered by changes in element size.

- For imbibition, change in pore morphology results drastic changes in end point relative permeability values. It is concluded that as size of secondary porosity features get smaller, end point relative permeability value of wetting phase increases.

CHAPTER 8

RECOMMENDATIONS

Pore network modeling is an effective tool in identification of flow mechanisms and determination of flow properties. By using the developed model in this study, it is shown that two – phase flow can be simulated in fissured and vuggy carbonates at pore scale. Also, effects of wettability on capillary pressure and relative permeability curves are examined. In this study, relative permeability values are determined by a new approach, rather than using Poiseuille's law. Improved studies can be conducted in order to compare the results obtained by using the aforementioned methodology and the ones obtained from Poiseuille's law and typical flow equations.

Further research studies can be conducted by using the aforementioned model and methodology, to determine three phase flow properties. Mechanisms like WAG or polymer injection can be simulated and corresponding flow properties, which are challenging to be determined experimentally, can be obtained. Moreover, by using pore space extraction tools, topologically equivalent pore network model can be used to simulate two or three phase flow in heterogeneous carbonates.

REFERENCES

Akin,S.,"Estimation of Fracture Relative Permeabilities From Unsteady State Corefloods", Journal of Petroleum Science and Engineering, 30, 2001, 1-14.

Al-Futaisi, A., Patzek, T. W., "Secondary Imbibition in NAPL- Invaded Mixed Wet Sediments", Journal of Contaminant Hydrology, 74, 2004, 61-81.

Al-Kharusi, A. S. Z., "Pore Scale Characterization of Carbonate Rocks", PhD Thesis, Imperial College, 2007.

Archie, G.E., "Classification of Carbonate Reservoir Rocks and Petrophysical Considerations", AAPG Bulletin, 36-6, 1952, 278-298.

Babadagli, T., Ershaghi, I., "Improved Modeling of Oil/Water Flow in Naturally Fractured Reservoirs Using Effective Fracure Relative Permeabilities", SPE 26076, Proceedings of the 1993 SPE Western Regional Meeting, Anchorage, Alaska, USA, 1993.

Bakke, S., Oren, P. E., "3-D Pore Scale Modeling of Sandstones and Flow Simulations in the Pore Network", SPE 35479, SPE Journal, Vol. 2, June 1997, 136-149.

Balhoff, M., "Modeling the Flow of Non-Newtonian Fluids in Packed Beds at the Pore Scale", PhD Thesis, Louisiana State University, 2005.

Bekri, S., Laroche, C., Vizika, O., "Pore Network Models to Calculate Transport and Electrical Properties of Single or Dual- Porosity Rocks", SCA 2005-35, Proceedings of 2005 International Symposium of the Society of Core Analysts, Toronto, Canada, 2005.

Bekri, S., Nardi, C., Vizika, O., "Effect of Wettability on the Petrophysical Parameters of Vuggy Carbonates: Network Modeling Investigation", SCA 2004-25, Proceedings of 2004 International Symposium of the Society of Core Analysts, Abu Dhabi, UAE, 2004.

Blunt, M., J, King, M., J, "Simulation and Theory of Two Phase Flow in Porous Media", Physical Review A, 46-12, December 1992, 7680-7702.

Blunt, M.J., "Flow in Porous Media – Pore Network Models and Multiphase Flow", Current Opinion in Colloid & Interface Science, 6, 2001, 197-207.

Blunt, M.J., "Pore Level Modeling of the Effects of Wettability", SPE Journal, 2, December 1997, 494-510.

Choquette, P.W, Pray, L.C., "Geologic Nomenclature and Classification of Porosity in Sedimentary Carbonates", AAPG Bulletin, 54, 1970, 207-250.

Dias, M. M., Payatakes, A. C., "Network Models for Two Phase Flow in Porous Media: 1. Immiscible Microdisplacement of Nonwetting Fluids", Journal of Fluid Mechanics, 164, 1986, 305-336.

Dodds, J.A., Lloyd, P.J., "A Model for the Void Structure in Multi-Component Sphere Packs Applied to Capillary Pressure Curves", Powder Technology, 5, 1971, 69- 76.

Dullien, F.A.L., "Porous Media: Fluid Transport and Pore Structure", 1992, San Diego, California: Academic Press Inc.

Dullien, F.A.L., Chatzis, I., El-Sayed, M.S., “Modeling Transport Phenomena in Porous Media by Networks Consisting of Non-Uniform Tubes”, SPE 6191, Proceedings of the 1976 Annual Fall Technical Conference and Exhibition of SPE of AIME, New Orleans, 1976.

Dunham, R.J., “Classification of Carbonate Rocks According to Depositional Texture”, Proceeding of AAPG Classification of Carbonate Rocks: A Symposium, 1962, 108-121.

Erzeybek, S., Akin, S., “Pore Network Modeling of Multiphase Flow in Fissured and Vuggy Carbonates”, SPE 113384, Proceedings of the 2008 SPE/DOE Improved Oil Recovery Symposium, Tulsa, OK, 2008.

Fatt, I., “The Network Model of Porous Media I. Capillary Pressure Characteristics”, Trans. AIME, 207, 1956, 144.

Fatt, I., “The Network Model of Porous Media II. Dynamic Properties of a Single Size Tube Network”, Trans. AIME, 207, 1956, 160.

Fatt, I., “The Network Model of Porous Media III. Dynamic Properties of Networks with Tube Radius Distribution”, Trans. AIME, 207, 1956, 164.

Fenwick, D.H., Blunt, M.J., “Network Modeling of Three-Phase Flow in Porous Media”, SPE Journal, March 1998, 86-97.

Hatiboğlu, C. H., “Automated Porosity Measurement Using Image Analysis Techniques”, M.Sc. Thesis, Middle East Technical University, 2002.

Heiba, A.A., Davis, H.T., Scriven, L.E., “Effect of Wettability on Two-Phase Relative Permeabilities and Capillary Pressures”, SPE 12172, Proceedings of the 1983 SPE Annual Technical Conference and Exhibition, San Francisco, CA, 1983.

Honarpour, M., Mahmood, S.M., SPE 18565, Relative Permeability Measurements: An Overview, SPE Technology Today Series, 1986.

Hughes, R.G., Blunt, M.J., "Network Modeling of Multiphase Flow in Fractures", Advances in Water Resources, 24, 2001, 409-421.

Hughes, R.G., Blunt, M.J., "Pore Scale Modeling of Rate Effects in Imbibition", Transport in Porous Media, 40, 2000, 295-322.

Hui, M.H., Blunt, M.J., "Pore Scale Modeling of Three-Phase Flow and the Effects of Wettability", SPE 59309, Proceedings of the 2000 SPE/DOE Improved Oil Recovery Symposium, Tulsa, OK, 2000.

Ioannidis, M.A., Chatzis, I., "A Dual-Network Model of Pore Structure for Vuggy Carbonates", SCA 2000-09, Proceedings of 2000 International Symposium of the Society of Core Analysts, Abu Dhabi, UAE, 2000.

Jardine, D., Andrews, D. P., Wischart, J. W., Young, J. W., "Distribution and Continuity of Carbonate Reservoirs", SPE 6139, Journal of Petroleum Technology, July 1977, 873-885.

Jia, C., Shing, K., Yortsos, Y. C., "Visualization and Simulation of Non-Aqueous Phase Liquids Solubilization in Pore Networks", Journal of Contaminant Hydrology, 35, 1999, 363-387.

Jia, L., "Reservoir Definition through Integration of Multiscale Petrophysical Data", Ph.D. Thesis, Stanford University, 2005.

Jin, G., Patzek, T. W., "Physics-Based Reconstruction of Sedimentary Rocks", SPE 83587, Proceeding of SPE Western Regional/ AAPG Pacific Section Joint Meeting, Long Beach, California, USA, 19-24 May, 2003.

Kamath, J., Xu, B., Lee, S.H., Yortsos, Y.C., "Use of Pore Network Models to Interpret Laboratory Experiments on Vugular Rocks", Journal of Petroleum Science and Technology, 20, 1998, 109-115.

Karaman, T., "Development of a Pore Network Model and a Neural Network Model To Be Coupled To Simulate Porous Medium", M.Sc. Thesis, Middle East Technical University, 2002.

Knackstedt, M. A., Sheppard, A. P., Sahimi, M., "Pore Network Modeling of Two Phase Flow in Porous Rock: The Effect of Correlated Heterogeneity", Advances in Water Resources, 24, 2001, 257 – 277.

Koplick, J., Lasseter, T.J., "Two Phase Flow in Random Network Models of Porous Media", SPEJ, February 1985, 89-100.

Larson, R.G., Scriven, L.E., Davis, H.T., "Percolation Theory of Two Phase Flow in Porous Media", Chemical Engineering Science, 36, 1981, 57-73.

Lenormand, R., Toubol, E., Zarcone, C., "Numerical Models and Experiments on Another in a Network of Capillary Ducts", Journal of Fluid Mechanics, 186, 1988, 165-187.

Lopez, X., Valvatne, P. H., Blunt, M. J., "Predictive Network Modeling of Single Phase Non-Newtonian Flow in Porous Media", Journal of Colloid and Interface Science, 264, 2003, 256-265.

Lu, C., Yortsos, Y. C., "A Pore Network Model of In-Situ Combustion in Porous Media", SPE 69705, Proceeding of SPE International Thermal Operations and Heavy Oil Symposium, Margarita, Venezuela, 12-14 March, 2001.

Lucia, F.J., “Petrophysical Parameters Estimated from Visual Descriptions of Carbonate Rocks: A Field Classification of Carbonate Pore Space”, Journal of Petroleum Technology, March 1983, 629- 637.

Lucia, F. J., Carbonate reservoir characterization, Berlin, Germany, Springer, 1999.

Mani, V., Mohanty, K. K., “Effect of Pore – Space Spatial Correlations on Two – Phase Flow in Porous Media”, Journal of Petroleum Science and Engineering, 23, 1999, 173 – 188.

Mazullo, S. J., “Overview of Porosity Evolution in Carbonate Rocks”, Kansas Geological Society Bulletin, 79, 1, 2004.

Moctezuma, A., Bekri, S., Laroche, C., Vizika, O., “A Dual Network Model for Relative Permeability of Bimodal Rocks: Application in a Vuggy Carbonate”, SCA2003-12, Proceedings of 2003 International Symposium of the Society of Core Analysts, Pau, France, 2003.

Mogensen, K., Stenby, E.H., “A Dynamic Two-Phase Pore-Scale Model of Imbibition”, Transport in Porous Media, 32, 1998, 299-327.

Moore, C.H., “Carbonate Reservoirs Porosity Evolution and Diagenesis in a Sequence Stratigraphic Framework”, 2001, Amsterdam, The Netherlands, Elsevier Scientific Publ. Co.

Murray, R.C., “Origin of Porosity in Carbonate Rocks”, Journal of Sedimentary Petrology, 30, 1, 1960, 59-84.

Nguyen, V.H., Sheppard, A.P., Knackstedt, M.A., Pinczewski, W.V., “The Effects of Displacement Rate and Wettability on Imbibition Relative Permeabilities”, SCA2005-39, Proceedings of 2005 International Symposium of the Society of Core Analysts, Toronto, Canada, 2005.

Nilsen, L. S., Oren, P.E. and Bakke, S., “Prediction of Relative Permeability and Capillary Pressure from a Pore Model”, SPE 35531, Proceedings of the European 3-D Reservoir Modeling Conference, Stavanger, Norway, 1996.

Okabe, H., “Pore Scale Modeling of Carbonates”, Ph.D. Thesis, University of London, Diploma, Imperial College, 2004.

Oren, P.E., Bakke, S., Arntzen, O.J., “Extending Predictive Capabilities to Network Models”, SPE 38880, Proceedings of the 1997 SPE Annual Technical Conference and Exhibition, San Antonio, Texas, 1997.

Patzek, T. W., Silin, D.B., “Shape Factor and Hydraulic Conductance in Noncircular Capillaries I. One-Phase Creeping Flow”, Journal of Colloid and Interface Science, 236, 2001, 295-304.

Patzek, T.W., “Verification of a Complete Pore Network Simulator of Drainage and Imbibition”, SPE 59312, Proceedings 2000 of the SPE/DOE Improved Oil Recovery Symposium, Tulsa, OK, 2000.

Peacock, D.C.P., Mann, A “Evaluation of the Controls on Fracturing in Reservoir Rocks”, Journal of Petroleum Geology, 28-4, 2005, 385-396.

Piri, M., “Pore-Scale Modeling of Three-Phase Flow”, Ph.D. Thesis, Imperial College, 2003.

Piri, M., Blunt, M.J., “Three- Dimensional Mixed Wet Random Pore Scale Network Modeling of Two and Three Phase Flow in Porous Media I. Model Description”, Physical Review E., 71, 2005, 26301/1-26301-30.

Radke, C.J., Kovscek, A.R., Wong, H., “A Pore-Level Scenario for the Development of Mixed Wettability in Oil Reservoirs”, SPE 24880, Proceedings of the 1992 SPE Annual Technical Conference and Exhibition, Washington, DC, 1992.

Romm, E.S., “Fluid Flow in Fractured Rocks”, Nedra Publishing House, Moscow, 1966.

SLB, Schlumberger, Carbonate Reservoirs, (Last accessed in April, 2008) http://www.slb.com/media/services/solutions/reservoir/carbonate_reservoirs.p

Sochi, T., “Pore-Scale Modeling of Non-Newtonian Flow in Porous Media”, PhD Thesis, Imperial College, 2007.

Tomeczek, J., Mlonka, J., “The Parameters of a Random Pore Network with Spherical Vesicles for Coal Structure Modeling”, Fuel, Vol. 77, 15, 1998, 1841-1844.

Uzun, I., “Use Of Pore Scale Simulators to Understand the Effects of Wettability on Miscible Carbon Dioxide Flooding and Injectivity”, M.Sc. Thesis, Middle East Technical University, 2005.

Valvatne, P.H., “Predicting Pore-Scale Modeling of Multiphase Flow”, Ph.D. Thesis, Imperial College, 2004.

Valvatne, P.H., Blunt, M.J., “Predictive Pore-Scale Network Modeling”, SPE 84550, Proceedings of the 2003 SPE Annual Technical Conference and Exhibition, Denver, Colorado, 2003.

Wilkinson, D., Willemsen, J.F., “Invasion Percolation: A New Form of Percolation Theory”, Journal of Physics A: Math. Gen., 1983, 16, 3365-3376.

Wilson-Lopez, R.V., Rodriguez, F., “A Network Model for Two-Phase Flow in Microfractures Porous Media”, SPE 92056, Proceedings of 2004 SPE International Petroleum Conference, Puebla, Mexico, 2004.

APPENDIX A

MATLAB CODE FOR PORE NETWORK CONSTRUCTION

```
%Matrix Construction Function (17.10.2007)
function [Model]=model_const(R_max,R_min,x,a,c,Approach,min,max,mu,sig,n)
clear all
fid1=fopen('pore_size.dat','r');
fid2=fopen('pore_properties.dat','r');
fid3=fopen('model_prop.dat','r');
fid4=fopen('contact_angles.dat','r');
fid5=fopen('pore_throat_size.dat','r+');
fid6=fopen('fissure_size.dat','r');
fid7=fopen('vug_size.dat', 'r');

pore_prop;
pore_throat;
Pore_Model_Cons;
model;
g_w;

%===== Pore Properties Function==========
%Inscribed radius calculation,total area calculation and pore size distribution
function [At,R_ins,alpha,nc] =pore_prop(R_max,R_min,x,a,c,Approach,n)
global At R_ins alpha n nc n_p theta_0 theta_1 theta_ow
%Lengths are in meter
n=fscanf(fid3, '%g %g',[1,1]);  %model size
n_p=n^3; %number of pores
Radius=fscanf(fid1,'%g', [2,n_p]); %Radius values are gathered.

%Constants, From Blunt (2000)
delta=0.3;
gamma=1.8;
x=0+(1-0)*rand(n_p,1);

%Inscribed radius calculation
R_max=0.000006535;
R_min=0.000001206;
R_ins=(R_max-R_min).*(-delta*log(x.*(1-exp(-1/delta))+exp(-1/delta))).^(1/gamma)+R_min;
%Inscribed Radius

%Distribution
maximum=max2(R_ins)/2;
minimum=min2(R_ins)/2;
m=mean(R_ins)/2;
s=std(R_ins)/2;
range_vals=[maximum;minimum;m;s];
fprintf(fid5,'%g\n', range_vals);
```

```
fclose(fid5)
hist(R_ins)
prop=fscanf(fid2,'%g',[1,3]);

a=prop(1);
if a==1;
dist1= normpdf(R_ins,m,s);
end
if a==2;
dist2= lognpdf(R_ins,m,s);
end

%Cross section type and total area calculation
Approach=prop(2);
c=prop(3); %Cross section type (Square:1, Equilateral Triangle:2, Circular:3)

%Alpha is half-angle of each corner of a polygon
if Approach==1; %Blunt's Total Area Approach
disp('Blunts Total Area Approach is used')
if c==1;
alpha=pi()/4; %For square,in radians
nc=4; %# of corners
At= nc.*R_ins.^2*cot(alpha); %Total area calculation, from Blunt 2001
end

if c==2;
alpha=pi()/6; %For equilateral triangle, in radians
nc=3; %# of corners
At= nc.*R_ins.^2*cot(alpha); %Total area calculation, from Blunt 2001
end
if c==3;
disp('Geometric Approach is used instead of Blunts Approach for circular cross sections')
alpha=0; %For circular, in radians
r=R_ins ; %Radius of circle
At=pi()*r.^2; %Total Area calculation by geometric approach
nc=1;
end
end

if Approach==2 %Geometric Approach
disp('Geometric Approach is used for Total Area Calculation')
if c==1;
alpha=pi()/4; %For square,in radians
E=2*R_ins;    %Edge of square
At=E.*E; %Cross sectional area
nc=4;
end
if c==2;
alpha=pi()/6; %For equilateral triangle, in radians
E=2*R_ins*sqrt(3); %Edge of equilateral triangle
H=3*R_ins;        %Height of equilateral triangle
At= E.*H/2;
nc=3;
end
if c==3;
alpha=0; %For circular, in radians
r=R_ins ; %Radius of circle
At=pi()*r.^2;
```

```
nc=1;
end
end

angles=deg2rad(fscanf(fid4,'%g',[2,3]));
theta_0=angles(1,1); %Contact angle during primary drainage before wettability change
theta_rec=angles(:,2); %Receding Contact Angle Range (radians)(Patzek,2000)
theta_1=theta_rec(1,1)+(theta_rec(2,1)-theta_rec(1,1))*rand((2*n-1)^3,1); %Contact angle during primary drainage after wettability change (radians)
theta_adv=angles(:,3); %Advancing Contact Angle Range (radians)(Patzek,2000)
theta_ow= theta_adv(1,1)+(theta_adv(2,1)-theta_adv(1,1))*rand((2*n-1)^3,1); %Advancing Contact Angle
end %End of Pore Properties function

%=====Pore Throat Properties Function======
%Pore throat size and distribution
function [R_throat,At_throat,l_throat]=pore_throat(min_t,max_t,mu,sig,n,R_ins)

global At R_ins alpha n nc n_p theta_0 theta_1 theta_ow
global R_throat At_throat l_throat n_t

n_t=(5*n^2-2*n)*(n-1); %Number of throats
%Lengths are in meter
fid5=fopen('pore_throat_size.dat','r');
range=fscanf(fid5,'%g');
min_t=range(2);
max_t=range(1);
delta=0.8;
gamma=1.6;

x=0+(1-0)*rand(n_t,1);
R_throat=(max_t-min_t).*(-delta*log(x*(1-exp(-1/delta))+exp(-1/delta))).^(1/gamma)+min_t;
%Randomly distributed throat radius (Blunt)
mu=mean(R_throat);
sig=std(R_throat);
l_throat=mu+ sig*randn(n_t,1);  %Randomly distributed throat length

%Eliminate zero and negative values of l_throat
for i=1:n_t
if l_throat(i,1)==0
l_throat(i,1)=0.0001; %Set zero values of l_throat to 0.0001
end
if l_throat(i,1)<0
l_throat(i,1)=abs(l_throat(i,1)); %Set negative values of l_throat to its absolute value
else
l_throat(i,1)=l_throat(i,1);
end
end

%Cross section is assumed as square
At_throat=4.*R_throat.^2*cot(pi/4); %Total area calculation, from Blunt 2001
end %End of Pore Throat Properties Function

%==========Pore Model Construction Function=========
%Pore Model Construction
%Lengths are in meter
function [Pore_Model_Const,Elm,Type]=Pore_Model_Cons(R_ins, R_throat, alpha, nc, At, n)
```

```
global At R_ins alpha n nc n_p theta_0 theta_1 theta_ow
global R_throat At_throat l_throat n_t
global Pore_Model_Const Pore_Model Location Elm Type Matrix_Model
format long
%Maximum coordination number of 3-D model is 6

%Required # of pore radius is gathered
R_p(:,1)=R_ins(:,1);

%Required # of pore throat radius is gathered. Control for pore throat radius distribution of
Pore_Model
R_t(:,1)=R_throat(:,1);

%========Pore Model Construction=========%
disp('Pore Model Before Construction')
Pore_Model=cell([2*n-1,2*n-1,2*n-1]);
%Location=cell([2*n-1,2*n-1,2*n-1]);
Pore_Model(:,:,:)={0};
disp(Pore_Model);
%Pores
a=1;
b=1;
c=1;%Counter for R_ins
num=1;
for k=1:1:2*n-1
if rem(k,2)~=0;
for j=1:1:2*n-1
   if rem(j,2)~=0;
      for i=1:2:2*n-1;
         Pore_Model(i,j,k)={[R_ins(c,1) At(c,1) theta_ow(a,1) theta_1(a,1) 0]};
         Location(i,j,k).C=1;
         Location(i,j,k).T='p';
         Elm(num,1)=i;
         Elm(num,2)=j;
         Elm(num,3)=k;
         Type(num,1)=1; %1 stands for pore
         num=num+1;
         a=a+1;
         c=c+1;
      end

      for i=2:2:2*n-2;
      Pore_Model(i,j,k)={[R_throat(b,1) At_throat(b,1) theta_ow(a,1)  theta_1(a,1) l_throat(b,1)]};
         Location(i,j,k).C=1;
         Location(i,j,k).T='t';
         Elm(num,1)=i;
         Elm(num,2)=j;
         Elm(num,3)=k;
         Type(num,1)=4; %4 stands for throat
         num=num+1;
         a=a+1;
         b=b+1;
      end
   else
      for i=1:2:2*n-1;
         Pore_Model(i,j,k)={[R_throat(b,1) At_throat(b,1) theta_ow(a,1)
           theta_1(a,1) l_throat(b,1)]};
         Location(i,j,k).C=1;
```

```
            Location(i,j,k).T='t';
            Elm(num,1)=i;
            Elm(num,2)=j;
            Elm(num,3)=k;
            Type(num,1)=4; %4 stands for throat
            num=num+1;
            a=a+1;
            b=b+1;
        end
        for i=2:2:2*n-2;
            Pore_Model(i,j,k)={[0 0 0 0 0]};
            Location(i,j,k).C=0;
            Location(i,j,k).T='m';
            Elm(num,1)=i;
            Elm(num,2)=j;
            Elm(num,3)=k;
            Type(num,1)=5; %5 stands for null
            num=num+1;
        end
    end
end

else
for j=1:1:2*n-1
    if rem(j,2)~=0;
        for i=1:1:2*n-1;
            Pore_Model(i,j,k)={[R_throat(b,1) At_throat(b,1) theta_ow(a,1) theta_1(a,1)
              l_throat(b,1)]};
            Location(i,j,k).C=1;
            Location(i,j,k).T='t';
            Elm(num,1)=i;
            Elm(num,2)=j;
            Elm(num,3)=k;
            Type(num,1)=4; %4 stands for throat
            num=num+1;
            a=a+1;
            b=b+1;
        end
    else
        for i=1:2:2*n-1;
            Pore_Model(i,j,k)={[R_throat(b,1) At_throat(b,1) theta_ow(a,1) theta_1(a,1)
              l_throat(b,1)]};
            Location(i,j,k).C=1;
            Location(i,j,k).T='t';
            Elm(num,1)=i;
            Elm(num,2)=j;
            Elm(num,3)=k;
            Type(num,1)=4; %4 stands for throat
            num=num+1;
            b=b+1;
            a=a+1;
        end
        for i=2:2:2*n-2;
            Pore_Model(i,j,k)={[0 0 0 0 0]};
            Location(i,j,k).C=0;
            Location(i,j,k).T='m';
            Elm(num,1)=i;
            Elm(num,2)=j;
```

```
        Elm(num,3)=k;
        Type(num,1)=5; %5 stands for null
        num=num+1;
      end
   end
end
end
end

Matrix_Model=Pore_Model;
matrix={'Pore_Radius','Throat_Radius','Throat_Length','Receeding_Ang','Advancing_Angle'};%;
R_throat, l_throat, theta_1, theta_ow};
xlswrite('Sim_Results.xls', matrix, 'Matrix_Prop', 'A1');
xlswrite('Sim_Results.xls', R_ins, 'Matrix_Prop', 'A2');
xlswrite('Sim_Results.xls', R_throat, 'Matrix_Prop', 'B2');
xlswrite('Sim_Results.xls', l_throat, 'Matrix_Prop', 'C2');
xlswrite('Sim_Results.xls', theta_1, 'Matrix_Prop', 'D2');
xlswrite('Sim_Results.xls', theta_ow, 'Matrix_Prop', 'E2');
end %End of Pore Model Construction Function

%============Model Construction Function=============%
%Inserts fissures and vugs into the matrix constructed by previous function. %Fissures and vugs are assummed to have square cross-sections.
function [Model,Model_Areas,num_p,num_t,num_fis,num_v,num_null]=model( Pore_Model, Location, n, n_t, n_p, theta_1, theta_ow, Elm,Type)
global Pore_Model Location n n_t n_p theta_1 theta_ow
global Model Model_Areas At_f At_v Type Elm num_p num_t num_fis num_v num_null

n_v=round(0.1*(n_t+n_p)); %Number of vugs
n_f=round(0.1*(n_t+n_p)); %Number of fissures

theta_1_new=theta_1(n_t+n_p+1:end);
theta_ow_new= theta_ow(n_t+n_p+1:end);

%Fissure Coordinates are assigned randomly
l_f=myrandint(1,1,[n-3:n-1]);
num_f=round(n_f/l_f);

%Constants, From Blunt (2000)
delta=0.8;
gamma=1.8;
xv=0+(1-0)*rand(n_v,1)
xf=0+(1-0)*rand(n_f,1);

%R_ins for Fissures are calculated
Fissure_R=fscanf(fid6,'%g %g',[2,1]);
R_f_min=Fissure_R(1);
R_f_max=Fissure_R(2);
R_f=(R_f_max-R_f_min).*(-delta*log(xf.*(1-exp(-1/delta))+exp(-1/delta))).^(1/gamma)+R_f_min
%Inscribed Radius
At_f= 4.*R_f.^2*cot(pi/4); %Total area calculation, from Blunt 2001. Fissures are assumed to have square cross-section

%R_ins for Vugs are calculated
Vug_R=fscanf(fid7,'%g %g',[2,1]);
R_v_min=Vug_R(1);
R_v_max=Vug_R(2);
```

```
R_v=(R_v_max-R_v_min).*(-delta*log(xv.*(1-exp(1/delta))+exp(1/delta))) ^(1/gamma)
+R_v_min; %Inscribed Radius
At_v= 4.*R_v.^2*cot(pi/4); %Total area calculation, from Blunt 2001.Vugs are assumed to have
square cross-section
dbstop error

%================Fissures are distributed==================%
a=1;
counter=1;
x_f=myrandint(1,1,[1:2*n-1]);
y_f=myrandint(1,1,[1:2*n-1-l_f]);
z_f=myrandint(1,1,[1:2*n-1]);
while counter<=num_f
if Location(x_f,y_f,z_f).T~='f' % & Location(x_f,y_f+l_f-1,z_f).T~='f';
if Location(x_f,y_f,z_f).C==1
   Pore_Model{x_f,y_f,z_f}(1)=R_f(a,1);
   Pore_Model{x_f,y_f,z_f}(2)=At_f(a,1);
   Location(x_f,y_f,z_f).C=1;
   Location(x_f,y_f,z_f).T='f';
   I=findn(Elm(:,1)==x_f & Elm(:,2)==y_f & Elm(:,3)==z_f);
   Type(I,1)=2; %2 stands for Fissure
else
   Pore_Model(x_f,y_f,z_f)={[R_f(a,1) At_f(a,1) theta_ow_new(a,1)
    theta_1_new(a,1) l_f]};
   Location(x_f,y_f,z_f).C=1;
   Location(x_f,y_f,z_f).T='f';
   I=findn(Elm(:,1)==x_f & Elm(:,2)==y_f & Elm(:,3)==z_f);
   Type(I,1)=2; %2 stands for Fissure
end

for j=1:l_f-1
   if Location(x_f,y_f+l_f-1,z_f).C==1
      Pore_Model{x_f,y_f+j,z_f}(1)=R_f(a+j,1);
      Pore_Model{x_f,y_f+j,z_f}(2)=At_f(a+j,1);
      Location(x_f,y_f+j,z_f).C=1;
      Location(x_f,y_f+j,z_f).T='f';
      I=findn(Elm(:,1)==x_f & Elm(:,2)==y_f & Elm(:,3)==z_f);
      Type(I,1)=2; %2 stands for Fissure
   else
      Pore_Model(x_f,y_f+j,z_f)={[R_f(a+j,1) At_f(a+j,1) theta_ow_new(a+j,1)
        theta_1_new(a+j,1) l_f]};
      Location(x_f,y_f+j,z_f).C=1;
      Location(x_f,y_f+j,z_f).T='f';
      I=findn(Elm(:,1)==x_f & Elm(:,2)==y_f & Elm(:,3)==z_f);
      Type(I,1)=2; %2 stands for Fissure
   end
end
a=a+l_f-1;
counter=counter+1;
x_f=myrandint(1,1,[1:2*n-1]);
y_f=myrandint(1,1,[1:2*n-1-l_f]);
z_f=myrandint(1,1,[1:2*n-1]);
else
x_f=myrandint(1,1,[1:2*n-1]);
y_f=myrandint(1,1,[1:2*n-1-l_f]);
z_f=myrandint(1,1,[1:2*n-1]);
end
end
```

```
%===============Vugs are distributed====================%
counter=1;
a=1;
i=1;
%Vug Coordinates are assigned randomly
x_v=myrandint(n_v,1,[1:2*n-1]);
y_v=myrandint(n_v,1,[1:2*n-1]);
z_v=myrandint(n_v,1,[1:2*n-1]);
while counter<=n_v
if Location(x_v(i),y_v(i),z_v(i)).T~='v' % & Location(x_f,y_f+l_f-1,z_f).T~='f';
if Location(x_v(i),y_v(i),z_v(i)).C==1
   Pore_Model{x_v(i),y_v(i),z_v(i)}(1)=R_v(a,1);
   Pore_Model{x_v(i),y_v(i),z_v(i)}(2)=At_v(a,1);
   Location(x_v(i),y_v(i),z_v(i)).C=1;
   Location(x_v(i),y_v(i),z_v(i)).T='v';
   I=findn(Elm(:,1)==x_v(i) & Elm(:,2)==y_v(i) & Elm(:,3)==z_v(i));
   Type(I,1)=3; %3 stands for Vug
else
    Pore_Model(x_v(i),y_v(i),z_v(i))={[R_v(a,1) At_v(a,1) theta_ow_new(a,1)
    theta_1_new(a,1) 0]};
   Location(x_v(i),y_v(i),z_v(i)).C=1;
   Location(x_v(i),y_v(i),z_v(i)).T='v';
   I=findn(Elm(:,1)==x_v(i) & Elm(:,2)==y_v(i) & Elm(:,3)==z_v(i));
   Type(I,1)=3; %3 stands for Vug
end
a=a+1;
counter=counter+1;
i=i+1;
else
x_v(i)=myrandint(1,1,[1:2*n-1]);
y_v(i)=myrandint(1,1,[1:2*n-1]);
z_v(i)=myrandint(1,1,[1:2*n-1]);
end
end
%%
num_p=0;
num_t=0;
num_fis=0;
num_v=0;
num_null=0;

for k=1:1:2*n-1;
for j=1:1:2*n-1;
for i=1:1:2*n-1;
   El_Type=Location(i,j,k).T;
   El_Loc(i,j,k)=Location(i,j,k).T;
   El_Cor(i,j,k)=Location(i,j,k).C;
   switch (El_Type)
      case 'p'
         num_p=num_p+1;
      case 't'
         num_t=num_t+1;
      case 'f'
         num_fis=num_fis+1;
      case 'v'
         num_v=num_v+1;
      case 'm'
         num_null=num_null+1;
```

```
   end

   if Location(i,j,k).C==1
      Model(i,j,k)=Pore_Model{i,j,k}(1);
      Model_Areas(i,j,k)=Pore_Model{i,j,k}(2);
      Angle_ow(i,j,k)= Pore_Model{i,j,k}(3);
      Angle_1(i,j,k)= Pore_Model{i,j,k}(4);
      ele_l(i,j,k)= Pore_Model{i,j,k}(5);
   end
end
end
end
hist(nonzeros(reshape(Model,(2*n-1)^3,1)))
radius=reshape(Model,(2*n-1)^3,1);
area_mod=reshape(Model_Areas,(2*n-1)^3,1);
angles1=reshape(Angle_1,(2*n-1)^3,1);
angles_ow=reshape(Angle_ow,(2*n-1)^3,1);
el_length=reshape(ele_l,(2*n-1)^3,1);
Loc_C=reshape(El_Cor,(2*n-1)^3,1);
Loc_T=reshape(El_Loc,(2*n-1)^3,1);

Model_backup={'Model_R','Area','Receeding_Ang','Advancing_Angle' 'Element Length' 'Number
of Pores' 'Number of Throats' 'Number of Fissures' 'Number of Vugs' 'Number of Nulls' 'Loc_C'
'Loc_T'};
xlswrite('Sim_Results.xls', Model_backup, 'Secondary Porosity', 'A1');
xlswrite('Sim_Results.xls', radius, 'Secondary Porosity', 'A2');
xlswrite('Sim_Results.xls', area_mod, 'Secondary Porosity', 'b2');
xlswrite('Sim_Results.xls',angles1 , 'Secondary Porosity', 'c2');
xlswrite('Sim_Results.xls', angles_ow, 'Secondary Porosity', 'd2');
xlswrite('Sim_Results.xls', el_length, 'Secondary Porosity', 'e2');
xlswrite('Sim_Results.xls', num_p, 'Secondary Porosity', 'f2');
xlswrite('Sim_Results.xls', num_t, 'Secondary Porosity', 'g2');
xlswrite('Sim_Results.xls', num_fis, 'Secondary Porosity', 'h2');
xlswrite('Sim_Results.xls', num_v, 'Secondary Porosity', 'i2');
xlswrite('Sim_Results.xls', num_null, 'Secondary Porosity', 'j2');
xlswrite('Sim_Results.xls', Loc_C, 'Secondary Porosity', 'k2');
xlswrite('Sim_Results.xls', Loc_T, 'Secondary Porosity', 'l2');

end %End of Model Function

%============Water Conductance Function===========%
%Poiseuille's law for flow in a circular cylinder approach is used (Blunt,2000).
function [W_conduct]=g_w(Model,n,Location)
global n
global Model Location Model_Areas
global W_conduct

for k=1:1:2*n-1;
for j=1:1:2*n-1;
for i=1:1:2*n-1;
   if Location(i,j,k).C==1;
      %Calculation of water conductance of pore in m^4
      W_conduct(i,j,k)=(pi*(sqrt(Model_Areas(i,j,k)/pi)+Model(i,j,k)).^4)/128;
   end
end
end
end
end %End of Water Conductance Function
```

```
%=========================================================%
global Model n Type Elm num_p num_t num_fis num_v num_null
pause
clf
plot3_Model([Elm(:,1) Elm(:,3) Elm(:,2)],[Type],'o',5);
disp('Model_Constructed=')
end%End of Model Construction Function
```

APPENDIX B

CODE FOR PRIMARY DRAINAGE

B.1. Flow In Primary Drainage

```
%======Primary Drainage Function =====%
function [P_cap]=Pres_Dist4(Pc_thres,Pore_Model)
clear
load model_prop.dat
global alpha n %From pore_prop function
global Pore_Model Location %From Pore_Model_Construction function
global Pc_thres Pc_drain Pc_ow_max b_pin Coord g_w g_nw Ac Ao S_water S_oil%From
Primary Drainage
global P_I Unfilled Filled_Cor kr_oil kr_water %Pressure
global sig_ow %Oil/Water interfacial tension (N/m)
global Model_Areas Model W_conduct At At_f At_v At_throat

sig_ow=model_prop(2);
%Pres=Pc_thres; %Pc_thres for drainage, Pc_thresh for imbibition
Model_Area=sum(reshape(Model_Areas,(2*n-1)^3,1));

g_nw=zeros(2*n-1,2*n-1,2*n-1);
g_w=zeros(2*n-1,2*n-1,2*n-1);
gIJ_w=zeros(2*n-1,2*n-1,2*n-1);
S_water=zeros(2*n-1,2*n-1,2*n-1);
S_oil=zeros(2*n-1,2*n-1,2*n-1);
Ao=zeros(2*n-1,2*n-1,2*n-1);
Ac=zeros(2*n-1,2*n-1,2*n-1);

count=1;
for k=1:1:2*n-1;
   for j=1:1:2*n-1;
      for i=1:1:2*n-1;
         if Location(i,j,k).C==1;
           Pc_thres(i,j,k)=feval(@Pri_Drain,Pore_Model{i,j,k}(4), Pore_Model{i,j,k}(1));
         g_w(i,j,k)=W_conduct(i,j,k);
            if Location(i,j,k).T=='t'
               g_wet.t(i,j,k)=g_w(i,j,k);
               g_nwet.t(i,j,k)=0;
            end
           S_water(i,j,k)=Model_Areas(i,j,k)/Model_Area;
           Coord(i,j,k)=count;
           Unfilled.x(count)=i;
           Unfilled.y(count)=j;
           Unfilled.z(count)=k;
           Phase(count)=0;
```

```
          count=count+1;
        end
      end
   end
end

g_total=W_conduct;
Pc_drain=zeros(2*n-1,2*n-1,2*n-1);
Total_Conductance=sum(sum(sum(W_conduct)));
kr_water=g_w/Total_Conductance;

%====Compare Calculated Capillary Pressures with Threshold Pressures====%
num=1;
t=1;
Filled.x(num)=0;
Filled.y(num)=0;
Filled.z(num)=0;
Mod(:,1)=Unfilled.x;
Mod(:,2)=Unfilled.y;
Mod(:,3)=Unfilled.z;

j=1; %Flow starts from the first column
P_list.P=nonzeros(Pc_thres(:,1,:));
P_list.Coordinates=nonzeros(Coord(:,1,:));
Sw=sum(sum(sum(S_water)));

while length(P_list.P)~=0
   [Pc,I]=min2(P_list.P);
   [Loc]=findn(Coord(:,:,:)==P_list.Coordinates(I));
   x1=Loc(1);
   y1=Loc(2);
   z1=Loc(3);
   Pc_drain(x1,y1,z1)=Pc;
   contr=any(x1==Filled.x(:)& y1==Filled.y(:) & z1==Filled.z(:));
   [Neigh,Indices]=feval(@Neigh_P,x1,y1,z1,Pc_thres);

if contr==0
      Filled.x(num)=x1;
      Filled.y(num)=y1;
      Filled.z(num)=z1;
      Capil_P(num)=Pc;
      %Calculation of Conductance for each phase at pore or throat

[g_nw(x1,y1,z1),g_w(x1,y1,z1),Ac(x1,y1,z1),Ao(x1,y1,z1)]=feval(@conduct_drain,Pc,Pore_Mod
el{x1,y1,z1}(4),Pore_Model{x1,y1,z1}(2),Pore_Model{x1,y1,z1}(1));
      if Location(x1,y1,z1).T=='t'
         g_nwet.t(x1,y1,z1)=g_nw(x1,y1,z1);
         g_wet.t(x1,y1,z1)=g_w(x1,y1,z1);
      end

%Calculation of Saturation
[S_oil(x1,y1,z1),S_water(x1,y1,z1)]=feval(@Cal_Sat,Ao(x1,y1,z1),Ac(x1,y1,z1),Model_Area);
      Water_Sat(num)=S_water(x1,y1,z1);
      Oil_Sat(num)=S_oil(x1,y1,z1);
      Total_Sat(num)=Water_Sat(num)+Oil_Sat(num);
      Phase(num)=1;
```

```
%Calculation of Relative Permeability
[kr_oil(x1,y1,z1),kr_water(x1,y1,z1)]=feval(@Cal_kr,g_nw(x1,y1,z1),g_w(x1,y1,z1),Total_Cond
uctance);

num=num+1;
end %End of if contr==0

   for a=1:length(Neigh) %Check for Neighbor elements
      if  Pc_drain(Indices.xx(a),Indices.yy(a),Indices.zz(a))==0;
         if Pc>=Neigh(a);
            Pc_drain(Indices.xx(a),Indices.yy(a),Indices.zz(a))=Pc; %Set Drainage
              Capillary of the element to Pc
            Filled.x(num)=Indices.xx(a);
            Filled.y(num)=Indices.yy(a);
            Filled.z(num)=Indices.zz(a);
            Capil_P(num)=Pc;
            Phase(num)=1;

%Calculation of Conductance for each phase
[g_nw(Indices.xx(a),Indices.yy(a),Indices.zz(a)),g_w(Indices.xx(a),Indices.yy(a),Indices.zz(a)),Ac
(Indices.xx(a),Indices.yy(a),Indices.zz(a)),Ao(Indices.xx(a),Indices.yy(a),Indices.zz(a))]=
feval(@conduct_drain,Pc,Pore_Model{Indices.xx(a),Indices.yy(a),Indices.zz(a)}(4),Pore_Model{I
ndices.xx(a),Indices.yy(a),Indices.zz(a)}(2),Pore_Model{Indices.xx(a),Indices.yy(a),Indices.zz(a)
}(1));

%Calculation of Saturation
[S_oil(Indices.xx(a),Indices.yy(a),Indices.zz(a)),S_water(Indices.xx(a),Indices.yy(a),Indices.zz(a))
]=feval(@Cal_Sat,Ao(Indices.xx(a),Indices.yy(a),Indices.zz(a)),Ac(Indices.xx(a),Indices.yy(a),Ind
ices.zz(a)),Model_Area);

Water_Sat(num)=S_water(Indices.xx(a),Indices.yy(a),Indices.zz(a));
Oil_Sat(num)=S_oil(Indices.xx(a),Indices.yy(a),Indices.zz(a));
Total_Sat(num)=Water_Sat(num)+Oil_Sat(num);

%Calculation of Relative Permeability
[kr_oil(Indices.xx(a),Indices.yy(a),Indices.zz(a)),kr_water(Indices.xx(a),Indices.yy(a),Indices.zz(a
))]=feval(@Cal_kr,g_nw(Indices.xx(a),Indices.yy(a),Indices.zz(a)),g_w(Indices.xx(a),Indices.yy(a
),Indices.zz(a)),Total_Conductance); %g_total(Indices.xx(a),Indices.yy(a),Indices.zz(a)));%

num=num+1;

%Eliminate the pressure of filled element if it is included in pressure list (P_list)
contr=any(Coord(Indices.xx(a),Indices.yy(a),Indices.zz(a))==P_list.Coordinates(:));

if contr==1
[Loc_f]=findn(Coord(Indices.xx(a),Indices.yy(a),Indices.zz(a))==P_list.Coordinates(:));
P_list.P(Loc_f)=[];
P_list.Coordinates(Loc_f)=[];
end

%Find neighbors of the filled element
[Neigh_f,Indices_f]=feval(@Neigh_P,Indices.xx(a),Indices.yy(a),Indices.zz(a), Pc_thres);
            for i=1:length(Neigh_f)
               if Pc_drain(Indices_f.xx(i),Indices_f.yy(i),Indices_f.zz(i))==0;
                     contr=any(Coord(Indices_f.xx(i),Indices_f.yy(i),Indices_f.zz(i))==P_list.Coordi
                     nates(:));
                  if contr==0
```

```
                        P_list.P(length(P_list.P)+1)=Pc_thres(Indices_f.xx(i),
                        Indices_f.yy(i),Indices_f.zz(i));
                        P_list.Coordinates(length(P_list.Coordinates)+1)=Coord(Indices_f.xx(i)
                        ,Indices_f.yy(i),Indices_f.zz(i));
                    end
                end
            end
else %Else of if contr==1
contr=any(Coord(Indices.xx(a),Indices.yy(a),Indices.zz(a))==P_list.Coordinates(:));
          if contr==0
          P_list.P(length(P_list.P)+1)=Pc_thres(Indices.xx(a),Indices.yy(a), Indices.zz(a));
          P_list.Coordinates(length(P_list.Coordinates)+1)=Coord(Indices.xx(a),
          Indices.yy(a),Indices.zz(a));
        end
end %End of if
end
end

P_list.P(I)=[];
P_list.Coordinates(I)=[];
Sw(t,1)=sum(sum(sum(S_water)));
Snw(t,1)=sum(sum(sum(S_oil)));
P_cap(t,1)=Pc;
kr_o(t,1)= sum(sum(sum(kr_oil)));
kr_w(t,1)=sum(sum(sum(kr_water)));
tom=Sw(t,1)+Snw(t,1);
t=t+1;
end

[Pc_ow_max]=max(P_cap);
[I_max]=findn(Pc_thres(:,:,:)==Pc_ow_max);
b_pin=(sig_ow/Pc_ow_max)*(cot(alpha)*cos(Pore_Model{I_max(1,1),I_max(1,2),
I_max(1,3)}(4))-sin(Pore_Model{I_max(1,1),I_max(1,2),I_max(1,3)}(4)));

num=1;
for j=1:1:2*n-1;
   for i=1:1:2*n-1;
      if Location(i,1,k).C==1 & Location(i,1,k).T~='t';
         In_P(num,1)=Pc_drain(i,1,k);
         Out_P(num,1)=Pc_drain(i,2*n-1,k);
         num=num+1;
      end
   end
end

drainage={'Sw','Capillary Pressure (Pa)','kr_w','kr_o'};
xlswrite('Sim_Results.xls', drainage, 'Drainage', 'A1');
xlswrite('Sim_Results.xls', Sw, 'Drainage', 'A2');
xlswrite('Sim_Results.xls', P_cap, 'Drainage', 'B2');
xlswrite('Sim_Results.xls', kr_w, 'Drainage', 'C2');
xlswrite('Sim_Results.xls', kr_o, 'Drainage', 'D2');

Filled_Cor(:,1)=nonzeros(Filled.x);
Filled_Cor(:,2)=nonzeros(Filled.y);
Filled_Cor(:,3)=nonzeros(Filled.z);
clf;
h=plot3k([Filled_Cor(:,1)    Filled_Cor(:,2)    Filled_Cor(:,3)],[Oil_Sat],'o',25,'Oil    Saturation
Distribution');
```

```
pause;
clf;
f=plot3k([Filled_Cor(:,1) Filled_Cor(:,2) Filled_Cor(:,3)], [Water_Sat], 'o', 25, 'Water Saturation Distribution');
```

B.2. Threshold Pressure Calculation

```
%Threshold Pressure for Primary Drainage
function [Threshold_P]=Pri_Drain(Rec_Ang,Radius)
global alpha sig_ow

if Rec_Ang+alpha>pi/2   %Control for presence of water in the corners
   error ('theta_1+alpha should be smaller than pi/2.Change theta_1 value')
   return
end %End of if (Pore_Model{i,j,k}(4)+alpha>pi/2)

%============Capillary Pressure Calculation==========%
%Threshold Capillary Pressure Calculation (Oren&Bakke,1997)
if Radius==0
   Threshold_P=inf;
end

alpha_1=alpha; %Maximum value of corner half angle
alpha_2=pi/4-alpha_1/2; %Minimum value of corner half angle
G=(sin(2*alpha_1)/2).*(2.+(sin(2.*alpha_1)./sin(2.*alpha_2))).^-2;

%Dimensionless shape factor
D=pi*(1-Rec_Ang/(pi/3))+3.*sin(Rec_Ang).*cos(Rec_Ang) (cos(Rec_Ang).^2)./(4*G);
Fd=(1.+sqrt(1+4*G*D./(cos(Rec_Ang)).^2))./(1+2.*sqrt(pi*G));

Threshold_P=(sig_ow*(1+2*sqrt(pi*G)).*cos(Rec_Ang)./Radius).*Fd;   %Threshold Capillary pressure (Pa)
```

B.3. Conductance Calculation

```
function [g_nwetting,g_wetting,Acor,Anw]=conduct_drain(Pres,Rec_Ang, Area, Radius)
global alpha nc  %From pore_prop function
global sig_ow %Oil/Water interfacial tension (N/m)

%Lengths are in m
%Conductance values are in m^4
%Angles are in degrees
%Pressure values are in Pa

%============Conductance Calculation=============%
r_ow=sig_ow/Pres; %Interfacial radius of curvature (m)

if alpha+Rec_Ang==pi/2; %(From Piri&Blunt, 2005)
   Acor=(r_ow*cos(alpha+Rec_Ang)/sin(alpha))^2*sin(alpha)*cos(alpha);
else
    Acor=nc.*r_ow.^2.*(cos(Rec_Ang).*(cot(alpha).*cos(Rec_Ang)-
    sin(Rec_Ang))+Rec_Ang+alpha-pi/2); %Area occupied by fluid in the corners. For primary
    drainage Ac=Aw (water area) (m^2)
end
Anw=Area-Acor; %Non-wetting phase area,oil area. Oil is present in the center of pore space. (m^2)
f=1; %Boundary condition at fluid/fluid interface. (1 represents no-flow boundary)
```

```
%Conductance Parameters
phi_1=pi/2-alpha-Rec_Ang;
phi_2=cot(alpha)*cos(Rec_Ang)-sin(Rec_Ang);
phi_3=(pi/2-alpha)*tan(alpha);

%Conductance calculations
g_wetting=(Acor.^2.*(1-sin(alpha))^2.*(phi_2.*cos(Rec_Ang)-phi_1)*phi_3^2)/
            (12*nc*(sin(alpha))^2*(1-phi_3)^2.*(phi_2+f*phi_1).^2);
%Wetting phase conductance. (Water is wetting phase) (m^4)

g_nwetting=pi*(sqrt(abs(Anw/pi))+Radius)^4/128;
%Non-wetting phase conductance. (Oil is non-wetting phase) (m^4)
```

APPENDIX C

CODE FOR IMBIBITION

C.1. Flow in Imbibition

```
%======Imbibibition=====%
function [P_cap]=Pres_Dist_imb(Pc_thres,Pore_Model)
clear
global alpha n %From pore_prop function
global Pore_Model Location %From Pore_Model_Construction function
global Pc_thres Pc_drain Pc_ow_max b_pin S_water S_oil g_nw g_w kr_oil kr_water Ao
Ac%From Primary Drainage
global sig_ow %Oil/Water interfacial tension (N/m)
global Model_Areas Model W_conduct Filledby

%Pres=Pc_thres; %Pc_thres for drainage, Pc_thresh for imbibition
Model_Area=sum(reshape(Model_Areas,(2*n-1)^3,1));
[Pc_threshold,theta_hing]=Imb;
count=1;
for k=1:1:2*n-1;
   for j=1:1:2*n-1;
      for i=1:1:2*n-1;
         if Location(i,j,k).C==1 & Pc_drain(i,j,k)~=0;
            Coord(i,j,k)=count;
            Pc_thres_imbibition(i,j,k)=Pc_threshold(i,j,k);
            theta_h_imb(i,j,k)=theta_hing(i,j,k);
            Uninvaded.x(count)=i;
            Uninvaded.y(count)=j;
            Uninvaded.z(count)=k;
            count=count+1;
         end
      end
   end
end

g_nwet_imb=g_nw;
g_wet_imb=g_w;
S_water_imb=S_water;
S_oil_imb=S_oil;
kr_oil_imb=kr_oil;
kr_water_imb=kr_water;
A_nwet_imb=Ao;
A_wet_imb=Ac;

Pc_imb=zeros(2*n-1,2*n-1,2*n-1);
Total_Conductance=sum(sum(sum(W_conduct)));
```

```
%%
%====Compare Calculated Capillary Pressures with Threshold Pressures====%
num=1;
t=1;
Invaded.x(num)=0;
Invaded.y(num)=0;
Invaded.z(num)=0;

%Flow starts from the first column (from left to right)
P_list.P=nonzeros(Pc_thres_imbibition(:,1,:));
P_list.Coordinates=nonzeros(Coord(:,1,:));

while length(P_list.P)~=0
   [Pc,I]=max2((P_list.P));
   [Loc]=findn(Coord(:,:,:)==P_list.Coordinates(I));
   x1=Loc(1);
   y1=Loc(2);
   z1=Loc(3);
   Pc_imb(x1,y1,z1)=Pc;
   Capil_P_imb(num)=Pc;
   contr=any(x1==Invaded.x(:)& y1==Invaded.y(:) & z1==Invaded.z(:));
   if contr==0
      Invaded.x(num)=x1;
      Invaded.y(num)=y1;
      Invaded.z(num)=z1;
      %Calculation of Conductance for each phase at pore or throat
      M=Filledby{x1,y1,z1}(4);
[g_nwet_imb(x1,y1,z1),g_wet_imb(x1,y1,z1),A_wet_imb(x1,y1,z1),A_nwet_imb(x1,y1,z1)]=imb
ibition_conduct(M,Pore_Model{x1,y1,z1}(3),theta_h_imb(x1,y1,z1),Pore_Model{x1,y1,z1}(4),Pc
,Pore_Model{x1,y1,z1}(2),Pore_Model{x1,y1,z1}(1));

      if Location(x1,y1,z1).T=='t'
         g_nwetting_imb.t(x1,y1,z1)=g_nwet_imb(x1,y1,z1);
         g_wetting_imb.t(x1,y1,z1)=g_wet_imb(x1,y1,z1);
      end
      %Calculation of Saturation

[S_oil_imb(x1,y1,z1),S_water_imb(x1,y1,z1)]=feval(@Cal_Sat,A_nwet_imb(x1,y1,z1),
A_wet_imb(x1,y1,z1), Model_Area);
      Water_Sat_imb(num)=S_water_imb(x1,y1,z1);
      Oil_Sat_imb(num)=S_oil_imb(x1,y1,z1);
      Total_Sat_imb(num)=Water_Sat_imb(num)+Oil_Sat_imb(num);

%Calculation of Relative Permeability
[kr_oil_imb(x1,y1,z1),kr_water_imb(x1,y1,z1)]=feval(@Cal_kr,g_nwet_imb(x1,y1,z1),g_wet_im
b(x1,y1,z1),Total_Conductance);
      num=num+1;
   end

   [Neigh,Indices]=feval(@Neigh_P,x1,y1,z1,Pc_thres_imbibition);
   for a=1:length(Neigh)
      if  Pc_imb(Indices.xx(a),Indices.yy(a),Indices.zz(a))==0;
         if Pc<=Neigh(a);
           Pc_imb(Indices.xx(a),Indices.yy(a),Indices.zz(a))=
           Pc_thres_imbibition(Indices.xx(a),Indices.yy(a),Indices.zz(a));
           %Set Imbibition Capillary of the element to Pc
        Capil_P_imb(num)=Pc;
         Invaded.x(num)=Indices.xx(a);
```

```
        Invaded.y(num)=Indices.yy(a);
        Invaded.z(num)=Indices.zz(a);
        M=Filledby{Indices.xx(a),Indices.yy(a),Indices.zz(a)}(4);

[g_nwet_imb(Indices.xx(a),Indices.yy(a),Indices.zz(a)),g_wet_imb(Indices.xx(a),Indices.yy(a),Ind
ices.zz(a)),A_wet_imb(Indices.xx(a),Indices.yy(a),Indices.zz(a)),A_nwet_imb(Indices.xx(a),Indic
es.yy(a),Indices.zz(a))]=
imbibition_conduct(M,Pore_Model{Indices.xx(a),Indices.yy(a),Indices.zz(a)}(3),theta_h_imb(Ind
ices.xx(a),Indices.yy(a),Indices.zz(a)),Pore_Model{Indices.xx(a),Indices.yy(a),Indices.zz(a)}(4),P
c,Pore_Model{Indices.xx(a),Indices.yy(a),Indices.zz(a)}(2),Pore_Model{Indices.xx(a),Indices.yy(
a),Indices.zz(a)}(1));

%Calculation of Conductance for each phase at pore or throat
        if Location(Indices.xx(a),Indices.yy(a),Indices.zz(a)).T=='t';
        g_nwetting_imb.t(Indices.xx(a),Indices.yy(a),Indices.zz(a))=g_nwet_imb
        (Indices.xx(a),Indices.yy(a),Indices.zz(a));
        g_wetting_imb.t(Indices.xx(a),Indices.yy(a),Indices.zz(a))=g_wet_imb
        (Indices.xx(a),Indices.yy(a),Indices.zz(a));
        end

%Calculation of Saturation
[S_oil_imb(Indices.xx(a),Indices.yy(a),Indices.zz(a)),S_water_imb(Indices.xx(a),Indices.yy(a),Ind
ices.zz(a))]=feval(@Cal_Sat,A_nwet_imb(Indices.xx(a),Indices.yy(a),Indices.zz(a)),A_wet_imb(I
ndices.xx(a),Indices.yy(a),Indices.zz(a)),Model_Area);

Water_Sat_imb(num)=S_water_imb(Indices.xx(a),Indices.yy(a),Indices.zz(a));
Oil_Sat_imb(num)=S_oil_imb(Indices.xx(a),Indices.yy(a),Indices.zz(a));
Total_Sat_imb(num)=Water_Sat_imb(num)+Oil_Sat_imb(num);

%Calculation of Relative Permeability
[kr_oil_imb(Indices.xx(a),Indices.yy(a),Indices.zz(a)),kr_water_imb(Indices.xx(a),Indices.yy(a),In
dices.zz(a))]=feval(@Cal_kr,g_nwet_imb(Indices.xx(a),Indices.yy(a),Indices.zz(a)),g_wet_imb(In
dices.xx(a),Indices.yy(a),Indices.zz(a)),
Total_Conductance);

num=num+1;

%Eliminate the pressure of filled element if it is included in pressure list (P_list)
contr=any(Coord(Indices.xx(a),Indices.yy(a),Indices.zz(a))==P_list.Coordinates(:));
        if contr==1
        [Loc_f]=findn(Coord(Indices.xx(a),Indices.yy(a),Indices.zz(a))== P_list.Coordinates(:));
        P_list.P(Loc_f)=[];
        P_list.Coordinates(Loc_f)=[];
        end

%Find neighbors of the filled element
[Neigh_f,Indices_f]=feval(@Neigh_P,Indices.xx(a),Indices.yy(a),Indices.zz(a),
                          Pc_thres_imbibition);
for i=1:length(Neigh_f)
if Pc_imb(Indices_f.xx(i),Indices_f.yy(i),Indices_f.zz(i))==0;
contr=any(Coord(Indices_f.xx(i),Indices_f.yy(i),Indices_f.zz(i))==P_list.Coordinates(:));
        if contr==0& Pc_thres_imbibition(Indices_f.xx(i), Indices_f.yy(i),
        Indices_f.zz(i)) ~=0;

        P_list.P(length(P_list.P)+1)=Pc_thres_imbibition(Indices_f.xx(i),
        Indices_f.yy(i),Indices_f.zz(i));
        P_list.Coordinates(length(P_list.Coordinates)+1)=Coord(Indices_f.xx(i),
        Indices_f.yy(i),Indices_f.zz(i));
```

```
        end
end
end

else
contr=any(Coord(Indices.xx(a),Indices.yy(a),Indices.zz(a))==P_list.Coordinates(:));
if contr==0 & Pc_thres_imbibition(Indices.xx(a),Indices.yy(a),Indices.zz(a))~=0;
            P_list.P(length(P_list.P)+1)=Pc_thres_imbibition(Indices.xx(a),
            Indices.yy(a),Indices.zz(a));
            P_list.Coordinates(length(P_list.Coordinates)+1)=Coord(Indices.xx(a),
            Indices.yy(a),Indices.zz(a));
end
end %End of if
end
end

P_list.P(I)=[];
P_list.Coordinates(I)=[];

Sw(t,1)=sum(sum(sum(S_water_imb)));
Snw(t,1)=sum(sum(sum(S_oil_imb)));
P_cap(t,1)=Pc;

kr_o(t,1)=sum(sum(sum(kr_oil_imb)));
kr_w(t,1)=sum(sum(sum(kr_water_imb)));
t=t+1;
end

imbibition={'Sw','Capillary Pressure (Pa)','kr_w','kr_o'};
xlswrite('Sim_Results.xls', imbibition, 'Imbibition', 'A1');
xlswrite('Sim_Results.xls', Sw, 'Imbibition', 'A2');
xlswrite('Sim_Results.xls', P_cap, 'Imbibition', 'B2');
xlswrite('Sim_Results.xls', kr_w, 'Imbibition', 'C2');
xlswrite('Sim_Results.xls', kr_o, 'Imbibition', 'D2');

[num_s, num_l, num_b, I_n, num_r]=Mechan_Num(Filledby);
mech_nums={'Snap-Off', 'Piston Like Advance', 'Pore Body Filling', 'I_n', 'Remained'};
xlswrite('Sim_Results.xls', mech_nums, 'Imbibition', 'e1');
xlswrite('Sim_Results.xls', num_s, 'Imbibition', 'e2');
xlswrite('Sim_Results.xls', num_l, 'Imbibition', 'f2');
xlswrite('Sim_Results.xls', num_b, 'Imbibition', 'g2');
xlswrite('Sim_Results.xls', I_n, 'Imbibition', 'h2');
xlswrite('Sim_Results.xls', num_r, 'Imbibition', 'i2');

Filled_Cor_Imb(:,1)=nonzeros(Invaded.x);
Filled_Cor_Imb(:,2)=nonzeros(Invaded.y);
Filled_Cor_Imb(:,3)=nonzeros(Invaded.z);

clf;
h=plot3k([Filled_Cor_Imb(:,1) Filled_Cor_Imb(:,2) Filled_Cor_Imb(:,3)], [Oil_Sat_imb], 'o', 25,
'Oil Saturation Distribution');
pause;
clf;
f=plot3k([Filled_Cor_Imb(:,1) Filled_Cor_Imb(:,2) Filled_Cor_Imb(:,3)], [Water_Sat_imb], 'o',
25, 'Water Saturation Distribution');
```

C.2. Threshold Pressure Calculation

```
%Waterflooding Threshold Pressure Calculation Function
%First check for snap-off, then piston like advance and pore body fillling
function [Pc_thresh_imb,theta_hin]=Imb(Location,Pore_Model,Pc_drain,n)

global n alpha%From pore_prop function
global Pore_Model Pc_ow_max b_pin g_w g_nw Ac Ao %From Pore_Model_Construction function
global Pc_drain Pc_thres Location%From Primary Drainage
global Filled_Cor %Pressure
global sig_ow Filledby Remained

%Lengths are in meter
%Angles are in radians
Filledby=cell([2*n-1,2*n-1,2*n-1]);
Pc_thresh_imb=zeros(2*n-1,2*n-1,2*n-1);

%Counters for Flow Mechanisms
num_pis=0;
num_snap=0;
num_body=0;

%=======Threshold Pressure Calculation for Imbibition====%
dbstop error
a=1;
for k=1:1:2*n-1;
for j=1:1:2*n-1;
for i=1:1:2*n-1;
%============================================================%
c=1;
if Location(i,j,k).C==1;
if Pc_drain(i,j,k)~=0;
if Pore_Model{i,j,k}(1)==0;
   Pc_thresh_imb(i,j,k)=Inf;
   theta_hin(i,j,k)=0;
end

if j==1;
%Elements are filled by Piston-like advance
[Pc_thresh_imb(i,j,k),theta_hin(i,j,k)]=feval(@piston_like,Pore_Model{i,j,k}(3),Pore_Model{i,j,k}(1),Pore_Model{i,j,k}(4),Pore_Model{i,j,k}(2));
   Filledby(i,j,k)={[i j k 'l' 0]};
   num_pis=num_pis+1;
else
   if Location(i,j-1,k).T=='t';
      %Check for possibility of snap-off
      snp=(Pore_Model{i,j-1,k}(1)/Pore_Model{i,j,k}(1));
      if snp<(1-tan(Pore_Model{i,j,k}(3))*tan(alpha))/2; %Mogensen&Stenby, 1998
         %Pore_Model{i,j,k}(1)/Pore_Model{i,j-1,k}(1)>3 %Ratio must satistfy Roof Criterion (Liping,2005)

[Pc_thresh_imb(i,j,k),theta_hin(i,j,k)]=feval(@snap_off,Pore_Model{i,j,k}(3),
Pore_Model{i,j,k}(1),Pore_Model{i,j,k}(4),Pore_Model{i,j,k}(2),Pc_drain(i,j,k));
         Filledby(i,j,k)={[i j k 's' 0]};
         num_snap=num_snap+1;
      else
         [Neigh_El]=feval(@Neigh_Whole,i,j,k);
```

```
        num=1;
        for a=1:length(Neigh_El.x)  %Determine # of filled neighbor elements
          if Pc_drain(Neigh_El.x(a),Neigh_El.y(a),Neigh_El.z(a))~=0;
            Neigh_Filling(num,1)=Neigh_El.x(a);
            Neigh_Filling(num,2)=Neigh_El.y(a);
            Neigh_Filling(num,3)=Neigh_El.z(a);
            c=c+1;
            num=num+1;
          end
        end
        c=c-1;
        if c==1 %Filling mechanism is either piston like or pore body filling

[Pc_thresh.Piston(i,j,k),theta_h.Piston(i,j,k)]=feval(@piston_like,Pore_Model{i,j,k}(3),Pore_Mod
el{i,j,k}(1),Pore_Model{i,j,k}(4),Pore_Model{i,j,k}(2));
          [Pc_thresh.PoreFill(i,j,k),theta_h.PoreFill(i,j,k)]=feval(@pore_filling_imb,
Pore_Model{i,j,k}(3),Pore_Model{i,j,k}(1),Pore_Model{i,j,k}(4),Pore_Model{i,j,k}(2),i,j,k,c,Nei
gh_Filling);

          if Pc_thresh.Piston(i,j,k)>Pc_thresh.PoreFill(i,j,k)
           %Piston like mechanism is prefered
            Pc_thresh_imb(i,j,k)=Pc_thresh.Piston(i,j,k);
            theta_hin(i,j,k)=theta_h.Piston(i,j,k);
            Filledby(i,j,k)={[i j k 'l' 0]};
            num_pis=num_pis+1;
          else
            Pc_thresh_imb(i,j,k)=Pc_thresh.PoreFill(i,j,k);
            theta_hin(i,j,k)=theta_h.PoreFill(i,j,k);
            Filledby(i,j,k)={[i j k 'b' c]};
          end

        else %Filling mechanism is pore body filling with I_c
          [Pc_thresh_imb(i,j,k),theta_hin(i,j,k)]=feval(@pore_filling_imb,
            Pore_Model{i,j,k}(3),Pore_Model{i,j,k}(1),Pore_Model{i,j,k}(4),
            Pore_Model{i,j,k}(2), i, j, k, c, Neigh_Filling);
          Filledby(i,j,k)={[i j k 'b' c]};
        end
      end %End of if Pore_Model{i,j,k}(1)/Pore_Model{i,j-2,k}(1)>3
    else
      [Neigh_El]=feval(@Neigh_Whole,i,j,k);

      num=1;
      for a=1:length(Neigh_El.x)  %Determine # of filled neighbor elements
        if Pc_drain(Neigh_El.x(a),Neigh_El.y(a),Neigh_El.z(a))~=0;
          Neigh_Filling(num,1)=Neigh_El.x(a);
          Neigh_Filling(num,2)=Neigh_El.y(a);
          Neigh_Filling(num,3)=Neigh_El.z(a);
          c=c+1;
          num=num+1;
        end
      end
      c=c-1;
      disp(Neigh_Filling)
      if c==1 %Filling mechanism is either piston like or pore body filling
        [Pc_thresh.Piston(i,j,k),theta_h.Piston(i,j,k)]=feval(@piston_like,
          Pore_Model{i,j,k}(3),Pore_Model{i,j,k}(1),Pore_Model{i,j,k}(4),
          Pore_Model{i,j,k}(2));
```

```
[Pc_thresh.PoreFill(i,j,k),theta_h.PoreFill(i,j,k)]=feval(@pore_filling_imb,Pore_Model{i,j,k}(3),P
ore_Model{i,j,k}(1),Pore_Model{i,j,k}(4),Pore_Model{i,j,k}(2),i,j,k,c,Neigh_Filling);


        if Pc_thresh.Piston(i,j,k)>Pc_thresh.PoreFill(i,j,k)
        %Piston like mechanism is prefered
           Pc_thresh_imb(i,j,k)=Pc_thresh.Piston(i,j,k);
           theta_hin(i,j,k)=theta_h.Piston(i,j,k);
           Filledby(i,j,k)={[i j k 'l' 0]};
        else
           Pc_thresh_imb(i,j,k)=Pc_thresh.PoreFill(i,j,k);
           theta_hin(i,j,k)=theta_h.PoreFill(i,j,k);
           Filledby(i,j,k)={[i j k 'b' c]};
        end

      else %Filling mechanism is pore body filling with I_c
         [Pc_thresh_imb(i,j,k),theta_hin(i,j,k)]=feval(@pore_filling_imb,Pore_Model{i,j,k}(3),
          Pore_Model{i,j,k}(1),Pore_Model{i,j,k}(4),Pore_Model{i,j,k}(2),i,j,k,c, Neigh_Filling);
         Filledby(i,j,k)={[i j k 'b' c]};
      end
   end %End of if Location(i,j-1,k).T=='t'
end %End of if j==1

else %Element was not invaded by wetting fluid
Pc_thresh_imb(i,j,k)=Pc_thres(i,j,k);
theta_hin(i,j,k)=0;
Filledby(i,j,k)={[i j k 'r' 0]};
Remained(a,1)=i;
Remained(a,2)=j;
Remained(a,3)=k;
a=a+1;
end
end %End of if Location(i,j,k).C==1;
%=========================================================%
end %End of i
end %End of j
end %End of k
%=========================================================%
disp(Pc_thresh_imb)
```

C.3. Threshold Pressure Calculation for Mechanism Type

C.3.1. Snap – Off

```
%Threshold Pressure for Snap-Off
function [Pc_snap,theta_h]=snap_off(Adv_Ang,Radius,Rec_Ang,Area,Pres)
global At R_ins alpha nc n_p n theta_0 theta_1 theta_ow
%From pore_prop function
global Pore_Model_Const Pore_Model
%From Pore_Model_Construction function
global Pc_thres Pc_ow_max b_pin  %From Primary Drainage
global sig_ow

%Lengths are in meter
%Angles are in radians
%==================Snap-Off====================%
%==Threshold Capillary Pressure Calculation==% (Oren&Bakke,1997)
```

```
%Spontaneous Snap-off
b=sig_ow*cos(Rec_Ang+alpha)/(Pc_ow_max*sin(alpha)); %Helland&Skaeveland, 2004
if Adv_Ang<pi/2-alpha %Spontaneous Snap-off
   Pc_snap=(sig_ow./Radius).*(cos(Adv_Ang)-2*sin(Adv_Ang)./(2*cot(alpha)));        %Threshold
Capillary pressure (Pa)
   ang=abs(Pc_snap).*b_pin.*sin(alpha)./sig_ow;
   if ang>1
      ang=1;
      Pc_snap=ang.*sig_ow./(b_pin*sin(alpha));
   end

   theta_h=acos(ang)-alpha; %Hinging Contact Angle (Blunt,2000).
   if theta_h<0;
      theta_h=pi+theta_h;
   end
end %End of Spontaneous Snap-Off

%Forced Snap-off
if Adv_Ang>pi/2-alpha; %Forced Snap-off
   if pi-alpha>=Adv_Ang;
      Pc_snap=Pc_ow_max.*(-1./cos(Rec_Ang+alpha));
      %Threshold Capillary pressure (Pa)
   end

   if Adv_Ang>pi-alpha;
      Pc_snap=Pc_ow_max.*cos(Adv_Ang+alpha)./cos(Rec_Ang+alpha);
      %Threshold Capillary pressure (Pa)
   end

   ang=abs(Pc_snap).*b_pin*sin(alpha)./sig_ow;
   if ang>1
      ang=1;
      Pc_snap=ang.*sig_ow./(b_pin*sin(alpha));
   end

   theta_h=acos(ang)-alpha; %Hinging Contact Angle (Blunt,2000).
   if theta_h<0;
      theta_h=pi+theta_h;
  end
end %End of Forced Snap-Off Loop
```

C.3.2. Piston Like Advance

```
%Threshold Pressure For Piston Like Advance
function [Pc_piston,theta_h]=piston_like(Adv_Ang,Radius,Rec_Ang,Area)
global At R_ins alpha nc n_p n theta_0 theta_1 theta_ow
%From pore_prop function
global Pore_Model_Const Pore_Model
%From Pore_Model_Construction function
global Pc_thres Pc_ow_max b_pin g_wet_pd g_nwet_pd G
%From Primary Drainage
global sig_ow

%Lengths are in meter
%Angles are in radians

%==================Piston-like Advance Filling==============%
%Threshold Capillay Pressure Calculations (Blunt,2000)
```

```
theta_max=acos((-sin(alpha+Rec_Ang)*sin(alpha))./ ((Radius*Pc_ow_max *
                        cos (alpha)/sig_ow)-cos(alpha+Rec_Ang))); %Blunt,2000
%=====Spontaneous Imbibition, Pc>0 (Blunt,2000)======%
if  Adv_Ang<=pi/2+alpha
   %theta_ow<=theta_max
   if Adv_Ang<=theta_max
      r=Radius; %Initial estimate for Effective Mean Radius of Curvature (m)
      Pc_thresh=sig_ow./r; %New value of Threshold Capillary Pressure (Pa)
      beta=asin(b_pin*sin(alpha)./r);  %Angle
      A_eff=(Radius^2/(2*tan(alpha)))(r*b_pin*sin(alpha+beta)/2)+(r^2* beta/2) ;
       % Effective Area (m^2)
      omega_eff=((Radius./tan(alpha))-b_pin)*cos(Adv_Ang)+r.*beta;
      %Effective Perimeter (m)
      r_new=A_eff./omega_eff;
      %New value of Effective Mean Radius of Curvature (m)
      er=abs(r_new-r); %Error
      %Iteration Loop for Calculation of Threshold Capillary Pressure and
      Effective Mean Radius of Curvature (Blunt,2000)
      while er>0.001; %Error Control
        r=r_new;
        Pc_thresh=sig_ow./r; %New value of Threshold Capillary Pressure (Pa)
        beta=asin(b_pin*sin(alpha)./r);
        A_eff=(Radius^2/(2*tan(alpha)))(r*b_pin*sin(alpha+beta)/2)+(r^2*beta/2);
        omega_eff=((Radius./tan(alpha))-b_pin)*cos(Adv_Ang)+r.*beta;
        r_new=A_eff./omega_eff;
        %Calculates new value of Effective Mean Radius of Curvature (m)
        er_new=abs(r_new-r);
        er=er_new;
     end
     r=r_new;
     Pc_thresh=sig_ow./r;
     %Threshold Capillary Pressure for spontaneous imbibition (Pa)
end

   %theta_ow>theta_max , Intermediate oil films are not created
   if Adv_Ang>theta_max
      Pc_thresh=2.*sig_ow.*cos(Adv_Ang)./Radius;
      %Threshold Capillary pressure (Pa)
   end
end %End of Spontaneous Imbibition Loop

%==Forced Imbibition , Pc<0, Intermediate oil films are created (Oren,1997)==%
if Adv_Ang>pi/2+alpha %& Adv_Ang>theta_max
   %Threshold pressure calculation is same with primary drainage
   %Adv_Ang angle was used as advancing angle

   alpha_1=alpha; %Maximum value of corner half angle
   alpha_2=pi/4-alpha_1/2; %Minimum value of corner half angle

   G=(sin(2*alpha_1)/2).*(2.+(sin(2.*alpha_1)./sin(2.*alpha_2))).^-2;
   %Dimensionless shape factor
   D=pi*(1-Adv_Ang/(pi/3))+3.*sin(Adv_Ang).*cos(Adv_Ang)-
      (cos(Adv_Ang).^2)./(4*G);
         if D<0;
         D=0;
         end
   Fd=(1.+sqrt(1+4*G*D./(cos(Adv_Ang)).^2))./(1+2.*sqrt(pi*G));
```

```
   Pc_thresh=(sig_ow.*(1+2*sqrt(pi*G)).*cos(Adv_Ang)./Radius).*Fd;
   %Threshold Capillary pressure (Pa)
end  %End of Forced Imbibition Loop
%================================================%
theta_h=acos(Pc_thresh*b_pin*sin(alpha)/sig_ow)-alpha;
Pc_piston=Pc_thresh;
```

C.3.3. Pore Body Filling

```
%Pore Body Filling
function [Pc_porefill,theta_h]=pore_filling_imb(Adv_Ang, Radius, Rec_Ang, Area, x, y, z,
num_of, Filling_N)
global alpha n nc%From pore_prop function
global Pore_Model Location %From Pore_Model_Construction function
global Pc_thres Pc_ow_max b_pin %From Primary Drainage
global W_conduct %From Water Conductance function
global sig_ow

%=====================Pore Body Filling==================%
%Threshold Capillay Pressure Calculations (Blunt,2000)
theta_max=acos((-sin(alpha+Adv_Ang)*sin(alpha))./  ((Radius*Pc_ow_max*cos(alpha)/sig_ow)-
cos(alpha+Adv_Ang))); %Blunt,2000

%====If theta_ow>theta_max, Invasion is similar to forced piston like imbibition====&
if Adv_Ang>theta_max %Pc<0 and intermediate oil films are created
   %Threshold pressure is same with primary drainage
   alpha_1=alpha; %Maximum value of corner half angle
   alpha_2=pi/4-alpha_1/2; %Minimum value of corner half angle

   G=(sin(2*alpha_1)/2)*(2+(sin(2*alpha_1)/sin(2*alpha_2)))^-2; %Dimensionless shape factor
   D=pi*(1-Adv_Ang/(pi/3))+3*sin(Adv_Ang)*
      cos(Adv_Ang) (Adv_Ang)^2/(4*G);
   if D<0;
      D=0;
   end
   Fd=(1+sqrt(1+4*G*D/(cos(Adv_Ang))^2))/(1+2*sqrt(pi*G));

   Pc_porefill=(sig_ow*(1+2*sqrt(pi*G))*cos(Adv_Ang)./Radius)*Fd;  %Threshold  Capillary
pressure (Pa)
end %End of Forced piston like imbibition

%====If theta_ow<theta_max=======%
if Adv_Ang<theta_max
   a=rand(1,num_of);
   g=rand(1,num_of);
   %Coefficient calculation for summation term
   coef=a(1,:).*g(1,:);
   sum=0;  %Summation Term

   for counter=1:num_of
         term=coef(1,counter)*Pore_Model{Filling_N(counter,1),
         Filling_N(counter,2),Filling_N(counter,3)}(1);
         sum=sum+term;
   end

   r_n=(1/cos(Adv_Ang))*(Radius+sum);
%Mean Radius of Curvature Calculation
   Pc_porefill=2*sig_ow/r_n; %Threshold Capillary Pressure Calculation
```

```
end

ang=abs(Pc_porefill)*b_pin*sin(alpha)/sig_ow;
if ang>1
   ang=1;
   Pc_snap=ang.*sig_ow./(b_pin*sin(alpha));
end

theta_h=acos(ang)-alpha; %Hinging Contact Angle (Blunt,2000).
if theta_h<0;
   theta_h=pi+theta_h;
end

end %End of pore filling loop
%=====================================================%
```

C.4. Conductance Calculation for Imbibition

```
%Capillary pressure and conductance calculations for Waterflooding (Imbibition Process)
function[g_nwet,g_wet,Aw_total,Ao]=imbibition_conduct(M,Adv_Ang,theta_h,Rec_Ang,Pres,
Area,Radius)

global alpha n nc%From pore_prop function
global Pore_Model Location %From Pore_Model_Construction function
global Pc_thres Pc_ow_max b_pin %From Primary Drainage
global W_conduct %From Water Conductance function
global sig_ow

if M=='s';
   %==================Snap-Off=====================%
   %==Threshold Capillary Pressure Calculation==% (Oren&Bakke,1997)
   %Spontaneous Snap-off
   r_ow=sig_ow./Pres; %Interfacial radius of curvature (m)
   phi_3=(pi/2-alpha)*tan(alpha); %Conductance parameter
   f=1; %Boundary condition at fluid/fluid interface. (1 represents no-flow boundary)

   if Adv_Ang<pi/2-alpha %Spontaneous Snap-off
      %=Conductance Calculation (Blunt,2000)=%
      if theta_h>=Adv_Ang %Pore is completely filled by water
         g_wet=(pi*(sqrt(Area/pi)+Radius).^4)/128; %in m^4 %Pore is completely filled by water
(m^4) (Wetting phase is water)
         g_nwet=0; %Non-Wetting phase is oil (m^4)
         Aw_total=Area;
         Ao=0;
      else %Pore is not filled by water. Remained same as at the end of Primary Drainage
         [g_nwet,g_wet,Aw_total,Ao]=feval(@conduct_drain,Pres,Rec_Ang,Area,Radius) ;
      end
   end %End of Spontaneous Snap-Off

   %Forced Snap-off
   if Adv_Ang>pi/2-alpha; %Forced Snap-off. Curvature is negative
      %==Conductance Calculation (Blunt,2000)==%
      if theta_h<Adv_Ang %Oil/Water/Solid Interface is pinned (Blunt,2000).
         Ac=nc.*r_ow.^2.*(cos(theta_h).*(cot(alpha).*cos(theta_h)-sin(theta_h))+theta_h+alpha-
pi/2);  %Area of Water in corners (m^2)
         if Ac<Area
         Ao=(Area-Ac); %Area of oil (m^2)
```

```
          %Conductance Parameters
          phi_1=pi/2-alpha-theta_h;
          phi_2=cot(alpha)*cos(theta_h)-sin(theta_h);
          phi_3=(pi/2-alpha)*tan(alpha);

          g_wet=(Ac.^2.*(1-sin(alpha))^2.*(phi_2.*cos(theta_h)-phi_1)*phi_3^2)./
                  (12*nc*(sin(alpha))^2*(1-phi_3)^2.*(phi_2+f*phi_1).^2);
%Wetting phase conductance. (Water is wetting phase) (m^4)
          g_nwet=(pi*(sqrt(Ao/pi)+Radius).^4)/128; %Conductance of water in center (m^4)
         else
            Ac=Area;
            Ao=0;
            g_wet=(pi*(sqrt(Area/pi)+Radius).^4)/128; %Conductance of water in center (m^4)
            g_nwet=0;
         end
        Aw_total=Ac;
      else %theta_h>= Adv_Ang;
         %Ac=nc.*r_ow.^2.*(cos(theta_h).*(cot(alpha).*cos(theta_h)-sin(theta_h))+theta_h+alpha-
pi/2);  %Area of Water in corners (m^2)
         Ac=nc.*r_ow.^2.*(cos(pi-Adv_Ang).*(cot(alpha).*cos(pi-Adv_Ang)-sin(pi-Adv_Ang))+
             (pi-Adv_Ang)+alpha-pi/2);  %Area of Oil layer + Area of water in corner (m^2)
         if Ac<Area
          Ao=(Area-Ac); %Area of oil (m^2)
          %Conductance Parameters
          phi_1=pi/2-alpha-theta_h;
          phi_2=cot(alpha)*cos(theta_h)-sin(theta_h);
          phi_3=(pi/2-alpha)*tan(alpha);

          g_wet=(Ac.^2.*(1-sin(alpha))^2.*(phi_2.*cos(theta_h)-phi_1)*phi_3^2)./
                  (12*nc*(sin(alpha))^2*(1-phi_3)^2.*(phi_2+f*phi_1).^2);
%Wetting phase conductance. (Water is wetting phase) (m^4)
          g_nwet=(pi*(sqrt(Ao/pi)+Radius).^4)/128; %Conductance of water in center (m^4)
         else
            Ac=Area;
            Ao=0;
            g_wet=(pi*(sqrt(Area/pi)+Radius).^4)/128; %Conductance of water in center (m^4)
            g_nwet=0;
         end
        Aw_total=Ac;
      end
   end %End of Forced Snap-Off Loop

   if Adv_Ang==pi/2-alpha
      Pres=0; %Threshold Capillary pressure (Pa) (Oren&Bakke,1997)
      g_wet=(pi*(sqrt(Area/pi)+Radius).^4)/128; %in m^4 %Pore is completely filled by water
(m^4) (Wetting phase is water)
      g_nwet=0; %Non-Wetting phase is oil (m^4)
      Aw_total=Area;
      Ao=0;
   end

end %End of snap-off

if M=='l'
   %=====================Piston-like Advance Filling==================%
   theta_max=acos((-sin(alpha+Rec_Ang)*sin(alpha))./((Radius*Pc_ow_max*cos(alpha)/sig_ow)-
                cos(alpha+Rec_Ang))); %Blunt,2000
   %Threshold Capillay Pressure Calculations (Blunt,2000)
```

```
   if  Adv_Ang<=pi/2+alpha
      %theta_ow<=theta_max
      %==Conducatance Calculation (Blunt,2000)==%
      g_wet=(pi*(sqrt(Area/pi)+Radius).^4)/128; %in m^4 %Pore is completely filled by water
(m^4) (Wetting phase is water)
      g_nwet=0; %Oil Conductance
      Ao=0;
      Aw_total=Area;
   end %End of Spontaneous Imbibition Loop

   %=====Forced Imbibition , Pc<0, Intermediate oil films are created (Blunt,2000)========%
   if Adv_Ang>=pi/2+alpha %& Adv_Ang>theta_max
      %Oil Films Stability Pressure (Oren&Bakke,1997)
      b2=2+cos(Adv_Ang)/sin(alpha);
      Pc_stab=-Pc_ow_max*(sin(alpha)/cos(Rec_Ang+alpha))*((1-b2^2)/(b2*cos(alpha)+sqrt(1-
                  b2^2*(sin(alpha))^2)));

      %===Conductance Calculation (Blunt,2000)===%
      if abs(Pres)<Pc_stab %Oil films do not collapse

         ang=abs(Pres).*b_pin*sin(alpha)./sig_ow;
         if ang>1
            ang=1;
            Pres=ang*sig_ow/(b_pin*sin(alpha));
         end

         theta_h=acos(ang)-alpha; %Hinging Contact Angle (Blunt,2000).
         if theta_h<0;
            theta_h=pi+theta_h;
         end

         r_ow=sig_ow./Pres; %Interfacial radius of curvature (m)
         Aw_corner=nc.*r_ow.^2.*(cos(theta_h).*(cot(alpha).*cos(theta_h)-
sin(theta_h))+theta_h+alpha-pi/2);  %Area of Water in corners (m^2)

         if alpha+Adv_Ang==pi/2; %(From Piri&Blunt, 2005)
         Ac=(r_ow*cos(pi-Adv_Ang)/sin(alpha))^2*sin(alpha)*cos(alpha);
         else
         Ac= nc.*r_ow.^2.*(cos(pi-Adv_Ang).*(cot(alpha).*cos(pi-Adv_Ang)-sin(pi-Adv_Ang))+
               pi-Adv_Ang+alpha-pi/2);  %Area of Oil layer + Area of water in corner (m^2)
         end
         %Ac=nc.*r_ow.^2.*(cos(pi-Adv_Ang).*(cot(alpha).*cos(pi-Adv_Ang)-sin(pi-Adv_Ang))
                +(pi-Adv_Ang)+alpha-pi/2);  %Area of Oil layer + Area of water in corner (m^2)
         Ao=(Ac-Aw_corner); %Area of oil (m^2)
         Aw_center=Area-Ac; %Area of water in the pore center (m^2)
         Aw_total=Aw_corner+Aw_center; %Total area of wetting phase (water) (m^2)

         phi_3=(pi/2-alpha)*tan(alpha); %Conductance parameter
         f=1; %Boundary condition at fluid/fluid interface. (1 represents no-flow boundary)
         g_wet_corner=(Ac^2*tan(alpha)*(1-sin(alpha))^2*phi_3^2)/(12*nc*(sin(alpha))^2*
                           (1-phi_3)*(1+f*phi_3)^2); %Conductance of water in corners (m^4)
         g_wet_center=(pi*(sqrt(Aw_center/pi)+Radius).^4)/128;
%Conductance of water in center (m^4)
         g_wet= g_wet_corner+g_wet_center; %Total Water Conductance (m^4)

         f1=1; %Boundary condition at fluid/fluid interface. (1 represents no-flow boundary)
         f2=1; %Boundary condition at fluid/fluid interface. (1 represents no-flow boundary)
```

```
        g_nwet=(Ao^3*(1-sin(alpha))^2*tan(alpha)*phi_3^2)/(12*nc*Ac*(sin(alpha))^2*
                    (1-phi_3)*(1+f1*phi_3-(1-f2*phi_3)*sqrt(Aw_corner/Ac))^2);
%Conductance of oil layer between water in center and water in corner (m^2)
      else %Pres>=Pc_stab, Oil films collapse
        g_wet=(pi*(sqrt(Area/pi)+Radius).^4)/128; %in m^4
%Pore is completely filled by water (m^4) (Wetting phase is water)
        g_nwet=0; %Oil Conductance
        Ao=0;
        Aw_total=Area;
      end

   end  %End of Forced Imbibition Loop
end %End of Piston-like

if M=='b'
   %=====================Pore Body Filling==================%
   %====If theta_ow>theta_max, Invasion is similar to forced piston like imbibition====&
   theta_max=acos((-
sin(alpha+Adv_Ang)*sin(alpha))./((Radius*Pc_ow_max*cos(alpha)/sig_ow)-
cos(alpha+Adv_Ang))); %Blunt,2000
   if Adv_Ang>theta_max %Pc<0 and intermediate oil films are created

      %Oil Films Stability Pressure (Oren&Bakke,1997)
      b2=2+cos(Adv_Ang)/sin(alpha);
      Pc_stab=-Pc_ow_max*(sin(alpha)/cos(Rec_Ang+alpha))*((1-b2^2)/(b2*cos(alpha)+
                  sqrt(1-b2^2*(sin(alpha))^2)));

      %===Conductance Calculation (Blunt,2000)===%
       if abs(Pres)<Pc_stab & Adv_Ang>=pi/2+alpha %Oil films do not collapse
         ang=(Pres)*b_pin*sin(alpha)/sig_ow;
         if ang>1
            ang=1;
            Pres=ang*sig_ow/(b_pin*sin(alpha));
         end

         theta_h=acos(ang)-alpha; %Hinging Contact Angle (Blunt,2000).
         if theta_h<0;
            theta_h=pi+theta_h;
         end

         r_ow=sig_ow./Pres; %Interfacial radius of curvature (m)
         Aw_corner=nc.*r_ow.^2.*(cos(theta_h).*(cot(alpha).*cos(theta_h)-sin(theta_h)) +theta_h+
                        alpha-pi/2); %Area of Water in corners (m^2)
         if alpha+Adv_Ang==pi/2; %(From Piri&Blunt, 2005)
         Ac=(r_ow*cos(pi-Adv_Ang)/sin(alpha))^2*sin(alpha)*cos(alpha);
         else
         Ac= nc.*r_ow.^2.*(cos(pi-Adv_Ang).*(cot(alpha).*cos(pi-Adv_Ang)-sin(pi-Adv_Ang))+
               pi-Adv_Ang+alpha-pi/2);  %Area of Oil layer + Area of water in corner (m^2)
         end
         Ao=Ac-Aw_corner; %Area of oil (m^2)
         Aw_center=Area-Ac; %Area of water in the pore center (m^2)
         Aw_total=Aw_corner+Aw_center; %Total area of wetting phase (water) (m^2)

         phi_3=(pi/2-alpha)*tan(alpha); %Conductance parameter
         f=1; %Boundary condition at fluid/fluid interface. (1 represents no-flow boundary)
         g_wet_corner=(Ac^2*tan(alpha)*(1-sin(alpha))^2*phi_3^2)/(12*nc*(sin(alpha))^2*
                           (1-phi_3)*(1+f*phi_3)^2); %Conductance of water in corners (m^4)
```

```
        g_wet_center=(pi*(sqrt(Aw_center/pi)+Radius).^4)/128;
%Conductance of water in center (m^4)
        g_wet= g_wet_corner+g_wet_center; %Total Water Conductance (m^4)
        f1=1; %Boundary condition at fluid/fluid interface. (1 represents no-flow boundary)
        f2=1; %Boundary condition at fluid/fluid interface. (1 represents no-flow boundary)

        g_nwet=(Ao^3*(1-sin(alpha))^2*tan(alpha)*phi_3^2)/(12*nc*Ac*(sin(alpha))^2*
                (1-phi_3)*(1+f1*phi_3-(1-f2*phi_3)*sqrt(Aw_corner/Ac))^2);
%Conductance of oil layer between water in center and water in corner (m^2)

      else %Pres>=Pc_stab, Oil films collapse
        g_wet=(pi*(sqrt(Area/pi)+Radius).^4)/128;
%Pore is completely filled by water .Water spontenously fills pore. Water Conductance (m^4)
        g_nwet=0; %Oil Conductance
        Aw_total=Area;
        Ao=0;
      end
   end

   %====If theta_ow<theta_max=======%
   if Adv_Ang<theta_max
      Aw_total=Area;
      g_wet=pi*(sqrt(Aw_total/pi)+Radius).^4/128;
      Ao=0;
      g_nwet=0;
   end %End of pore filling loop
end %End of Pore_Filling

if M=='r' %Remained Same
   g_wet=pi*(sqrt(Area/pi)+Radius).^4/128; %Water Conductance (m^4)
   g_nwet=0;
   Aw_total=Area;
   Ao=0;
end
```